An Investigation into the Ferric Leaching of Chalcopyrite - a Sub-Process in the Bioleaching of Chalcopyrite

by
Elizabeth Geethika Jeevaratnam
B.Sc. (Eng.) Chemical

Dissertation prepared in partial fulfilment of the requirments
for the degree of
M.Sc. (Eng.) Chemical

In the Department of Chemical Engineering
University of Cape Town
November 2001

Acknowledgements

I would like to thank the following people for their contribution over the past two years:

My supervisor, Professor Geoff Hansford, for giving me the opportunity to do my masters and his guidance and encouragement throughout my thesis

Giles Searby for his endless assistance in correcting my thesis and all his help in the lab.

A-Professor Peter Harris, Syd Allison, Paul Kruger (Mintek), Michele Warick (Billiton), Helen Divey, Stephanie La Grange, Shireen Mjacu and Granville de la Cruz for their technical assistance

Sue Jobson, for doing all the orders for the experiments and her enthusiasm.

Everyone in the Department of Chemical Engineering for their company. Special thanks to Ben Knights, Evelyn Dhilawayo, Mark Pickering, Malose Mamashela ,Glordina Gordan and Jo-Ann Moon for the laughs and great times.

Special thanks to the BIOMIN group; Nick Dempers, Ashraf Jaffer, Tendai Furamera and Ashli Breed for their technical assistance and encouragement.

To all the guys in the office, Madelyn Johnstone-Roberts, Foluke Daramola, Valerie Lamaignere, Christian Techer for the great company in the office

To my best friends Ada Chirinos, Nadine Chin, Linda Mesani and Angelik Deltgen for all their encouragement and support during the hard times of the thesis and making my final year in Cape Town a memorable one.

To Stuart Domijan for all his support and encouragement during the tough times of the thesis and the late nights checking the grammar of my thesis.

To my parents, for their encouragement and support throughout my years at University of Cape Town.

Sasol for their financial support

Finally, I would like to thank God for giving me the strength to defeat all odds and carry me through my years at this university.

Summary

The current focus of research in the UCT Minerals Bioprocessing Research Unit is to develop an understanding of the chalcopyrite bioleaching sub-processes. This thesis forms part of the greater study on bioleaching, investigating the ferric leaching sub-process. The objective of this thesis was two-folds. Firstly, a detailed literature review was undertaken to develop a better understanding of the ferric leaching of chalcopyrite and the cause of passivation during chalcopyrite leaching. Secondly, leach experiments on pyrite were used to establish the applicability and reproducibility of measuring the rate of ferric leaching at a constant redox potential, using the methodology developed by Kametani and Aoki (1985). Following this, chalcopyrite ferric leach experiments were conducted to obtain the redox potential range where chalcopyrite leaching occurs.

The rate of chalcopyrite leaching in a sulfate media decreases with time due to the formation of a passivating layer. This has been described by many researchers as parabolic kinetics (Dutrizac, 1982; Beckstead *et al.,* 1976; Munoz *et al.,* 1979 and Dutrizac and Mac Donald, 1974). The nature of the passivating layer is still under considerable debate. Current theories of passivation include either the formation of jarosite, ferric hyroxy sulfate, sulfur or iron deficient polysulfide like covellite (Klauber *et al.*, 2001, Parker *et al.,* 1981, Munoz *et al,* 1976, Warren *et al.,* 1985 and Parker *et al.,* 1981). Recent research has suggested that different passivating layers are formed during the various stages of chalcopyrite leaching. These include a ferric hydroxy sulfate layer followed by jarosite over extended period of time (Klauber *et al.,* 2001 and Parker *et al.,* 2001). Current investigations are underway to establish whether semiconductor properties of the mineral affects the type of passivating layer formed.

To date, most of the work has been performed at temperatures higher than those at which chalcopyrite bioleaching occurs and with varying pH and redox potentials. There has been little consideration of the potential difference between the suspended particles surface and the solution. This problem can be overcome by conducting experiments at a constant solution redox potential. Kametani and Aoki (1985) first presented a method of maintaining a constant redox potential by using potassium permanganate as an oxidant to continuously re-oxidise ferrous-iron to ferric-iron. This method was then adopted by our research group to determine the initial rates of chalcopyrite leaching. Preliminary rates of chalcopyrite leaching were presented in the thesis by Furamera (2000). Further work was required to firmly establish the rates of chalcopyrite leaching and the optimal redox potential range within which

chalcopyrite leach occurs. This involved optimising the redox potential control system to obtain better redox potential control during the chalcopyrite leach experiment.

To validate the use of potassium permanganate to control redox potential, it was necessary to test the applicability and reproducibility of measuring the rate of leaching using this method. Preliminary experiments on the ferric leaching of pyrite at constant redox potential were performed. Pyrite was chosen as a base case since the kinetics and stoichiometry of pyrite are well established. The rates were compared to the rates obtained in the dynamic leach experiments performed by May (1997), Figure 1. The rates were comparable and fitted well with the Butler-Volmer equation. The results showed that the technique was applicable and reproducible.

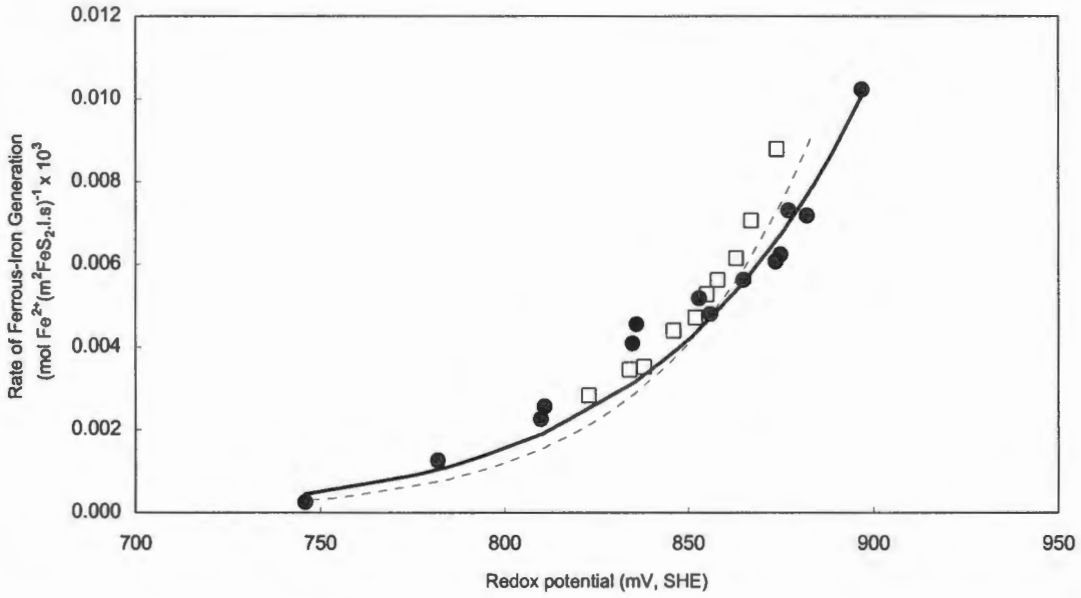

Figure 1: Comparison of Butler-Volmer fit to current data and experimental data (May, 1997)
[●] Experimental Data; [□] May (1997)
[—] Butler-Volmer fit to current data; [---] Butler-Volmer fit to data by May (1997)

Both dynamic and controlled ferric leach experiments were conducted. Dynamic leach experiments were initially performed to establish the reaction stoichiometry. Previous research has shown that ferric leaching of chalcopyrite proceeds according to one of the following reactions (Beckstead *et al.,* 1976; Munoz *et al.,* 1979; Dutrizac and MacDonald, 1974; Dutrizac, 1989 and 1982 and Jones and Peters, 1976).

$$CuFeS_2 + 4Fe^{3+} \rightarrow Cu^{2+} + 5Fe^{2+} + 2S_o \qquad [1]$$

$$CuFeS_2 + 16Fe^{3+} + 8H_2O \rightarrow Cu^{2+} + 17Fe^{2+} + 2SO_4^{2-} + 16H^+ \qquad [2]$$

Variable ferrous-iron to copper ratios were observed at 35°C and 70°C during the course of the reaction. These results are similar to the results observed by Jones

and Peters (1976). Other researchers have established a constant ferrous-iron to copper ratio of 5 (Dutrizac, 1989 and Munoz *et al.*, 1979).

Following the dynamic leach experiments, controlled redox potential experiments were conducted. During these ferric leach experiments the redox potential was constantly maintained by the controlled addition of potassium permanganate using an automatic titration unit. The rate of ferrous-iron generated was calculated from the amount of potassium permanganate added to re-oxidise it back to ferric-iron. The rate was calculated based on the following relationship:

$$-5r_{KMnO_4} = -r_{Fe^{2+}} \qquad [3]$$

Figure 2 shows a comparison of the rate of ferrous-iron generation at different redox potentials at 35°C and 70°C.

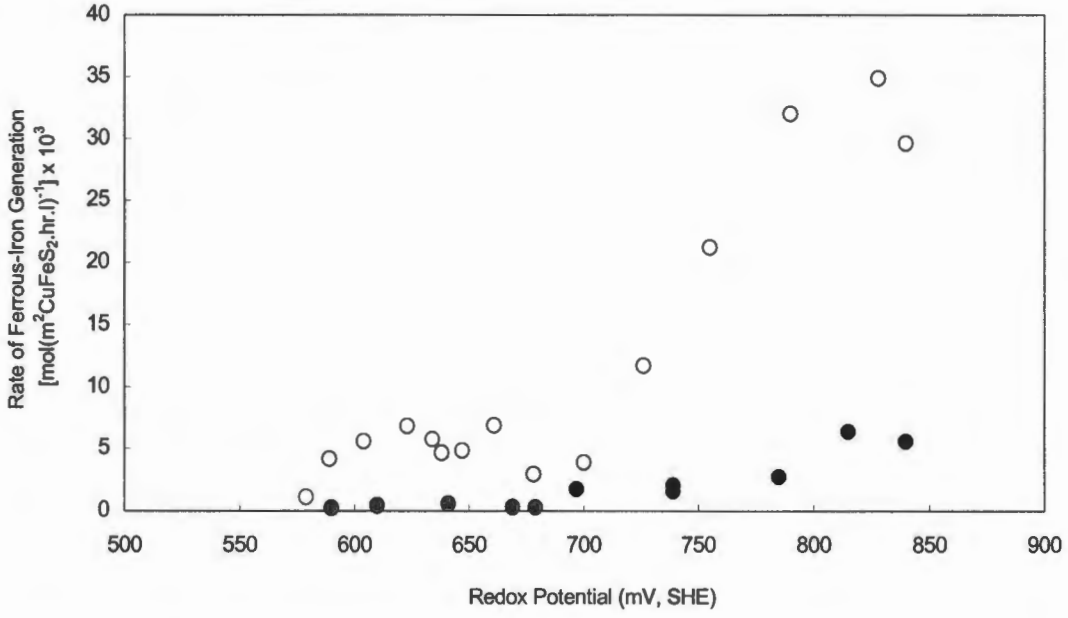

Figure 2: Comparison of initial rate of ferrous-iron generation at 35°C and 70°C.
Rate of ferrous iron generation was calculated using the rate of permanganate addition
[O] 70°C, [●] 35°C; pH = 1.5, Total Iron = 10g/ℓ

From the above diagram it can be seen that there are two regions of enhanced ferrous-iron generation, namely 580 mV to 650 mV (SHE) and 700 mV to 800 mV (SHE). According to Kametani and Aoki (1985), the increase in ferrous-iron generation at redox potentials above 700 mV (SHE) is caused by an increase in pyrite leaching, or a change in the mechanism of leaching due to a change in the nature of chalcopyrite. Iron analysis did not indicate a distinct increase in iron at higher redox potentials. The contribution of ferric leaching of sphalerite to the increase in rate of ferrous-iron generation was found to be negligible, at the different redox potential.

The amount of copper extracted was monitored throughout the duration of the experiments. Figure 3 shows a comparison of the copper extraction at 35°C and 70°C. Above 780 mV, there is a decrease in the rate of copper extraction at 70°C and 35°C. Higher rates of copper extraction were observed at the higher temperature.

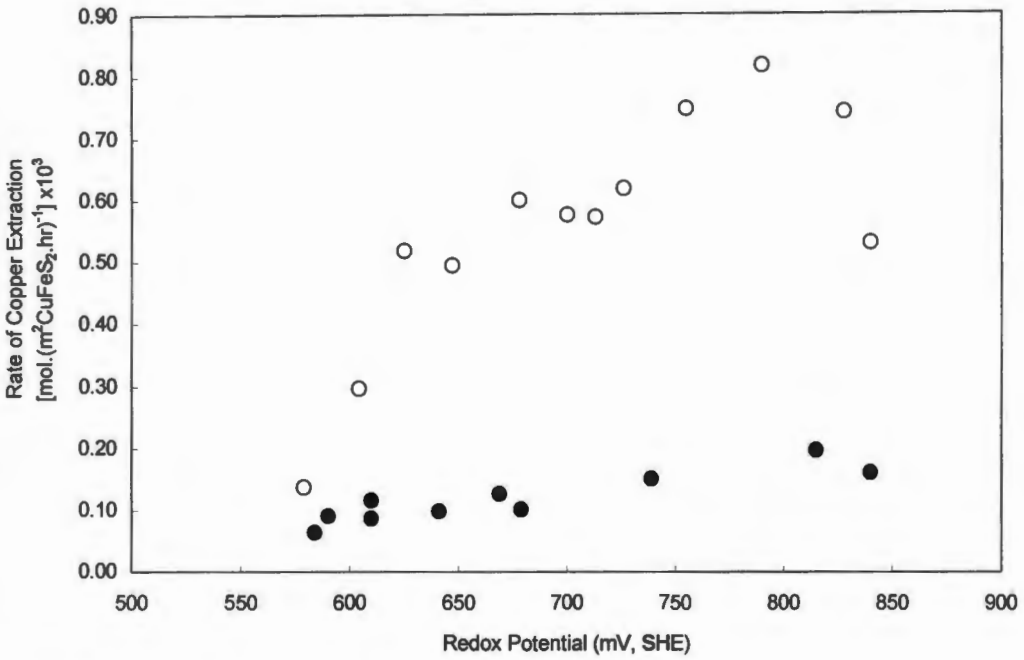

Figure 3: Initial rate of copper extraction versus redox potential
[O] 70°C, [●] 35°C, pH = 1.5, Total Iron = 10g/ℓ

To confirm the redox potential range where chalcopyrite leaching occurs, the experimental results have been compared with those from previous researchers. The data presented by Kametani and Aoki (1985) was reworked in order to normalise the rate. Following which, the difference in temperature was accounted for by using the Arrhenius equation. Figure 4 shows agreement in the redox potential range within which chalcopyrite leaching occurs. However, the experimental rates are higher than those of Kametani and Aoki (1985) within the redox potential range of 720 mV and 800 mV (SHE).

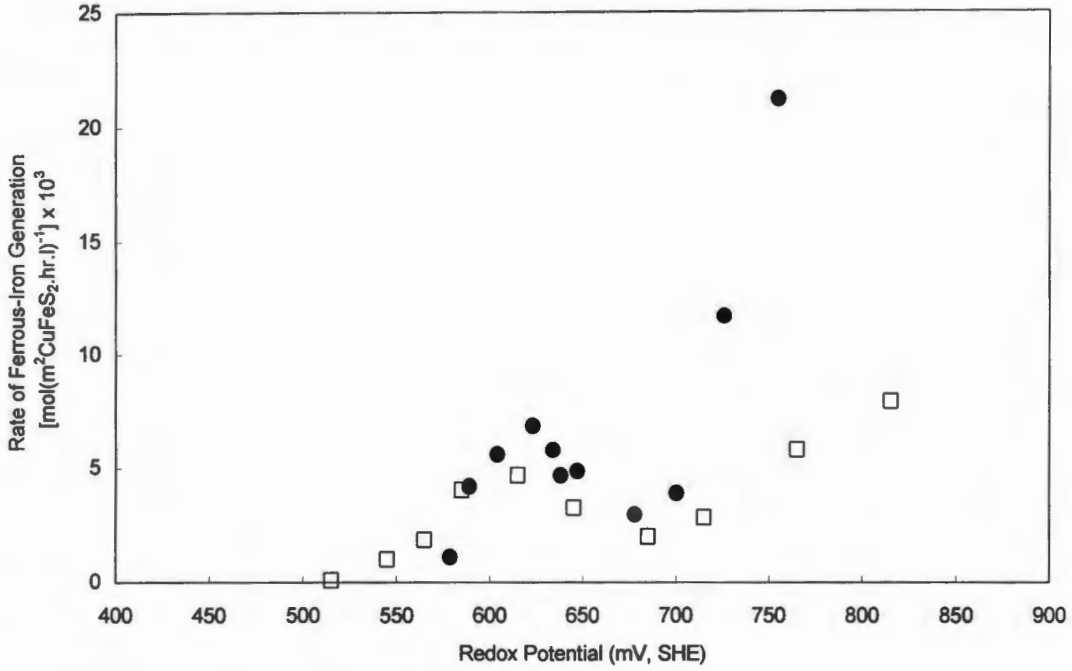

Figure 4: Comparison of the rate of ferrous-iron generation
[●] Experimental data; [□] Kametani and Aoki (1985)

Hiroyoshi *et al.* (2000) used a much purer chalcopyrite concentrate to determine the optimal redox potential range where chalcopyrite leaching occurs. Figure 5 shows that the redox potential range where chalcopyrite leaching occurs was from 530 to 580 mV (SHE). This range is considerably lower and narrower than the optimal redox potential range observed by Kametani and Aoki (1985), and the results presented in this thesis.

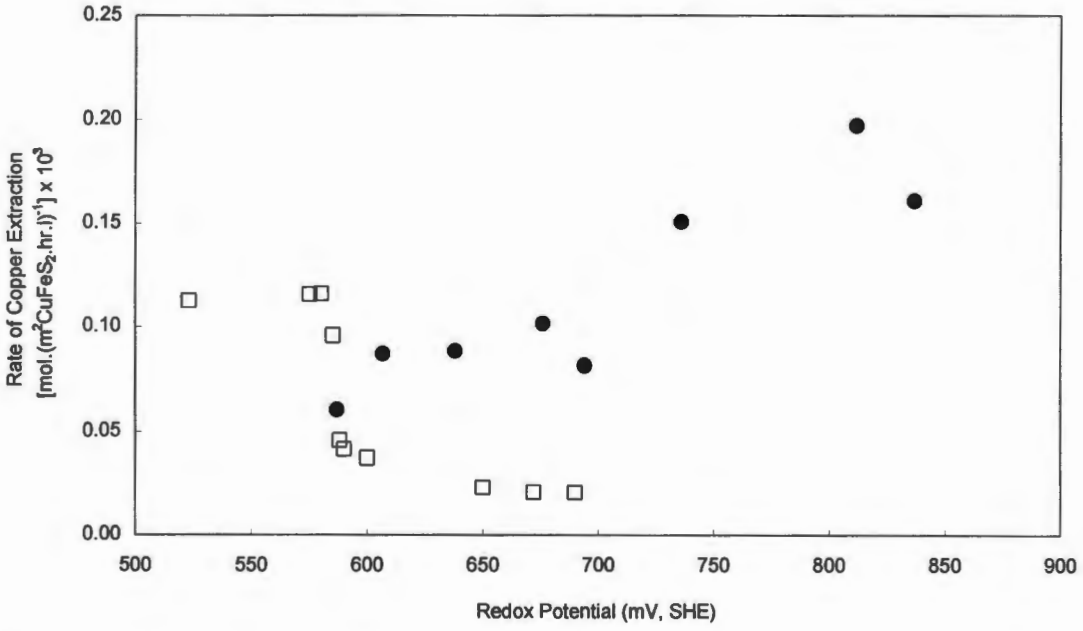

Figure 5: Comparison of the rate of copper extracted between experimental data at 35°C and re-evaluated rate data at 25°C from Hiroyoshi *et al.* (2000)
[●] Experimental data [□] Hiroyoshi *et al.* (2000)

The results show that there is a possibility that the optimal chalcopyrite leaching redox potential range is dependent on the type of concentrate used. The concentrates used in this investigation and those used by Kametani and Aoki (1985) are similar and exhibited similar behaviour, whereas the purer chalcopyrite concentrate exhibited a lower optimal redox potential range.

Hiroyoshi *et al.* (1997) performed leach experiments using ferric and ferrous sulfate media on four different concentrates. It was observed that three of the four concentrates reported better copper extraction in a ferrous sulfate system. However, the concentrate which had the most impurities showed negligible difference in the rate of copper extraction in the ferric nor the ferrous sulfate system. Based on these findings, leach experiments were conducted in this study over an extended period of time in a ferrous and ferric sulfate system. The results also indicated a negligible difference in the rate of copper extraction between the two systems.

This study has established that the methodology for determining the rate of chalcopyrite leaching at constant redox potential is valid. In this investigation, the initial rates of chalcopyrite leaching were established using only one concentrate. Further work using chalcopyrite concentrates of varying purity is needed to establish whether the redox potential range, where chalcopyrite leaching occurs varies with the type of concentrate used.

Table of Contents

List of Figures

List of Tables

Nomenclature

		Units
α	transfer co-efficient	m^2
α	fraction extracted	
k	rate constant	
η	over potential	mV
i	current density	$A.m^{-2}$
i_o	exchange current density	$A.m^{-2}$
E^o	standard redox potential	mV
E	redox potential	mV
RT/zF	Nernst Parameter	mV
r_{Fe2+}	rate of ferrous production	$mol.m^2CuFeS_2^{-1}.s^{-1}$
AAS	atomic adsorption spectroscopy	
AES	auger electron spectroscopy	
CESL	Cominco Engineering Service Limited	
SEM	scanning electron microscopy	
SHE	standard hydrogen electrode	
SSE	sum of squares of error	
XRD	x-ray diffraction	
XPS	x-ray photoelectron spectroscopy	

Chapter One

Introduction

Bioleaching is now an established technology for the pre-treatment of gold ores and concentrates, and the leaching of copper from whole copper ores in heaps (Brierley and Brierley, 2001 and Haines and Van Aswegen, 1990). Bioleaching is a robust metallurgical process with many advantages, including low capital expenditure and operating costs, shorter construction times, operational simplicity and environmental advantages to pressure oxidation and smelting (Brierley and Brierley, 2001). Recently, the bioleach technology developed for arsenopyrite/pyrite concentrates has been extended to incorporate chalcopyrite concentrates. Both Billiton and Mintek have established two independent commercial approaches to stirred tank chalcopyrite concentrate leaching which are in the pilot plant scale development stage (Miller *et al.*, 1999 and Dew *et al.*, 1999).

Chalcopyrite is the most abundant, naturally occurring copper sulphide mineral, therefore it is a major commercial source of copper (Habashi, 1990). This combined with the in-depth understanding of the bioleach process could make chalcopyrite concentrate bioleaching a commercially viable process.

In order to optimise the plant operating parameters, it is necessary to have a complete understanding of the chalcopyrite bioleaching mechanism and kinetics. A study conducted on the bioleaching of pyrite has provided strong evidence that the bioleaching of sulfide minerals proceeds via a multi-sub-process mechanism (Boon *et al.*, 1995). Based on the bioleaching mechanism developed for pyrite, a current review by Hansford and Vargas (2001) outlined the general application of this mechanism to other sulfide minerals. The bioxidation of sulfide mineral involves a primary acidic and ferric–iron oxidation reaction, which can be represented as:

$$MS_x + Fe^{3+} \rightarrow M^{x+} + Fe^{2+} + S_x(?) \qquad [1.1]$$

The role of the bacteria is to regenerate ferric-iron by oxidising the ferrous-iron and sulfur product for metabolic growth according to the following reactions:

$$4Fe^{2+} + O_2 + 4H^+ \rightarrow 4Fe^{3+} + 2H_2O \qquad [1.2]$$

$$S_x(?) + 2xO_2 + 2xe^- \rightarrow xSO_4^{2-} \qquad [1.3]$$

The proposed mechanism has been supported by the findings of Schippers and Sand (1999), who described the bioleaching of chalcopyrite as proceeding via a polysulfide route. The mineral is acid soluble and reacts with the ferric-iron to yield elemental sulfur. This proceeds by the formation of an intermediary polysulfide according to the following mechanism (Schippers and Sand, 1999):

$$CuFeS_2 + Fe^{3+} + 2H^+ \rightarrow Cu^{2+} + H_2S_n + 2Fe^{2+} + e^-(n=2) \quad [1.4]$$

$$H_2S_n + 2Fe^{3+} \rightarrow 0.25S_8 + 2Fe^{2+} + 2H^+ \quad [1.5]$$

$$0.25S_8 + 3O_2 + H_2O \rightarrow 2SO_4^{2-} + 4H^+ \quad [1.6]$$

In this process the continual regeneration of the ferric-iron sustains the leaching process and a low pH is maintained within the system, by the sulphur oxidation process. The bacterial-oxidation of ferrous-iron has been found to be a function of the ferric to ferrous-iron ratio (Boon, 1996). Likewise, the ferric leaching of chalcopyrite is also a function of the ferric to ferrous iron ratio (Kametani and Aoki, 1985). A constant solution redox potential can be maintined within a continuous bacterial leach system, due to the continuous regeneration of ferric-iron.

The multiple sub-process mechanism implies that each sub-process can be independently studied and modelled to predict the overall performance of the bioleach reactors at different operating conditions. Thus the ferric leaching of chalcopyrite forms an important subprocess of bioleaching.

The UCT Mineral Bioprocessing Research Unit is currently investigating the kinetics of each sub-process of chalcopyrite bioleaching. This thesis forms part of the greater study, investigating the initial rate of chalcopyrite ferric leaching at constant redox potential.

Considerable research has been done on the ferric leaching of chalcopyrite. However, the reaction conditions of the published studies were different from those encountered in bioleaching. In particular, the leach experiments were conducted at higher leach temperatures, and varying pH and solution redox potentials. Bioleaching takes place under a low temperature range of 35 to 70°C, within a pH range of 1 to 2 and a constant redox potential. In a ferric leach experiment, the difference between the mineral and solution redox potential is partially overcome by the use of an oxidising agent, to continuously regenerate ferric-iron and maintain a constant redox potential. Kametani and Aoki (1985) established such a method for determining chalcopyrite leach kinetics at various redox potentials.

1.1 OBJECTIVE OF THESIS

The thesis has two objectives. Firstly, to provide a thorough review of the literature on the kinetics of chalcopyrite leaching and on the nature of the passivating layer formation on chalcopyrite. Secondly, to establish the initial rates of chalcopyrite ferric leaching under bioleach conditions.

The potassium permanganate titration method, established by Kametani and Aoki (1985) has been used by Furamera (2000) to obtain initial rates of chalcopyrite leaching. The initial focus of this thesis was to further the work done by Furamera (2000) and establish profiles for the redox potential leach window at different temperatures. However, due to discrepancies in results obtained by Furamera (2000), the objectives of the thesis were shifted to improving the methodology, so as to obtain better control of redox potential and to obtain reproducible results. In doing so, the objectives deviated towards establishing:

- The validity of the use of potassium permanganate titration method to control redox potential by using pyrite as a base case, given that the leach kinetics of pyrite are well established, and
- The optimal redox potential range and the rate of ferric leaching of chalcopyrite at thermophilic (70°C) and mesophilic (35°C) conditions.

1.2 STRUCTURE OF THESIS

The structure of the thesis is outlined below

- **Chapter Two**: A general review of the literature review on the different type of processes used for copper extraction for chalcopyrite. This is followed by, a thorough review of the literature on the ferric leaching of chalcopyrite, and the different theories on the cause of passivation during chalcopyrite leaching.
- **Chapter Three**: Re-evaluation of previously published data on the effect of redox potential on the rate of chalcopyrite leaching.
- **Chapter Four**: A description of the materials and methods used for the constant potential chalcopyrite and pyrite leach experiments.
- **Chapter Five:** The results and discussion section is divided into two sections; firstly, the rate of pyrite leaching at constant redox potential, and, secondly, the rate of chalcopyrite leaching. The first section focused on validating the method of constant potential leaching using pyrite, and the second section looks at the rate of chalcopyrite leach within redox potential range of 550 to 850 mV (SHE).
- **Chapter Six:** A comparison of the results obtained from the chalcopyrite leach experiments with those from the published data.
- **Chapter Seven:** Conclusions and recommendations.

Chapter Two

Literature Review

Based on the current understanding of the bioleaching multiple sub-process mechanism, ferric leaching and proton attack of the mineral is an important sub-process. This literature review begins with a brief description of the chalcopyrite bioleaching process, as well as the alternative processes available for copper extraction from chalcopyrite. This is followed by a detailed literature review, which concentrates on the following topics:

- A comparison of the chalcopyrite ferric leach stoichiometry and kinetics in sulfate and chloride medium.
- A description of the characteristics of the chalcopyrite mineral and the factors affecting the leaching of chalcopyrite.
- A detailed review on the nature of the passivating layer and factors affecting the formation of the passivating layer.
- The different methods of measuring chalcopyrite leach kinetics.

The aim of this literature review is to establish the state of the art in chalcopyrite ferric leaching, which forms part of a sub-process in the chalcopyrite bioleaching mechanism.

2.1 COPPER PRODUCTION

Copper can be extracted from oxides and primary (chalcopyrite) and secondary copper sulfides (covellite, bornite, chalcocite and enargite) ores using pyrometallurgical processing, or hydrometallurgical processes, such as pressure oxidation and bacterial leaching. Smelting, pressure oxidation and bacterial leaching are all developing and competing processes, which will be discussed in this section. Emphasis will be placed on the copper bioleaching process.

2.1.1 Copper Bioleaching

Bacterial leaching is the microbially mediated extraction of metals from mineral sulfides. While bioleaching for the extraction of copper has been practised since the 16th Century, it was only in 1947, that the bacterium *Acidithiobacillus ferrooxidans* was isolated from acidic mine water and the process was understood to be bacterially catalysed (Colmer and Hinkle, 1947). The genus *Thiobacillus* has recently

been reclassified and the species *Thiobacillus ferrooxidans* has been renamed *Acidithiobacillus ferrooxidans* (Kelly and Wood, 2000).

Bioleaching has environmental advantages over roasting with regard to the quality of gaseous and liquid effluent (Van Aswegen, 1993). Other advantages that bioleaching has over pressure oxidation include the milder conditions employed in bioleaching such as, the mild acidity and slightly elevated temperatures, as opposed to high pressures, temperatures and acidity (Haines and Van Aswegen, 1990). Copper oxides are found closer to the surface than sulfides and are mined first for dump and heap leaching using sulphuric acid. However, only twenty percent of world's copper resources occur as oxides and have already been extensively exploited (Habashi, 1999).

At present, bioheap leaching of secondary copper ores is extensively practised in Chile and North America, and some parts of Australia. Eleven copper bioheap operations have been commissioned since 1980 (Brierley and Brierley, 2001). The largest existing commercialised secondary copper bioheap leach process is Quebrada Blanca. This facility processes 17 300 tons of sulfide ore and produces 206 tons of London Metal Exchange grade copper per day (Brierley, 1999 and Schnell, 1997).

Chalcopyrite is the most difficult copper sulfide to bioleach. Waste dumps irrigated over four to six years only recover 15% of copper from chalcopyrite (Schnell, 1997). The rate of chalcopyrite leaching in a sulfate media decreases with time due to the formation of a passivating layer, this has been described by researchers as parabolic kinetics (Dutrizac, 1982; Beckstead *et al.,* 1976; Munoz *et al.,* 1979 and Dutrizac and MacDonald, 1974). The nature of the passivating layer is under considerable debate. A detailed review of the different theories on the passivating layer is discussed in a later section, Section 2.7.

Billiton and Mintek have established pilot plant operations using stirred tank bacterial oxidation technology to leach copper from chalcopyrite rich concentrates. Pilot plant trials undertaken at Billiton Process Research Unit, and another at BacTech Mt. Lyell pilot-plant operation have demonstrated the effective use of thermophilic bacteria to leach finely ground concentrate. Both processes obtained high copper recoveries up to 97% using thermophilic bacteria *(Sulfolobus),* which operate at 70°C as opposed to 31% using mesophilic bacteria, which grow at an optimal temperature range of 35 to 45°C (Dew *et al.,* 1999 and Miller *et al.,* 1999).

The Mintek-Bactech Process has also developed an indirect commercial approach to chalcopyrite concentrate bioleaching in which the bio-oxidation occurs in a separate step. A high concentration of ferric iron is produced in a separated reactor heated to 70°C and the ferric solution is contacted with the chalcopyrite concentrate (Pinches *et al.*, 1997 as cited by Brierley and Brierley 2001). The cost associated with the heating of the ferric liquor and the cooling before recirculation to the bacterial reactor would make the direct thermophilic bacterial leaching a favourable process (Brierley and Brierley, 2001).

2.1.2 Alternative Routes

Conventionally, smelting produces copper metal, which then requires further refining. The high levels of sulfur dioxide emission makes this process unfavourable. Mining operations have taken corrective measures either voluntarily or under pressure from legislation to minimise sulphur dioxide emissions. Some of the corrective actions include; the attachment of sulfuric acid producing plants, the use of tall stacks to dispose sulfur dioxide and the replacement of furnaces used during smelting. The reverbatory furnaces, which produce the most amount of sulfur dioxide, has been replaced by flash smelting furnaces which produce sulfur dioxide in concentrations suitable for sulfur acid production (Habashi, 2001). The problem of dust has generally been overcome by the use of wet scrubbers and electrostatic precipitators (Habashi, 2001).

Economic considerations do not always make smelting an appropriate method of treating metal sulfides. These include:

- Operations where the project is not large enough to sustain the initial capital expenditure of smelting and refining (Brierley, 1997).
- Mines which are in remote areas and require transportation costs (Brierley, 1997).
- Excessive energy consumption and dust formation on application to low-grade concentrates.
- High costs incurred in treating dirty concentrates (high level of Pb, Bi, Se, Te, Hg) (Dreisinger, 2001)

As a result of these factors, hydrometallurgical processes have been considered as an alternative. Hydrometallurgical alternatives are more favourable for the extraction of copper from low-grade ores. With the scarcity of high-grade ores, copper extraction from low-grade ores needs to be considered in order to meet copper demand.

Pressure oxidation involves exposing the mineral of interest to oxygen in an acid medium at elevated temperatures and pressures. Pressure oxidation is capital intensive, due to the operating conditions and material of construction required for the autoclaves. Chalcopyrite concentrates may be pressure leached commercially using variable solution and temperature conditions (Dreisinger, 2001). A variety of feasible routes for chalcopyrite, sulfate-based, pressure leaching processes have been developed. These include the Cominco Engineering Services Limited (CESL), Activox, Dynatec and Total Pressure Oxidation (TPO) processes (Dreisinger, 2001). A brief process description of different types of pressure oxidation processes are tabulated below.

Table 2.1: Operating conditions for Activox, CESL and TPO processes

	ACTIVOX	CESL	TOTAL PRESSURE OXIDATION
Pressure	Low	Medium	
Temperature (°C)	100	150	200
Size of particles	5 – 15 microns	45 microns	50-100 microns
Final recovery method	SX/EW*	SX/EW*	SX/EW*

* Solvent extraction followed by electrowinning

Dreisinger (2001) and Taylor and Jansen (1999) have performed a detailed review of the different pressure oxidation processes. Based on their reviews, the advantages and disadvantages of these processes have been discussed in this section.

The Activox process operates at low pressure. The advantage of using low pressure is the lower capital investments in autoclaves and the production of elemental sulphur, which minimises oxygen consumption. However, fine grinding of the concentrate is required to overcome the resistance to leaching at low temperatures (Dreisinger, 2001). The producers claim that compared to smelting, the Activox process has significantly low capital cost, and metal recoveries at least as good as smelting. It is economically viable for processes in which the production of copper is less than 10000 tpa (Taylor and Jansen, 1999).

The CESL process involves the use of a chloride catalyst and an additional second stage atmospheric leach operation to improve copper extraction. The benefit of using high temperature, is that it avoids the need for ultrafine grinding. In comparison to smelting, the CESL process claims to reduce the amount of capital required and the operating costs by half. The process is economically viable for large installations (Taylor and Jansen, 1999).

In the Total Pressure Oxidation Process, within one hour of leaching more than 99% copper can be extracted. High temperatures and the use of oxygen for complete oxidation is costly and such a process would only be considerable under certain circumstances (Dreisinger, 2001). These processes demonstrate the advances in pressure oxidation to overcome the limitation of chalcopyrite leaching, and indicate potential for commercialisation.

2.2 LEACHING OF SULFIDE MINERALS

Decomposition of sulfide minerals in an aqueous medium can be classified into the following categories; the molecular oxygen and sulfur transfer mechanism, electrochemical mechanism or a combination of both mechanisms (Peters and Doyle, 1989). These mechanisms are discussed in detail in this section.

2.2.1 Molecular Oxygen and Sulfur Transfer Mechanism

Sulfide minerals are leached by the use of an oxidising agent, which oxidises sulfide to elemental sulfur or sulfate, thereby releasing the metal ion into solution. Unlike

most base metal oxides, sulfides do not dissolute easily in acid solution and require an oxidising agent (Dutrizac and MacDonald, 1974). The use of the most inexpensive oxidant, oxygen, is limited by the low reactivity of molecular oxygen. Oxidation of sulfide minerals using oxygen can only be achieved under high pressures and temperatures; under milder conditions other chemical species that exhibit higher oxidation potentials such as chloride, cupric ions and ferric-iron ions are needed (Hearne *et al.*, 1998). Acidic ferric solution has proven to be a powerful and cheap leachant for sulfide dissolution under non-autoclave conditions (Linge, 1976).

Most base metal sulfides require a moderately strong oxidising agent to improve their dissolution in an acidic medium. For an oxidant to leach a mineral, its potential must be higher than the electrochemical potential of the mineral (Riekkola-Vahanen and Heimala, 1993). Ferric-iron ions are strong oxidising agents with an oxidation potential of approximately 700 V (SHE). Ferric-iron can be applied either in a sulfate or chloride medium. The kinetics of chalcopyrite leaching using ferric chloride and sulfate media are discussed later in this report. The typical oxidation of sulfide mineral is as follows:

$$MS + 2Fe^{3+} \rightarrow M^{2+} + 2Fe^{2+} + S^{\circ} \qquad [2.1]$$

The regeneration of ferric-iron in solution promotes the chemical oxidation of the sulfide mineral with the formation of ferrous-iron and elemental sulfur. Ferric-iron can be regenerated using autotrophic bacteria, MnO_2 and $NaClO_3$ or electrolytic anodic oxidation (Murr *et al.*, 1978).

2.2.2 Electrochemical Mechanism

Electrochemistry is an important consideration in the study of the oxidation of sulfide minerals. Sulfide minerals such as chalcopyrite are electronic conductors. When these minerals undergo oxidation, the leaching process is electrochemical in nature. Electrochemical mechanisms are promoted by high over voltages supplied by high redox potentials, or accelerated by high temperatures. Electrochemical processes are unique in that the solid assumes a uniform potential throughout, if the ohmic resistance is considered negligible. The chemical reaction may be directly influenced by the potential and may also serve to stabilise the intermediate solid phases (Wadsworth, 1987).

Corrosion theory can be applied to the electron conducting solids in hydrometallurgical systems (Wadsworth, 1987). During the corrosion process two types of mixed potential regimes can be operative; corrosion and galvanic couples. The corrosion type involves a single phase, having both anodic and cathodic reactions on a mineral. The galvanic couple is operational when two or more solids are in contact. Each solid assumes an anodic or cathodic behaviour. Natarajan (1992) studied galvanic interactions within a chalcopyrite concentrate and reported preferred oxidation of specific minerals.

Before oxidation can occur, the solution redox potential must exceed the rest potential of the mineral. When a metal sulfide is placed in a solution containing an oxidant (e.g. Fe^{3+}), having a more positive redox potential, a corrosion cell will be established, resulting in the anodic dissolution of the mineral and cathodic reduction of the oxidant

Half cell reactions:

$$MS \rightarrow M^{m+} + S^{\circ} + me^{-} \quad [2.2]$$

$$N^{n+} + e^{-} \rightarrow N^{(n-1)+} \quad [2.3]$$

The mineral is a short-circuited electrochemical cell (Natarajan, 1982) that assumes a mixed potential between the half-cell potentials of the anodic and cathodic reactions. Potentials more positive than the equilibrium potential drive the half-cell reaction in the anodic direction, and potentials more negative than the equilibrium potential drive the reaction in the net cathodic direction.

The net current density for a system is the sum of the anodic and cathodic reaction The mixed potential, E, occurs when the net current density is zero, i.e. when the anodic and cathodic current are equal and opposite. Therefore the kinetics of the electrochemical process involves the anodic and cathodic reaction influenced by the voltage biases controlled by the mixed potential generated during the leaching. (Wadsworth, 1987).

2.2.3 Redox Potential Measurements

Redox potential is an important measurement and control parameter used in the sulfide mineral decomposition mechanisms outlined above. Leaching experiments are carried out with the ore immersed in a suspension media containing ferric and ferrous irons. The measured redox potential can be related to ratio of oxidising to reducing agent via the Nernst equation, Equation 2.4.

$$E = E^{\circ} + \frac{RT}{zF} \ln \frac{[M^{ox}]}{[M^{red}]} \quad [2.4]$$

In this system, free ferric-iron in the solution is the oxidising agent and free ferrous-iron in solution is the reducing agent. This gives the following form of the Nernst equation

$$E = E^{\circ} + \frac{RT}{zF} \ln \frac{[Fe^{3+}]}{[Fe^{2+}]} \quad [2.5]$$

E° is the standard potential and is related to the ease with which electrons are removed from the oxidised species. Each system has a characteristic E°. The redox potential is measured by placing an inert metal electrode such as platinum in solution and comparing its potential with that of a reference electrode. The reference electrode possesses a stable potential which is unaffected by the solution potential.

The metal electrode acquires the potential of the solution by a process of electron interchange, which can be expressed by the Nernst equation.

The Nernst equation relates the measured potential to the ratio of the activities of the redox couple. It is assumed that during the ferric to ferrous-iron conversion, the ferric/ferrous redox couple is the dominate redox couple. The formation of other complexes have negligible effect on the overall exchange current density, and therefor the redox potential (Dry, 1984). The formation of a cuprous/cupric redox couple, had negligible effect on the measured redox potential at cupric ion concentrations of up to 0.1M (Hiroyoshi *et al.*, 2000).

It is common practice to refer all redox potential to the Standard Hydrogen Electrode (SHE) assumed to have zero potential at all temperatures. The SHE is however not always suitable for practical use, other electrodes are more convenient (Record, 1965). The relationships between the SHE and other electrode potentials are recorded in the following table.

Table 2.2: Relationships between various electrode potentials referred to the SHE at 25° C for common reference electrodes – European convention (Record, 1965)

REFERENCE ELECTRODE	mV
Saturated Calomel Electrode (S.C.E)	+ 244
3.5 M KCl, Calomel Electrode	+ 250
1.0 M KCl, Calomel Electrode	+ 285
Saturated Silver, Silver Chloride Electrode	+ 198
Saturated Mercury, Mercurous Sulfate Electrode	+ 658

In the bioleach system, the redox potential is also used as a quick and easy method for early detection of the reduction in the bacterial activity, such as an increase in ferrous-iron concentration (Breed, 2000).

2.3 CHEMICAL PROPERTIES OF CHALCOPYRITE

Chalcopyrite is a complex sulfide. It has a tetrahedral structure, with a unit cell crystal structure consisting of two metal atoms, copper and iron, surrounded by four sulfur atoms in a tetrahedral arrangement as shown in Figure 2.1. It is covalently bonded, with each bond being bonded to its neighbours by sp^3 hybrid orbitals. Chalcopyrite can exist in two ionic states, $Cu^{+}Fe^{3+}(S^{2-})_2$ and $Cu^{2+}Fe^{2+}(S^{2-})_2$ (Habashi, 1978). A description of the physical and electrical properties of chalcopyrite are illustrated in Table 2.3.

Table 2.3: The mineral properties of chalcopyrite (Habashi, 1978 and Hiskey, 1993)

PROPERTY	VALUE
Structure	Tetragonal
Density($g.cm^{-3}$)	4.087
Hardness (Moh)	3.5 – 4
Surface cleavage	011
Molar mass ($g.mol^{-1}$)	184
Resistivity (Ωm)	$2x10^{-4} – 3x10^{-1}$
Cp ($J\ mol^{-1}\ K^{-1}$) 298-830K	$88.71+5.19e^{-2}T +7.45e-^{5}T^{2}$

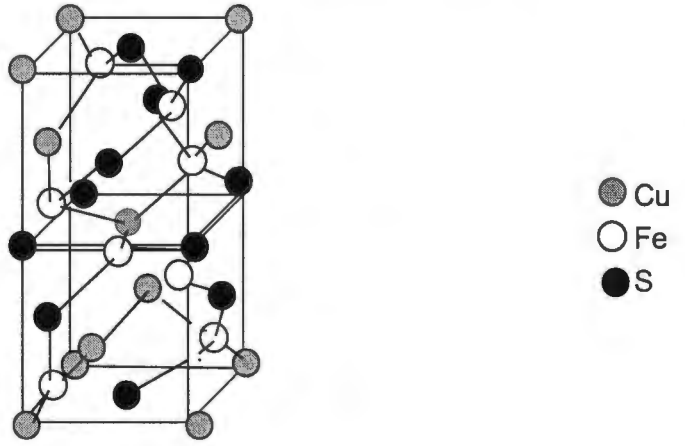

Figure 2.1: Schematic representation of a chalcopyrite crystal

2.4 FERRIC LEACH STOICHIOMETRY

The overall ferric leaching of chalcopyrite in a sulfate or chloride media at ambient pressure is often represented by either of the following two reactions (Munoz *et al.,* 1979; Dutrizac and MacDonald, 1974; Dutrizac, 1989 and 1982 and Jones and Peters, 1976).

$$CuFeS_2 + 4Fe^{3+} \rightarrow Cu^{2+} + 5Fe^{2+} + 2S_o \qquad [2.6]$$

$$CuFeS_2 + 16Fe^{3+} + 8H_2O \rightarrow Cu^{2+} + 17Fe^{2+} + 2SO_4^{2-} + 16H^+ \qquad [2.7]$$

A detailed review of the ferric-iron stoichiometry in a sulfate and chloride medium is discussed in detail below.

2.4.1 Ferric Leach Stoichiometry in Sulfate Media

Most of the research performed on the ferric sulfate leaching of chalcopyrite supports the formation of elemental sulfur as opposed to sulfate formation (Munoz *et al.,* 1979; Dutrizac and MacDonald, 1974 and Linge, 1976). It has been shown that 94% of the sulfide was converted to elemental sulfur and only 6% to sulfate formation in a 70-hr leach experiment at 95°C. A constant ferrous-iron to copper ratio of 5 was established (Dutrizac, 1989). Jones and Peters (1976) reported 18% sulfate formation after 17 days, and even greater amounts at shorter periods of time.

Initially, a high ferrous-iron to copper ratio (>10) was observed which decreased to 7.5 after about 15 days of leaching. Jones and Peters (1976) proposed that the preferential iron dissolution at the start could have resulted in the high ferrous-iron to copper ratio

Dutrizac (1989) proposed that the leaching mechanism might involve a direct attack of sulfide minerals, according to the following equation:

$$CuFeS_2 + 2H_2SO_4 \rightarrow CuSO_4 + FeSO_4 + 2H_2S_{aqueous} \quad [2.8]$$

The dissolved H_2S is subsequently oxidised by ferric sulfate according to the following equation:

$$2H_2S_{aqueous} + 2Fe_2(SO_4)_3 \rightarrow 4FeSO_4 + 2H_2SO_4 + 2S^\circ \quad [2.9]$$

The formation of a polysulfide intermediate is in agreement with the chalcopyrite bioleaching mechanism proposed by Schippers and Sand (1999). However, the overall reaction is represented by Equation 2.6] and 2.7.

The lack of dominance of either of these equations during the leaching reaction would imply a varying stoichiometry; hence a varying ferrous-iron to copper ratio. Most research has been conducted using mixed concentrates, and the researchers have only reported the extent of copper extraction with time. Few have reported on the change in ratio of ferrous-iron to copper production with time (Dutrizac, 1989 and Jones and Peters, 1976). Leaching of other sulfides such as sphalerite and pyrite in the concentrate would also contribute to the increase in ferrous-iron concentration in the system. Unless a very pure chalcopyrite concentrate is used, it is difficult to clearly establish the stoichiometry of chalcopyrite leaching.

2.4.2 Ferric Leach Stoichiometry in Chloride Media

Accurate stoichiometric predictions of elemental sulfur formation were observed in ferric chloride medium. Analytical data at 50°C and 90°C indicated that 96% of the oxidised sulfide reported to elemental sulfur (Dutrizac, 1989 and 1978, and Jones and Peters, 1976).

2.5 COMPARISON OF FERRIC SULFATE AND CHLORIDE LEACH KINETICS

Hydrochloric acid leaching is more aggressive than sulfuric acid leaching, this is ascribed to the formation of chlorine within the system (Habashi and Toor, 1979 as cited by Habashi, 1978). Similarly, there are reports of chalcopyrite oxidising more readily in the presence of chloride than in the sulfate medium (Dutrizac and MacDonald, 1974 and Dutrizac, 1981). Nevertheless, sulfate is the preferred medium because the downstream electrowinning process which produces copper cathodes of wire-drawing quality is more suited for the sulfate medium than the chloride medium (Dutrizac, 1989). Furthermore, ferric-iron applied in sulfate media is

preferable because of the availability of sulfuric acid (Dutrizac and MacDonald, 1974).

In the bacterial system, a sulfate medium is used due to the toxicity of chloride ions to the bacterial culture. Lawson *et al.*, (1995) found *Acidithiobacillus ferrooxidans* to be affected detrimentally at chloride concentrations of about 14 mmol.l^{-1} and Dew *et al.*, (1997) reported that the BIOX® culture was inhibited at chloride concentrations of 140 mmol.l^{-1}.

The enhanced leaching rate in the presence of chlorides has been noted by a number of researchers. Activation energy in chloride solution is about 42kJ/mol whilst for sulfate solution, the corresponding value is 75kJ/mol (Dutrizac, 1982). Ferric leaching of natural chalcopyrite over the temperature range of 50 to 100°C with chlorides exhibits a constant rate over time, this has been described by researchers as linear kinetics (Dutrizac, 1978).

Leaching in a sulfate medium results in a decrease in the rate of leaching over time. This has been described by many authors as parabolic kinetics (Dutrizac, 1982; Beckstead *et al.*, 1976; Munoz *et al.*, 1979 and Dutrizac and Mac Donald, 1974). Over extended leach periods, linear kinetics were observed in sulfate media (Jones and Peters, 1976). Similar leach kinetics were observed in subsequent research by Hirato *et al.* (1987), where chalcopyrite leaching exhibited an initial parabolic kinetics, followed by linear kinetics after an extended period of time. An analysis of the leached surface, at various stages of the leach period, showed that the sulfur layer formed on the chalcopyrite surface pealed off with time, leaving behind a roughened surface. Under these circumstances the leach kinetics became linear.

Dutrizac (1978) demonstrated that the addition of cupric chloride ($CuCl_2$) during a ferric chloride leach experiment accelerated the reaction; therefor increasing the rate of reaction as the reaction proceeds. Electrochemical studies have shown that cupric chloride accepts electrons more rapidly than ferric chloride, thus enhancing the rate as the product $CuCl_2$ increases. The increasing rate enhancement opposes the rate retardation caused by the electron transfer slowing down between Fe^{2+} and Fe^{3+} ions as the reaction proceeds (Parker *et al.*, 1981).

2.6 FACTORS AFFECTING THE RATE OF FERRIC LEACHING

The rate of chalcopyrite ferric leaching in a sulfate medium decreases with time. (Beckstead *et al.*, 1976; Dutrizac, 1981 and Munoz *et al.*, 1979). The rates have been found to be strongly dependent on the following factors:

a) Temperature

b) Surface area

c) Redox Potential

Other parameters such as pH and ferric-iron concentrations have been considered to be a weaker function of leaching rate (Dutrizac, 1981 and 1978, Munoz *et al.*, 1976).

The effect of each of these factors on the leach kinetics will be discussed in detail in this section. Since the focus within this research group is to establish leach kinetics at constant redox potential, previously published data on the effect of redox potential on leach kinetics has been re-evaluated and reported in Chapter Three. However, a brief description of the effect of redox potential on ferric leach kinetics has been outlined in this section.

2.6.1 Effect of Temperature on Leaching

The rates of copper extraction have been reported to increase with an increase in temperature (Dutrizac, 1982 and 1978; and Munoz *et al.*, 1979). The effect of temperature on copper extraction is illustrated in Figure 2.2

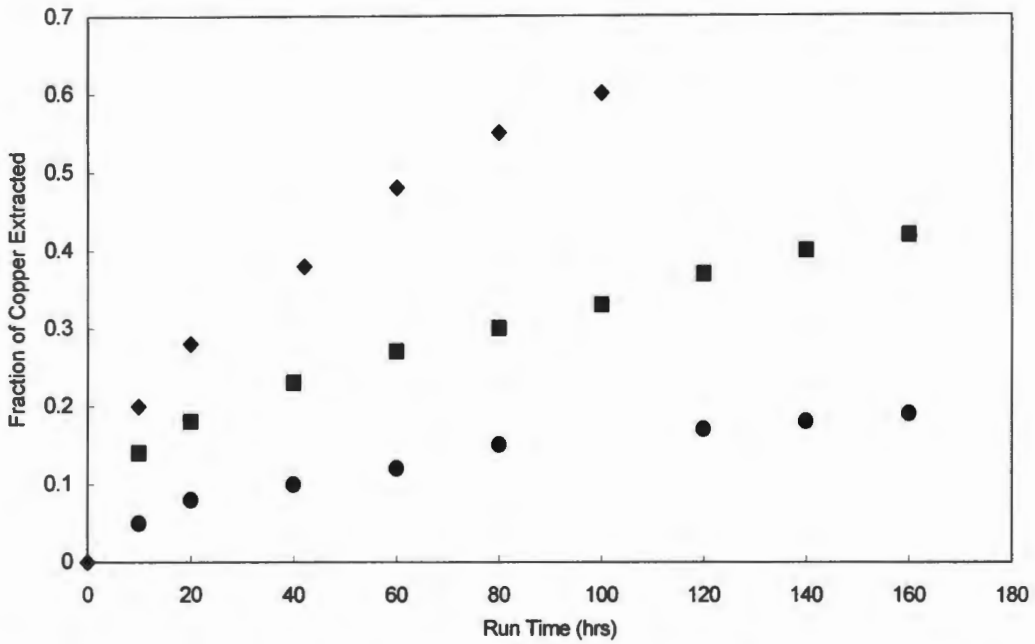

Figure 2.2: Reworked plot of copper extraction from monosized chalcopyrite using 1.0M H_2SO_4, 0.25M $Fe_2(SO_4)_3$, 0.5 pct solids and 1200 rpm. [Munoz *et al.*, 1979] [◆] 90° C; [■] 75 °C; [●] 60 °C

Most studies cover a temperature range of up to 150°C. A study on the effect of temperature on chalcopyrite leaching showed a significant increase in the rate of copper extraction above 120°C. This has been attributed to the melting of the protective sulfur coating formed around the chalcopyrite particle (Braithwaite and Wadsworth, 1976). The authors also reported a difference in activation energies at temperatures below the melting point of sulfur of (22.2kcal/mol) and (8.9kcal/mol) above melting point of sulfur, indicating a shift in mechanism from diffusion control to reaction control. It appears that an increase in temperature limits the extent of passivation, and a higher copper extraction is thus obtained.

2.6.2 Effect of Particle Size on Leaching

Due to the refractory nature of the chalcopyrite mineral, fine grinding of the mineral promotes rapid chalcopyrite leaching. Higher rates of leaching were reported for

smaller particles (Munoz *et al.*, 1979; Beckstead *et al.*, 1976 and Dutrizac, 1981). Fraction of copper extracted at various size fractions is illustrated in Figure 2.3.

Research by Jones and Peters (1976) showed that the rate of chalcopyrite leaching is independent of the particle size. However, this finding has not been supported by other researchers, it is not known why they did not observe an area dependency for the rate of chalcopyrite leaching.

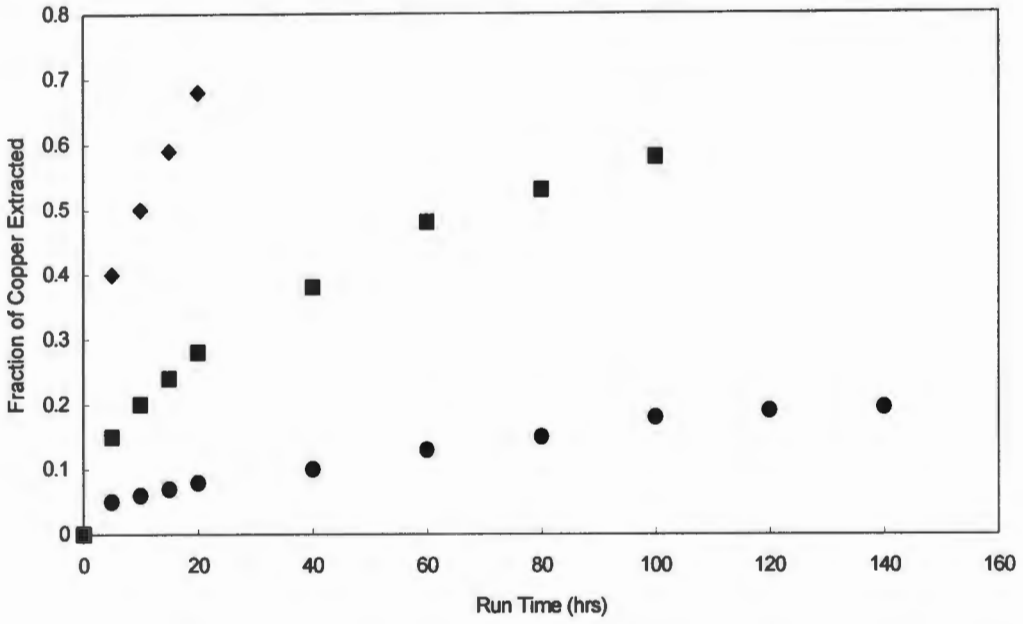

Figure 2.3: Reworked plot of copper extraction from monosized chalcopyrite using 1.0M H_2SO_4, 0.25M $Fe_2(SO_4)_3$, 0.5 pct solids and 1200 rpm. [Munoz *et al.*, 1979] [◆]4μm; [■] 12μm; [●]47μm

The rate of copper extraction per unit area is the same for all size fractions. Assuming spherical particle and similar physical properties, a normalised extraction of copper per unit area can be calculated. The normalisation of the rate makes it easier to compare rates of leaching with other published data.

2.6.3 Effect of Mass Transfer on Leaching

The chalcopyrite leaching kinetics is independent of the stirring speeds (Dutrizac and MacDonald, 1969 as cited by Dutrizac, 1989). Adequate stirring is only required to maintain particles in suspension (Beckstead *et al.*, 1976 and Dutrizac, 1978). This implies that mass transfer does not control the rate of leaching across the liquid boundary.

2.6.4 Effect of Redox Potential on Leaching

The rate of chalcopyrite leaching is dependent on redox potential (Kametani and Aoki, 1985 and Hiroyoshi *et al.*, 2000). The published data on the effect of redox potential has been re-evaluated to establish the redox potential range within which

chalcopyrite leaching occurs. Literature has shown that chalcopyrite leaching occurs at low redox potentials; 520 to 580 mV (SHE) (Hiroyoshi *et al.*, 2000) and 550 to 700 mV (SHE) (Kametani and Aoki, 1985). A detailed description on the process of re-evaluation of published data and the results have been explained in detail in Chapter Three. The results indicated that there are variations in the redox potential range within which chalcopyrite ferric leaching occurs. A recent study by Peterson *et al.* (2001) on the thermophilc bioleaching of chalcopyrite suggested that the rate was not dependent on the redox potential but rather on a possible passivating layer. Experiments indicated enhanced leaching at redox potentials of approximately 600 mV (SHE). Their results indicated no relationship between redox potential and the stagnant and exponential phase of chalcopyrite leaching. There is a need to further investigate the effect of redox potential on the ferric leaching of chalcopyrite.

2.6.5 Effect of Galvanic Interactions on Leaching

Chalcopyrite ore usually exists as a combination of different types of sulfides. When two sulfide minerals come into contact with leaching media a galvanic cell is established. The most active mineral would be selectively corroded while the less active minerals are cathodically protected.

Natarajan (1992) recorded the interaction of chalcopyrite, sphalerite and pyrite in a bioleaching system. The measured rest potentials (E_h) in a bioleach system are as follows:

Table 2.4: Table of rest potentials of different sulfide minerals

MINERAL	mV)
Pyrite	700
Chalcopyrite	560
Sphalerite	400

The relative ease with which a mineral may be degraded depends on its rest potential. The mineral rest potential in turn depends on the nature of the mineral and the type of semi-conduction exhibited, either p-or n-type (Barrett *et al.*, 1991). Sphalerite is the most active mineral in a spalerite-pyrite-chalcopyrite concentrate and undergoes selective anodic dissolution according to the following equation:

$$ZnS \rightarrow Zn^{2+} + S^0 + 2e^- \qquad [2.10]$$

In a chalcopyrite-pyrite concentrate, chalcopyrite would be selectively leached, since it is a more active mineral than pyrite. Thus, it behaves anodically with respect to pyrite. Anodic dissolution with respect to chalcopyrite can be expressed as follows:

$$CuFeS_2 \rightarrow Cu^{2+} + Fe^{2+} + 2S^0 + 4e^- \qquad [2.11]$$

The rate of chalcopyrite dissolution can be accelerated in the presence of pyrite. The coupled chalcopyrite-pyrite systems have shown improved copper metal dissolution than when leaching a single mineral (Natarajan, 1990). A number of factors such as temperature, the relative surface area of the anodic and cathodic minerals and the

efficiency of contact between the mineral will affect galvanic interactions between the mineral. The reaction conditions such as pH, conductivity, oxygen concentration and the presence of other redox species, also play a role in galvanic interaction (Natarajan and Iwasaki, 1985). The galvanic interaction of minerals existing in an ore shows that corrosion can only occur once the applied potential exceeds the rest potential.

2.6.6 Effect of pH on Leaching

It has been reported that acid may play a role in the initial attack of mineral in a leaching process (Dutrizac, 1989). This is supported by the polysulfide leaching mechanism for chalcopyrite bioleaching proposed by Schippers and Sand (1999), which involves an acid and ferric attack on the mineral. In a BIOX® process the optimal pH for the bioleach is between 1.2 and 2 (Dew *et al.,* 1997).

Previous research has shown that acid concentration has a negligible effect on the rate of chalcopyrite leaching in a ferric sulfate leach system (Dutrizac and MacDonald, 1974). However, sufficient acid concentration (>0.1M) should be present to maintain a low pH in the system, in order to prevent iron hydrolysis and precipitation at low temperatures (Dutrizac and MacDonald, 1974; Dutrizac, 1981 and Munoz *et al*, 1979).

As opposed to the negligible effect of pH on the ferric-iron leach system, a recent study on the effect of pH in a ferrous sulfate system indicated that the rate of chalcopyrite leaching in a ferrous sulfate medium is strong function of pH (Hiroyoshi *et al.*, 1997). In a ferrous sulfate system the amount of copper extracted increases with decreasing pH. Experiments conducted at initial pH of 4 and 1 showed a significant increase in copper extraction at the lower pH.

There is a need to establish the effect of acid during the initial phases of the leaching process and quantify it in terms of the ferric leaching.

2.6.7 Effect of Ferric- Iron Concentration on Leaching

The rate of chalcopyrite leaching is nearly independent of the ferric concentration above a concentration of 0.01M (Munoz *et al.*, 1979; Dutrizac, 1981 and Hirato *et al.,* 1987). At lower ferric concentrations there is considerable disagreement on the range within which the rate of leaching is dependent on the ferric-iron concentration. Half-order leach rate dependency on the ferric-iron concentration was observed within the initial phases of ferric sulfate leaching (Munoz *et al.,* 1979). Table 2.5 summarises the literature findings on the effect of ferric-iron on leach kinetics.

Table 2.5: The effect of ferric-iron on the rate of leaching reaction

AUTHOR	RANGE	RATE OF FERRIC LEACHING
Jones and Peters (1976)	0.03–1M	Increase in rate up to 1M Rate inhibition beyond 1M
Munoz *et al.* (1979)	0.06–0.5M	Rate α $[Fe^{3+}]^{0.5}$ for initial reaction phase rate independent for $[Fe^{3+}]$
Dutrizac (1981)	0.01–2M	Rate α $[Fe^{3+}]^{0.12}$ for entire reaction
Hirato *et al.*, (1987)	0.001–1M	rate α $[Fe^{3+}]$ up to 0.1M

2.7 PRODUCT LAYER PASSIVATION

Chalcopyrite leaching in a sulfate medium results in a decrease in the rate of leaching with time. This has been attributed to the formation of a reaction product on the mineral surface that hinders further leaching. The cause of passivation during chalcopyrite leaching is still under considerable debate. Literature has presented a number of possibilities concerning the nature of the passivating layer. In most studies the nature of these films has been identified using detailed surface analysis of the leached chalcopyrite surface by Scanning Electron Microscopy, SEM, coupled with X-ray diffraction analysis, X-ray Photoelectron Spectroscopy, XPS or Auger Electron Spectroscopy, AES.

Both XPS and AES are excellent analytical tools for surface analysis. AES penetrates to a few atomic layers thick (20 to 50A°) and is more surface sensitive than XPS, which penetrates to a depth of up to 25nm. AES provides elemental information, whereas XPS has the added capability of providing chemical state information.

2.7.1 Characteristics and Composition of the Passivating Layer

Both surface studies and electrochemical methods have been performed to investigate the passivating layer formed during the ferric leaching of chalcopyrite. Different theories on the role and nature of the passivating layer have been suggested. The film has the following possible effects:

1. It slows the rate of transfer of attacking oxidant species or ions from the bulk electrolyte to the chalcopyrite reaction surface.
2. It slows the rate of transfer of electrons and product ions and species from the reacting surface to the bulk electrolyte.
3. It slows the rate of the electron transfer to the oxidant in the bulk electrolyte.
4. It allows the transfer of ions from the electrolyte to the surface, or, visa versa,
5. It entirely coats the surface and prevents the attacking oxidants from contacting the active chalcopyrite surface

Table 2.6: Summary table of passivating layer and its effect on ion, electron and species transport during the ferric leaching of chalcopyrite presented by previous workers

AUTHOR	NATURE OF LAYER	EFFECT ON TRANSPORT
Jones and Peters (1976) Dutrizac (1978); Munoz *et al.*, (1979); Duitrizac, (1989) Hirato *et al.* (1986)	Porous sulfur	1 or 2 or 3 or 5
Braithwaite and Wadsworth (1976), Duitrizac, (1978)	Iron precipitates like hematite or jarosite and sulfur	1 or 2 or 3 or 5
Tiwari *et al.*, (1980), Parker *et al.*, (1981)	A semiconducting iron deficient polysulfide like covellite or chalcocite or bornite	1 or 2 or 3
Warren *et al.*, (1982), Biegler and Horne, (1985) Hackl *et al.*, (1995) Holliday and Richmond (1990)	Two iron deficient polysulfide layers of differing nature like CuS and Cu_2S	1 or 2 or 3

Most authors claim that the decreasing rate of leaching with time observed in ferric sulfate leaching is caused by a diffusion limitation of ions through a dense, tenacious sulfur layer formed at the chalcopyrite surface (Dutrizac, 1978 and 1989 and Munoz *et al.*, 1979). These leach experiments were performed at various leach times of up to 100 hours. Over extended leach periods of up to 55 days Jones and Peters (1976) observed the formation of elemental sulfur only on certain fissures or grain boundaries. A subsequent study, on the morphology of the surface using SEM and Electron Probe Microanalyser analysis on leached surfaces over periods of up to 30 days, showed that the elemental sulfur formed on the aggregates becomes partly peeled off from the surface, leaving a roughened surface (Hirato *et al.*, 1987). Under such circumstances the leaching rates became linear (Hirato *et al.*, 1987 and Jones and Peters, 1976).

Further supporting evidence of passivation by a sulfur layer was demonstrated by Munoz *et al.* (1979). In their study, the activation energy for the reaction, 83.7 kJ/mol, was approximately the same as that for transport of electrons through elemental sulfur, 96 kJ/mol, calculated from conductivity and electron mobility measurements. Using the Wagner theory of oxidation they argued that the rate-limiting step is the transport of electrons through the elemental sulfur layer, corresponding to the two-half reactions

Anodic: $$CuFeS_2 \rightarrow Cu^{2+} + Fe^{2+} + 2S + 4e^- \quad [2.12$$

Cathodic: $$4Fe^{3+} + 4e^- \rightarrow 4Fe^{2+} \quad [2.13$$

The Wagner theory of oxidation is based on the formation of a protective sulfur layer during leaching, with the leach rate limited by the transport of electrons through the

insulating sulfur layer. The model was supported by kinetic data. Slow parabolic reaction kinetics were predicted by the Wagner's theory of oxidation, which relates the electrical conductivity of the elemental sulfur reaction product to the rate of reaction. The predicted reaction rate, calculated from physiochemical properties of the reaction system, indicated good agreement with the experimentally determined rates. A schematic representation of the transport of electrons through sulfur layer is illustrated in Figure 2.4

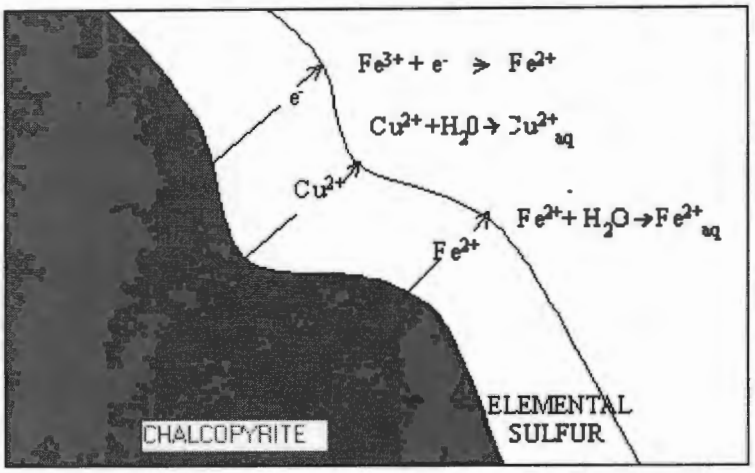

Figure 2.4: Acid ferric sulfate leaching of chalcopyrite – rate control by electronic transport through elemental sulfur reaction product layer [Munoz *et al.*, 1979].

A significant increase in leaching rates was observed by the addition of silver ions, which activate the chalcopyrite surface (Miller and Portillo, 1979). The layer of silver sulfide formed on the chalcopyrite surface prevents the direct formation of elemental sulfur on chalcopyrite. The elemental sulfur formed on the Ag_2S crystallites formed a non-porous sulfur layer.

The catalytic effect of silver is attributed to the formation of conductive compounds such as Ag_2S. The conductive compound in the coating barrier neutralises its passivation effect by acting as a channel for electron flow through the barrier (Rossi, 1990). A detailed analysis of the mechanism involved in the use of silver for chalcopyrite oxidation is discussed in a later section.

Parker *et al.* (1981) rejected the argument of passivation caused by the build up of sulfur, based on the fact that extensive formation of sulfur during ferric chloride leaching of chalcopyrite had a negligible effect on the leach kinetics. In a recent study, SEM analysis on leached chalcopyrite residue indicated the formation of a more crystalline and porous sulfur product on chalcopyrite leached in a chloride medium than a sulfate medium (Lu *et al.*, 2000). The authors suggest that the presence of chloride ions in solution fosters the formation of a much more porous sulfur layer, thus in a chloride system negligible passivation was observed because

the porosity of the sulfur layer permits the diffusion of reactants through the sulfur product film.

Linge (1976) proposed that the processes inside the chalcopyrite lattice are the slow steps in oxidation and pore diffusion is not the rate limiting step, thus rejecting sulfur as a possible passivating substance.

Electrochemical studies on the behaviour of chalcopyrite provide additional insight into the passivation phenomenon. The effect of oxidation products on the potentiostatic oxidation of chalcopyrite under ferric sulfate, ferric chloride and cupric chloride solutions were investigated. Data from these studies tend to support a second passivation theory; that the passivating layer is a compact, intermediate sulfide layer, and dispelled the long held understanding that passivation was due to sulfur formation.

During anodic dissolution, there is an initial preferential release of iron from the chalcopyrite lattice, to form an copper-rich polysulfide layer on the chalcopyrite surface (Warren *et al.,* 1982 and Linge, 1976). Formation of this intermediate was supported by AES results, which demonstrate that the ratio of Cu/Fe, on surfaces less than 1μm, was approximately 1.6 (Hackl *et al.,* 1995). The following mechanism is proposed at low potential between 500 to 700 mV:

$$CuFeS_2 \rightarrow Cu_{1-x}Fe_{1-y}S_{2-z} + xCu^{2+} + yFe^{2+} + zS^{\circ} + 2(x+y)e^{-} \qquad [2.14]$$

The intermediate defect structure of $Cu_{1-x}Fe_{1-y}S_{2-z}$ (S_1) decomposes further to form a second intermediate CuS_n. These are proposed to be bornite and covellite respectively (Warren *et al.*, 1982). This intermediate polysulfide has been referred to as a metal-deficient polysulfide with semi-conductor properties different to chalcopyrite (Parker *et al.,* 1981; Tiwari *et al.,* 1980; Warren *et al.,* 1982; Linge, 1976 and Ammou-Chokrum *et al.*, 1981). It was proposed that this layer grows at the chalcopyrite surface through a mechanism of solid-state diffusion of the cation at different rates (Burkin, 1969, Parker *et al.,* 1981 and Ammou-Chokrum *et al.,* 1981). The polysulfide layer was thought to slow the transport of ions and electrons during the leaching process (Parker *et al.,* 1981).

Hiroyoshi *et al.* (2000) used gibbs free energy to support the formation of Cu_2S as an intermediate. They proposed that the chalcocite oxidises easier than chalcopyrite resulting in the enhanced copper extraction by the oxidation of chalcocite to copper (II) ions in the presence of oxygen and ferrous-irons. However, analytical techniques were not used to confirm the presence of this intermediate.

Ammou-Chokroum *et al.* (1981) proposed that the rate of dissolution is governed by the formation of a compact diffusion layer and that the outer sulfur layer is porous enough not to be rate limiting. Ammou-Chokroum *et al.* (1981) performed electrochemical oxidation studies on chalcopyrite in acid chloride medium. However, recent studies by Lu *et al.* (2000) suggests that the sulfur layer formed during chloride leaching is more porous than the sulfur layer formed during leaching in sulfate medium. Therefore, in a sulfate medium, sulfur can not be discarded as a

possible passivating layer since the sulfur layer is not as porous as that formed during ferric chloride leaching.

Braithwaite *et al.*, (1976) using SEM, analysis on leached samples suggested that hematite and sulfur where the compositions of the passivating layer.

In recent publications, Klauber *et al.* (2001) and Parker *et al.* (2001) carefully used XPS analysis of leached chalcopyrite surfaces to predict the possible passivating species. The XPS analysis was conducted carefully at low temperatures to minimise the loss of volatile species from the surface. This was done because the ultrahigh vacuum used during the XPS surface analysis procedure, will evaporate the bulk elemental sulfur unless the surface is maintained at temperature below 200K (Smart *et al.*, 1999). Chemical leach experiments were conducted over a short period of time using both ferric and ferrous sulfate media at a temperature of 50°C and pH of 1.5 (Klauber *et al.*, 2001). Only elemental sulfur was identified as a possible passivating layer. Neither metal-deficient sulfide nor polysulfides were identified as major surface layer components during initial leaching. More elemental sulfur was observed on chalcopyrite leach surfaces that were leached in ferric sulfate medium. The authors suggest that other researchers might have overlooked the possibility of sulfur as a passivating agent, due to experimental techniques used.

Subsequent leach experiments were conducted under bioleach and chemical leach conditions over an extended period of time, and the findings were presented in a paper by Parker *et al.* (2001). Elemental sulfur, pyritic disulfide and ferric hydroxy sulfate were identified on leached surfaces. An independent study on the reactivity of polysulfides indicated that polysulfides were extremely reactive and could not be considered as a stable surface species. Ferric hydroxy sulfate is a precursor to jarosite formation, and has been identified as the passivating layer during ferric leaching. Bulk precipitation of jarosite was observed on chemical and bioleached surfaces over an extended leach period, and ferric hydroxy sulfate was observed as a precursor to jarosite on chemically leached surface over a shorter period of time.

The theory of the build up of jarosite or iron-sulfur compounds as a possible passivating layer was further supported by copper and iron analysis performed on chalcopyrite bioleaching experiments at 70°C in airlift and stirred tank reactor (Peterson *et al.*, 2001).

Based on these different theories, it is difficult to conclude which of these passivating layers are indeed present during the acidic ferric sulfate leaching of chalcopyrite. The nature of the mineral and the presence of encrustation of sulfates and flotation reagent residues, as revealed by XPS analysis, may contribute further to the decrease in leaching rates (Rossi, 1990). In the recent 2000/2001 annual report by AJ Parker Coorporate Research Centre for Hydrometallurgy, it is reported that initial results suggested that different chalcopyrite leaching behaviour arise between n and p- type conducting chalcopyrite. Further work is currently in progress to establish if the semiconductor properties of the chalcopyrite effect the nature of the passivating layer.

2.7.2 Factors Affecting the Formation of Passivating Layer

Various factors such as redox potential, temperature and pH have been proposed to have an effect on the formation of the passivating layer. The effects of these factors are discussed in this section.

Effect of potential

Anodic polarisation studies performed on chalcopyrite electrodes have revealed the existence of a passive region within which the current is constant, with increasing potential. Potential ranges between the approximate rest potential of mineral and 900mV (SHE) have been identified as passive regions for any of the proposed passivating layers, such as bornite and covellite (Warren *et al.*, 1982, Holiday and Richmond, 1990 and Parker *et al.*, 1981). At higher potentials, chalcopyrite oxidises completely to Cu^{2+} and Fe^{3+}, due to the greater amount of material forced to dissolve by the higher current resulting from the higher potential (Warren *et al.*, 1982 and Gomez *et al.*, 1996).

Kametani and Aoki (1985) found incomplete chalcopyrite oxidation within the redox potential ranges of 515 to 545 mV (SHE). The XRD analysis of leach residue indicated the presence of CuS within this redox potential region. Complete oxidation to elemental sulfur at higher potentials between 585 to 645 mV (SHE) was observed. Based on literature, these intermediates act as passivating layers during chalcopyrite leaching. Therefore it is necessary to operate at an optimal redox potential range in order to minimise the effect of passivation.

Effect of temperature

The passivating layer is thermally unstable and breaks down at higher temperatures (Braithworth and Wadsworth, 1976; Hackl *et al.*, 1995 and Parker *et al.*, 1981). Parker *et al.* (1981) proposed that the polysulfide was thermally unstable and decomposed to form sulfur and lesser polysulfides when heated from 25°C to 80°C. Hackl *et. al.* (1995) proposed that at higher temperatures the yield of sulfur decreases with little or no sulfur formed at temperatures higher than 200°C, indicating that the sulfur layer formed is thermally unstable and that the sulfur chain fragments and oxidises to sulfate before forming S_8 rings.

Effect of pH

Gomez *et al.* (1996) observed that pH had no effect at room temperature, but that at a higher temperature of 68°C, the more acidic medium hampered the mineral oxidation by increasing the potential range of the passive region. However, this behaviour has not been reported by other researchers.

2.7.3 Mechanism for the Passivating Layer Formation

Two mechanisms for the build up of a passivating layer have been proposed. These include the formation of a metal deficient polysulfide layer or the formation of a ferric hydroxy sulfate.

Several authors support the theory of the formation of a polysulfide layer, which acts as a passivating layer during chalcopyrite leaching (Warren *et al.,* 1982, Parker *et al.,* 1981 and Hackl *et al.,* 1995). Under these circumstances, the generalised equations for the formation and dissolution of the passivating polysulfide layer, have been expressed by Hackl *et al.,* (1995) according to the following equations:

$$CuFeS_2 \rightarrow Cu_{1-x}Fe_{1-y}S_2 + cCu^{2+} + yFe^{2+}\ 2(x+y)e^- \quad [2.15]$$

$$Cu_{1-x}Fe_{1-y}S_2 \rightarrow\ + Cu_{1-x-z}S_2 + zCu^{2+} + (1-y)Fe^{2+} +\ 2(z+1-y)e^- \quad [2.16]$$

$$Cu_{1-x-z}S_2 \rightarrow (1-x-z)Cu^{2+} + 2S^{\circ} + 2(1-x-z)e^- \quad [2.17]$$

In the instance that covellite is assumed to be the intermediate, the following reactions can be developed for the formation and dissolution of the intermediate. These include the ferric leaching of chalcopyrite itself, the formation of a possible polysulfide and the further decomposition of the polysulfide layer.

Initial ferric leaching takes place according to the following possible reactions:

$$CuFeS_2 + 2Fe^{3+} \rightarrow Cu^{2+}\ 5Fe^{2+} + 2S^0 \quad [2.18]$$

$$CuFeS_2 + 16Fe^{3+} + 8H_2O \rightarrow Cu^{2+} + 17Fe^{2+} + 2SO_4 + 8H^+ \quad [2.19]$$

$$CuFeS_2 + 2Fe^{3+} \rightarrow CuS + 3Fe^{2+} + S^0 \quad [2.20]$$

The assumed rate determining step could be the ferric leaching of the polysulfide film followed by its decomposition

$$CuS + 2Fe^{3+} \rightarrow Cu^{2+} + 2Fe^{2+} + S^0 \quad [2.21]$$

$$CuS \rightarrow Cu^{2+} + 2e^- + S^0 \quad [2.22]$$

Recent publication by Parker *et al.* (2001) proposed the following mechanism for chalcopyrite leaching based on their XPS analysis study. The copper (I) in the chalcopyrite in the presence of oxygen forms cuprous oxide according to the following reaction:

$$Cu_2O + 2H^+ \rightarrow 2Cu^{2+} + H_2O + 2e^- \quad [2.23]$$

The disulfide dimer (S_2^{2-}) undergoes acidic dissolution according to the following reactions:

$$Fe-S-S\ + H^+ \rightarrow\ Fe-S-SH^+ \quad [2.24]$$

$$Fe-S-SH^+ + H^+ \rightarrow\ Fe-S^{2+} + H_2S \quad [2.25]$$

Then the ferric leaching of the pyritic sulfide occurs according to following reaction:

$$FeS_2 + 6Fe^{3+} + 3H_2O \rightarrow\ 7Fe^{2+} + S_2O_3^{\ 2-} + 6H^+ \quad [2.26]$$

The thiosulfate undergoes further oxidation to produce elemental sulfur, polythionate and sulfate according to the following equations:

$$8S_2O_3^{2-} + H^+ \rightarrow S_8 + 7SO_3^{2-} + HSO_3^- \quad [2.27]$$

$$2S_2O_3^{2-} + 2Fe^{3+} \rightarrow 2Fe^{2+} + S_4O_6^{2-} \quad [2.28]$$

$$S_4O_6^{2-} + SO_3^{2-} \rightarrow S_3O_6^{2-} + S_2O_3^{2-} \quad [2.29]$$

$$HSO_3 + \tfrac{1}{2}O_2 \rightarrow SO_4^{2-} + H^+ \quad [2.30]$$

2.8 ENHANCEMENT OF LEACH KINETICS

Different methods have been developed to enhance the chalcopyrite leach kinetics. These include the use of external agents such as silver ions and carbon particles as well as the use of ferrous-iron which act as an auto-catalytic process. The different leach rate enhancement mechanisms have been discussed in this section.

2.8.1 Use of Silver Ions

A strategy designed to increase chalcopyrite leaching rates is the addition of silver (catalytic) ions. The catalytic mechanism for silver ion is as follows:

$$CuFeS_2 + 4Ag^+ \rightarrow 2Ag_2S_{(\text{surface of chalcopyrite})} + Cu^{2+} + Fe^{2+} \quad [2.29]$$

$$Ag_2S_{(\text{surface of chalcopyrite})} + 2Fe^{3+} \rightarrow 2Ag^+ + 2Fe^{2+} + S^o \quad [2.30]$$

SEM analysis of silver catalysed leached samples indicated very porous well defined sulfur crystallites. The uncatalysed reaction indicated a smooth tenacious layer of elemental sulfur (Miller and Portillo, 1979). The electrochemical reaction (Equation 2.30) occurs at the surface of silver sulfide crystallite. Elemental sulfur replaces the Ag_2S crystallite, forming a porous, non-protective layer. The silver ion acts as a transfer agent while the silver sulfide film, which is constantly restored, prevents extensive sulfur formation at the chalcopyrite surface.

2.8.2 Using $CuFeS_2$/C aggregates

The rate of copper dissolution from aggregates of $CuFeS_2$ and C can be enhanced by the presence of conductive carbon particles. Intimate mixing and pressing of the mixture forms the $CuFeS_2$/C aggregates. The SEM analysis indicated that the sulfur product layer formed on leached chalcopyrite surfaces differed significantly in structure to that formed in the absence of carbon. The addition of particles of carbon alters the structure of sulfur, and facilitates the transport of electrons through the sulfur-product layer. The addition of carbon to solid sulfur increases the conductivity in comparison to pure sulfur (Wan *et al.*, 1984[b]).

$CuFeS_2$/C aggregates form a galvanic coupling, so that electron transfer would be part of a mechanism of galvanic corrosion, in which carbon would act as a cathode, allowing the reduction of Fe^{3+} ions (Wan *et al.*, 1984[a]).

2.8.3 Ferrous-Promoted Leaching

Hiroyoshi *et al.* (2000), proposed that the oxidative leaching of chalcopyrite with dissolved oxygen and ferric- iron ions is promoted by the presence of high concentrations of ferrous-iron and cupric ions. This is an autocatalytic process, which does not require an external promoter to increase chalcopyrite leaching. The authors proposed the following model for ferrous-iron promoted chalcopyrite leaching. Chalcopyrite leaching proceeds via an intermediate :

$$CuFeS_2 \rightarrow Cu_2S \rightarrow Cu^{2+} \qquad [2.32]$$

The chalcopyrite leaching proceeds via two steps:

1). Reduction of chalcopyrite to Cu_2S by ferrous-iron in the presence of cupric ions.

$$CuFeS_2 + 3Cu^{2+} + 3Fe^{2+} \rightarrow 2Cu_2S + 4Fe^{3+} \qquad [2.33]$$

2) Oxidation of Cu_2S to cupric ion and elemental sulfur.

$$2xCu_2S + 8xH^+ + 2xO_2 \rightarrow 4xCu^{2+} + 2xS + 4xH_2O \qquad [2.34]$$

$$2(1-x)Cu_2S + 8(1-x)Fe^{3+} \rightarrow 4(1-x)Cu^{2+} + 2(1-x)S + 8(1-x)Fe^{2+} \qquad [2.35]$$

Thermodynamics were used to prove the steps in this reaction. They however did not perform XRD analysis to confirm the possibility of the formation of Cu_2S. Chalcopyrite leach experiments indicated enhanced copper extraction at low redox potentials between 520 to 580 mV (SHE). At higher redox potentials, the rate of copper extraction decreases because of the low ferrous-iron concentration.

All these processes have indicated enhanced copper extraction from chalcopyrite, ferrous-promoted chalcopyrite leaching is more favourable, since it is an autocatalytic process which does not require external agents to increase copper extraction. Further, experiments are required to confirm the viability of this mechanism.

2.9 MEASURING THE RATE OF FERRIC LEACHING

Several methods have been applied to measure the rate of chalcopyrite leaching. The simplest method involved developing the rate of leaching based on the amount of copper extracted during the leach experiment. This method did not take into consideration the electrochemical nature of leaching sulfide minerals. The more effective methods have taken this into consideration and developed techniques of measuring the rate of ferric leaching using dynamic or constant redox potential methods.

In the dynamic leaching method, the redox potential drops during the leaching and is measured on line. In the static method, the redox potential is kept constant during

the leaching reaction. It is expected that at a constant redox potential, a better control of the reaction kinetics can be obtained, since it takes into account the difference in potential between the mineral and leach solution. The details of available methods are discussed in this section.

2.9.1 Dynamic Redox Potential

A dynamic redox method was established to determine the rate of leaching of pyrite and arsenopyrite respectively. The redox potential behaviour can be related to a rate leaching of the mineral using the Nernst equation, Equation 2.2, which is differentiated to give an expression for rate as follows (May *et al.*, 1997):

$$r_{FeS_2} = \frac{\frac{zF}{RT}\frac{dE}{dt}}{\frac{(3n+2)}{[Fe^{3+}]} + \frac{(3n+3)}{[Fe^{2+}]}} \text{.....mol.l}^{-1}\text{.s}^{-1} \qquad [2.36]$$

When n = 0 there is formation of sulfur and a value of n = 4 indicates formation of sulfate. The redox potential is the key variable, which is used to determine the rate of leaching.

2.9.2 Constant Potential Methods

Oxidation in suspension differs in some respects from an electrode reaction in that it is not possible to measure the potential difference between the suspended particles and the solution directly. This makes it difficult to compare leaching reactions and electrode processes directly (Kametani and Aoki, 1985). At the same time the semi-conducting properties of pulverised minerals vary during oxidation (Kametani ,1982, as cited by Kametani and Aoki, 1985). The problem of difference in suspension potential can be partially overcome by conducting experiments at a constant redox potential.

The maintenance of a constant redox potential can be achieved by the use of an externally applied current (Crundwell and Harvey, 1997) or the use of an oxidising agent (Kametani and Aoki, 1985).

Crundwell and Harvey (1997) used an electrolysis cell divided into two sections by an ion exchange membrane with leaching experiments being carried out in one of the compartments. By changing the current to the cell the redox potential in the leaching compartment was controlled. The current was measured by the potential difference across a precision resistor. The redox potential was controlled within 1.0 mV of the set point.

This method offers very elaborate control over the applied potential. It seems to be limited by increased solids loading. The shape of the reaction vessel would not allow effective suspension of the solid particles, which is essential to prevent mass transfer limitation of the rate of leaching.

Kametani and Aoki (1985) conducted experiments in a one-litre reaction vessel. The suspension potential was measured using a rotating platinum electrode with a reference electrode. A controller regulated the addition of potassium permanganate solution so as to maintain the desired potential.

The constant potential method provides the most reliable way of monitoring the rate since it can overcome the potential difference between the solution and the suspended particles. This method offered the greatest versatility in terms of varying operating conditions and simplicity in operation.

2.10 MODELLING FERRIC LEACH KINETICS

Chalcopyrite leaching exhibits two regions of leaching; initial chemical control and diffusional control of the rate. For a spherical particle, in which the reaction rate is controlled by the transport through the reaction product layer, the following relationship between fraction extracted (α) with time was developed (Munoz *et al.*, 1979 and Beakstead *et al.*, 1976):

$$F(\alpha) = 1 - \tfrac{2}{3}\alpha - (1-\alpha)^{\frac{2}{3}} = k_p t \qquad [2.38]$$

Kametani and Aoki (1985) reported that chalcopyrite leaching is reaction controlled and presented the following model:

$$1 - (\alpha - 1)^{\frac{1}{3}} = k_r t \qquad [2.39]$$

The shrinking core models do not take into consideration the electrochemical nature of the leaching sulfide mineral. There is increasing evidence that leaching is dependent on the redox potential (Warren *et al.*, 1982 and Kametani and Aoki, 1985). Electrochemical theories are currently being used to model the sulfide mineral leach kinetics, these have been discussed in the following section.

The simplest electrochemical model assumes a linear relationship between the solution redox potential and mineral rest potential (Nagpal *et al.*, 1994). More comprehensive models are based on the Butler-Volmer equation for corrosion reactions, limited by charge transfer at the interphase. The Butler- Volmer equation for a simple electron transfer reaction is represented by the following equation:

$$i = i_o\left(\exp\left(\frac{(1-\alpha)F\eta}{RT}\right) - \exp\left(\frac{-\alpha F\eta}{RT}\right)\right) \qquad [2.40]$$

The value η is the over potential, which is the difference between the equilibrium potential and applied potential. α is the transfer coefficient and is an intrinsic characteristic of the large-transfer reaction and determines what fraction of the electrical energy results from the displacement of the potential from equilibrium effects the rate of electrochemical transformation. The values η and α determine the relationship between the rate of the charge transfer reaction and the potential

difference across the interface. The symmetry factor for the reduction of ferric-iron at a platinum electrode has been shown to be 0.58 (Bockris and Reddy, 1970).

May (1997) reported a version of the Butler-Volmer equation that could be used to determine rate directly:

$$r = r_o\left(\exp(\alpha\beta(E-E^\circ) - \exp((1-\alpha)\beta(E-E^\circ)\right) \quad [2.41]$$

Subsequently, Holmes and Crundwell (1999) developed a rate expression for the dissolution of pyrite. Based on the observation that dissolution of pyrite is dependent on the redox potential and concentration of H^+, the following expression was developed for the current density due to dissolution of pyrite:

$$i_{FeS_2} = k_{FeS_2}[H^+]^{\frac{1}{2}}\left(\exp(\frac{\alpha_{FeS_2}FE}{RT}\right) \quad [2.42]$$

An expression for the rate of leaching of pyrite was developed:

$$r_{FeS_2} = \frac{k_{FeS_2}[H^+]^{\frac{1}{2}}}{14F}\left(\frac{k_{FeS_2}[Fe^{3+}]}{k_{FeS_2}[H^+]^{\frac{1}{2}} + k_{Fe^{2+}}[Fe^{2+}]}\right) \quad [2.43]$$

Chalcopyrite leaching undergoes various phases during the leaching, making it difficult to model chalcopyrite leach kinetics to an electrochemical model. There has not been any evidence of the use of electrochemical theories to model chalcopyrite leach kinetics.

2.11 THE CURRENT UNDERSTANDING OF CHALCOPYRITE FERRIC LEACHING

Ferric leaching of chalcopyrite in a sulfate medium has been reported to exhibit an initial chemical control regime followed by a diffusion controlled regime. The decrease in rate has been attributed to the formation of a passivating layer on the mineral surface, which hinders further leaching. Different explanations have been offered for the decrease in the rate of leaching. These include:

- Formation of elemental sulfur on the surface
- Formation of a metal-deficient polysulfide layer
- Formation of jarosite

The nature of the passivating layer is still under considerable debate. However, recent publications by Klauber *et al.* (2001) and Parker *et al.* (2001) have shown that during the different time periods of acidic chemical and bioleaching, different passivating layers are formed. Parker *et al.* (2001), performed careful XPS analysis and demonstrated that ferric hydroxy sulfate, which is a precursor for jarosite

formation, and subsequent jarosite formation are the proposed passivating layers. In their study, neither metal-deficient polysulfides nor polysulfides were detected.

It appears that there is a possibility that the passivation substance is dependent on the nature of the mineral, solubilisation process and the operating conditions such as redox potential and temperature. Current research is underway to establish whether the semiconducting properties of chalcopyrite have an effect on the nature of the chalcopyrite leaching, hence affecting the nature of the passivating layer formed.

Electrochemical theories are currently being used to model the sulfide mineral leach kinetics. There has not been any evidence of the use of electrochemical theories to model chalcopyrite leach kinetics.

Most researchers have performed leach experiments at varying redox potentials. There is a need to take the electrochemical nature of the reaction into consideration. When the mineral comes into contact with the oxidant such as ferric iron, a corrosion cell develops which results in the anodic oxidation of the mineral and cathodic reduction of the oxidant. During the oxidation process, it is not possible to measure the potential difference between the mineral and the leach solution directly. The problem of difference in potential can be overcome by conducting experiments at constant redox potential.

The method of using potassium permanganate to maintain a constant redox potential was initially presented by Kametani and Aoki (1985). Potassium permanganate regenerates ferric-iron by re-oxidising the ferrous-iron, thus maintaining a constant redox potential. This method can be used to determine the initial rate of chalcopyrite leaching.

Experiments that have been conducted have been at higher temperatures and long leach times. There is limited literature on the initial rates of chalcopyrite leaching. There is a need to study the ferric leach sub-process at different constant redox potentials and temperatures within the range typical to the bioleach system.

Table 2.7, is a summary of the literature review on ferric leaching of chalcopyrite. It summarises the experimental conditions and the observed kinetics of chalcopyrite leaching.

Table 2.7: Summary of Literature Findings and Conditions Applied

Reference	Type of Study / Lixiviant used and Potential Ranges	$CuFeS_2$ Source and Particle Size	Temp	Fe / Cu	S_o / S_o+SO_4	Kinetics, Proposed Mechanism and Nature of Passivating Layers
Beckstead *et al.*, 1976	Ferric sulfate leach 0.25M Fe_2SO_4; 1M H_2SO_4	Pima 12μm & 47μm	50-90 °C	5	-	**Kinetics:** Parabolic - rate limited by ferric diffusion through product layer $CuFeS_2 + 4Fe^{3+} \rightarrow Cu^{2+} + 5Fe^{2+} + 2S^0$
Braithworth *et al.*, 1976	In situ ferric sulfate leach Oxygen at 40 -1620 psia. SEM and EDAX surface study	Bingham +65-100μm +200-270μm	90 °C	Vary	vary	**Kinetics:** Parabolic: Mixed reaction diffusion control with rate limitation by O_2 diffusion through product layer **Passivating Layer:** S^o and Hermatite
Jones and Peters, 1976	Ferric sulfate leach 1M $Fe_2(SO_4)_3$; 0.2M H_2SO_4	Craigmont	90°C	5	72%	**Kinetics:** Mixed, linear and then parabolic kinetics $CuFeS_2 + 4Fe^{3+} \rightarrow Cu^{2+} + 5Fe^{2+} + 2S^0$ $CuFeS_2 + 16\ Fe^{3+} + 8H_2O \rightarrow Cu^{2+} + 17Fe^{2+} + 2SO_4^{2-}\ 16H+$ **Passivating Layer:** Sulfur
	Ferric chloride leach 1M $FeCl_3$;; 0.2M HCl	Craigmont	90°C		100%	**Kinetics**: Linear with rate being 5 –20 times larger than sulfate $CuFeS_2 + 4\ Fe^{3+} \rightarrow Cu^{2+} + 5Fe^{2+} + 2S^0$

Reference	Type of Study	$CuFeS_2$ Source and Particle Size	Temp	Fe / Cu	S_o / S_0+SO_4	Kinetics, Proposed Mechanism and Nature of Passivating Layers
Dutrizac 1978	Ferric sulfate leach 0.1M $Fe_2(SO_4)_3$ leach	Temagami Lake 150-200μm 0.5-3g/l	30-95°C	5		**Kinetics**: Parabolic $CuFeS_2 + 4 Fe^{3+} \rightarrow Cu^{2+} + 5Fe^{2+} + 2S^0$ **Passivating Layer:** Sulfur and Iron precipitate
	Ferric chloride Leach 0.1M $FeCl_3$; 0.3MHCl	Synthetic	50-90 °C		96%	**Kinetics:** Linear $CuFeS_2 + 4 Fe^{3+} \rightarrow Cu^{2+} + 5Fe^{2+} + 2S^0$ No passivation
Munoz *et al*, 1979	Ferric sulfate leach 0.25M $Fe_2(SO_4)_3$; 1MH_2SO_4	Pima Slurry 4,12,47 μm	60-90°C	5	-	**Kinetics**: Parabolic - Mixed reaction diffusion control of electrons through Sulfur product layer being limiting $CuFeS_2 + 4 Fe^{3+} \rightarrow Cu^{2+} + 5Fe^{2+} + 2S^0$ **Passivating Layer**: Sulfur
Tiwari *et al*,1980	In situ ferric sulfate. Leach O_2 and SO_2 mixture XRD surface analysis	Pima	93°C	5.3	-	**Kinetics**: unspecified $CuFeS_2 + 2.16Fe_2(SO_4)_3 + 0.21H_2 \rightarrow Cu^{2+} + 5.3FeSO_4\ 1.95S^0 + 0.21H_2SO_4 +$ $2Fe^{2+} + 4 H^+ + O_2 \rightarrow 2Fe^{3+} + 2H_2O$ Cu pttn: $Cu^{2+} + S^0 + SO_2 + 2H_2O \rightarrow CuS + SO_4^{2-} + 4H^+$ **Passivating Layer:** CuS

Reference	Type of Study	$CuFeS_2$ Source and Particle Size	Temp	Fe / Cu	S_o / S_o+SO_4	Kinetics, Proposed Mechanism and Nature of Passivating Layers
Parker *et. al*, 1981	Electrochemical oxidation in ferric sulfate 0.1 - 1M $Fe_2(SO_4)_3$ Electrochemical oxidation In ferric chloride 0.5 M - 1M $FeCl_3$ Potentiostatic oxidation in chloride and sulfate media 200 to 600mV (S.C.E)	Messina, Baxter, Springs, Craigmont Used massive ore to make electrodes	80 - 90°C 25 - 85°C	-	-	**Kinetics**: parabolic - Reaction rate is diffusion controlled by the slow transport of Cu^+ and Fe^{2+} through Sp layer. For $CuFeS_2$ corrosion in 200 to 600mV range $CuFeS_2 \rightarrow Cu^{2+} + 5Fe^{2+} + 2S^0 + 4e^-$ $CuFeS_2 \rightarrow Cu^+ + Fe^{2+} + 2S^0 + 3e^-$ $CuFeS_2 + 16\ Fe^{3+} + 8H_2O \rightarrow Cu^{2+} + 17Fe^{2+} + 2SO_4^{2-} + 16H^+$ **Passivating Layer:** Semiconducting metal deficient polysulfide. Nature of Sp layer different in chloride (lower Sp) and higher Sp in sulfate media. Sp layer is more thermally stable in sulfate lixiviant as compared to chloride..
Dutrizac, 1982	Ferric sulfate leach 0.1M $Fe_2(SO_4)_3$ Ferric chloride 0.1M $FeCl_3$; 0.3M HCl	Transvaal Arizona, Quebec, Craigmont, Montana, Ontario, Manitoba, Mattagami, Kiddcreek 20-29μm,	50-95°C 50-95°C		95% 76%	**Kinetics:** Parabolic $CuFeS_2 + 8H_2O + 16\ Fe^{3+} \rightarrow Cu^{2+} + 17Fe^{2+} + 16H^+ + 2SO_4^{2-}$ **Passivating Layer:** unspecified **Kinetics**: Paralinear $CuFeS_2 + 4\ Fe^{3+} \rightarrow Cu^{2+} + 5Fe^{2+} + 2S^0$

Reference	Type of Study	$CuFeS_2$ Source and Particle Size	Temp	Fe / Cu	S_0 / S_0+SO_4	Kinetics, Proposed Mechanism and Nature of Passivating Layers
Warren *et al*, 1982	Anodic dissolution of $CuFeS_2$ in acidic media 1 M H_2SO_4 Potentiodynamic oxidation in acidic sulfate medium 500-1100 mV (SHE)	New Mexico, Ontario, Craigmont, Mt Lyle, Mt. Isa, Transvaal	25°C	vary	vary	Kinetics: Parabolic Initial reaction control with diffusional rate limitation throughout product film 500-700mV (SHE) $CuFeS_2 \rightarrow Cu_{1-x}Fe_{1-y}S_{2-z} + xCu^{2+} + Cu^{2+} + yFe^{2+} + zS^0 + 2(x+y)e^-$ For y>x For 700 –750 mV $Cu_{1-x}Fe_{1-y}S_{2-z} \rightarrow (2-z)CuS_{(n-s)} + (1-y)Cu^{2+} + (1-y)Fe^{2+} + 2(1-y)e^-$ At lower potentials less than 700mV: $CuS_{(n-s)} \rightarrow Cu^{2+} + S^0 + 2e^-$ At higher than 700mV: $CuS_{(n-s)} \rightarrow Cu^{2+} + 0.25SO_4^{2-} + 0.75S^0 + 2e^-$ **Passivating Layer**: $Cu_{1-x}Fe_{1-y}S_{2-z}$ is S1 and $CuS_{(n-s)}$ is S2. Both intermediate films are speculated to be copper sulphides
McMillan *et. al*, 1982	Sulfate, chloride, bromate, nitrate and chromate leaches and anodic dissolution of $CuFeS_2$ in acidic media 0.2 M acetic acid.	n-type Kidd Creek, Messina 20-29μm	90 °C	-	-	**Kinetics:** Parabolic in bormate media **Passivating Layer**: Solid electrolyte Interphase made up of iron deficient copper sulphide, which is electrochemically insulating but allows transfer of ionic species.
Buckley and Woods, 1984	Anodic dissolution in acidic media	Mt Lyle	25 °C	-	-	**Kinetics:** unspecified **Passivating Layer:** Metal deficient copper disulphide $Cu_{1.1}FeS_{2.8}$ from acetic acid exposure

Reference	Type of Study	$CuFeS_2$ Source and Particle Size	Temp	Fe / Cu	S_0 / S_0+SO_4	Kinetics, Proposed Mechanism and Nature of Passivating Layers
Beigler and Horne , 1985	Anodic dissolution of $CuFeS_2$ in acidic media 1M HCl, 1M $HClO_4$; 1M HNO_3, 1M H_2SO_4 Potentiodynamic oxidation in acidic media	Mt. Lyle And Moonta	25°C	Vary initial stages 2 – 6.6	100%	Step 1: Anodic dissolution: $CuFeS_2 \rightarrow Cu_aFe_bS_c + (1-a)Cu^{2+} + (1-b)Fe^{2+} + (2-c)S + (4-2a-2b)e^-$ Step 2: Cathodic reduction $Cu_afe_bS_c + 2(c-a/2)H^+ + (2c-2b-a)e^- \rightarrow a/2Cu_2S + bFe^{2+} + (c-a/2)H_2S$ And $(2-c)S + (4-2c)H^+ + (4-2c)e^- \rightarrow (2-c)H_2S$ For 0.75>a>0.375, 0<b<1 For a = 0.75 $CuFeS_2 \rightarrow 0.75CuS + 0.25Cu^{2+} + Fe^{2+} + 1.25S^o + 2.5e^-$ **Passivating Layer:** Metal deficient polysulphide ($2CuFeS_2 \rightarrow Cu_{0.75}S$ or $CuS \rightarrow Cu_2S$) and S^0
Hirato *et al.*, 1986	Electrochemical oxidation and leaching with ferric chloride 0.2 M $FeCl_3$ SEM surface study	Shakanai mine	52-90°C	1	100%	**Kinetics** Linear - half order dependence on $FeCl_3$ Anodic: $CuFeS_2 \rightarrow Cu^{2+} + 5Fe^{2+} + 2S^0 + 4e^-$ Cathodic: $FeCl_2^+ + e^- \rightarrow FeCl_2$ Passivating Layer: Porous S^o on fringes of mineral surface
Dutrizac, 1989	Ferric chloride leaching 0.2 M $FeCl_3$	Messina 10-14, 20-29, 29-37μm	30- 90°C	6	94%	**Kinetics**: Parabolic – Diffusion model applied with limitation of transport through S^0 layer. Ferric sulfate leach accompanied by direct acid attack and H_2S oxidation to S^0. $CuFeS_2 + 2 Fe_2(SO_4)_3 \rightarrow CuSO_4 + 5Fe SO_4 + 2S^0$ $CuFeS_2 + 8 Fe_2(SO_4)_3 + 8H_2O \rightarrow CuSO_4 + 17Fe SO_4 + 8H_2S0_4$ $CuFeS_2 + 2 H_2SO_4 \rightarrow CuSO_4 + 5Fe SO_4 + 2H_2S(aq)$ $2H_2S(aq) + 2 Fe_2(SO_4)_3 \rightarrow H_2SO4 + 4Fe SO_4 + 2S^0$ **Passivating Layer**: Granular, thick S^o

Reference	Type of Study	$CuFeS_2$ Source and Particle Size	Temp	Fe / Cu	S_0 / S_0+SO_4	Kinetics, Proposed Mechanism and Nature of Passivating Layers
Holiday and Richmond, 1990	Anodic dissolution of $CuFeS_2$ in acidic media Xray photoelectron spectroscopic study 0 to 600mV (SCE)	Mt Issa	25C	5	-	Overall reaction Anodic; $2CuFeS_2 + 6H^+ + 2e^- \rightarrow Cu_2S + 3H_2S + 2Fe^+$ Cathodic: $Cu_2S \rightarrow 2Cu^{2+} + S0 + 4e$- **Passivating Layer:** CuS or Cu_2S
Murr and Hiskey, 1993	Ferric sulfate leach	Transvaal 48-65,100-150,200-270μm	95°C			**Passivating Layer:** Xray spectrum showed presence of sulfur
Hackl *et al*, 1995	O_2 pressure leaching in sulfate medium 0.69 and 1.38Mpa O_2 Partial pressure	Messina, Gibraltar 14μm	110-220°C	>>1	-	**Kinetics:** Mixed reaction/ diffusion model with initial rate control by ion diffusion through polysulphide layer. Reversion to chemical control when layer decomposes $CuFeS_2 \rightarrow Cu_{1-x}Fe_{i-y}S_2 + xCu^{2+} + yFe^{2+} + 2(x+y)e^-$ (fast) $Cu_{1-x}Fe_{1-y}S_2 \rightarrow Cu_{1-x-z}S_2 + zCu^{2+} + (1-y)Fe^{2+} + 2(z+1-y)e^-$ (slow) $Cu_{1-x-z}S_2 \rightarrow (1-x-z)Cu2+ + 2S^o + 2(1-x-z)e$- (slowest) **Passivating Layer:** At 110°C passivating layer is iron deficient copper disulphide indicated: $Cu_{1-x}Fe_{1-y}S_2$ Polysulphide CuS_n for n>2 At 200°C no passivation
Gomez *et al.*, 1996		Transvaal	25–70°C			**Passivating Layer** Cu rich, Fe poor polysulfide differing in structure
Klaber *et al.*, 2001	Ferric sulfate leach 0.2M $Fe(SO_4)_3$ XPS analysis	Mt. Isa Mines 1 -200μm	50°C			**Passivating Layer:** Sulfur and disulfide,

Chapter Three

Re-evaluation of Previously Published Data

Published data by Kametani and Aoki (1985) and Hiroyoshi *et al.* (2000) on the effect of redox potential on chalcopyrite leaching was re-evaluated by the Biomineral Processing research group in the Department of Chemical Engineering at UCT. This was done in order to standardise the rate of leaching since the experiments from different authors were conducted under different conditions. All calculated rates of leaching were normalised to a rate per unit area, to allow easier comparison of the rates with other published data. A detailed description of the procedures used to rework the data, followed by conclusions on the optimal redox potential range where chalcopyrite ferric leaching occurs, are presented in this section.

Kametani and Aoki (1985) performed chalcopyrite leach experiments within the redox potential range of 520 to 880 mV (SHE) at 90°C, using ultrafine particles of a mean size of 6μm. The concentrate consisted of 75% chalcopyrite, 17% pyrite and small quantities of ZnS (3%) and PbS (2%). Potassium permanganate was used as an oxidising agent to continuously re-oxidise the ferrous-iron to ferric-iron, thus maintaining a constant redox potential. The oxidation of ferrous-iron by potassium permanganate proceeds via the following reaction:

$$MnO_4^- + 5Fe^{2+} + 8H^+ \rightarrow Mn^{2+}\ 5Fe^{3+} + 4H_2O \qquad [3.1]$$

Due to the uncertainty of the spontaneity and stoichiometry of the reaction under the different temperature and pH conditions, experiments were carried out to verify these aspects within our research group. The results by Furamera (2000) conclusively showed that the permanganate oxidation reaction was instantaneous and the stoichiometry was not affected by changes in pH and temperature.

Kametani and Aoki (1985) reported the amount of potassium permanganate used to oxidise the ferrous-iron to ferric-iron at the various redox potentials. This data is represented in Figure 3.1.

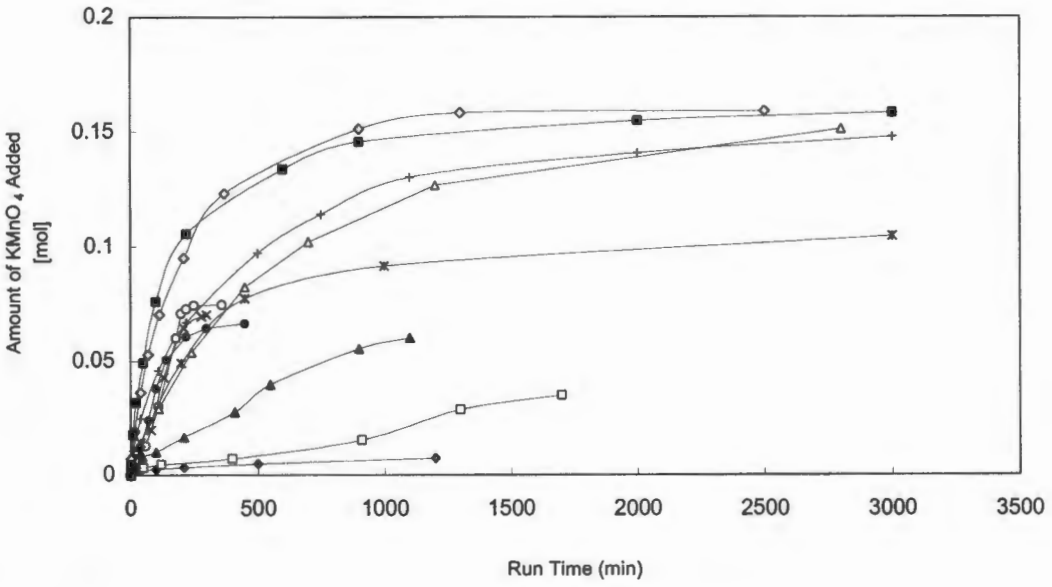

Figure 3.1: The amount of potassium permanganate added
[♦] 515 mV, [□] 545 mV,[▲]565 mV [●] 615 mV [O] 645 mV [✳]685 mV
[Δ] 715 mV [+] 765 mV [◊] 815 mV,

The rate of ferrous-iron generated from oxidation of mineral can be calculated from the amount of potassium permanganate added to re-oxidise the ferrous-iron to ferric-iron for a continuous leaching process. All the experiments were allowed to go to completion. The results showed an initial fast reaction rate followed by a slower rate. The faster rate was linked to reaction controlled region (Munoz *et al.,* 1979). Based on potassium permanganate additions, the amount of ferrous-iron generation at any time was calculated. The rate of ferrous-iron generation due to ferric leaching of the sulfide minerals can be represented as follows:

$$-5r_{KMnO_4} = -r_{Fe^{2+}} \qquad [3.2]$$

Figure 3.2, indicates the calculated rate of ferrous-iron generation at different redox potentials. The data was normalised to copper extraction per unit area. The rate of ferrous-iron generation increased with increasing potential up to a critical redox potential of 640 mV (SHE). The rate then decreased again up to 720 mV (SHE), thereafter increased with increasing potential from 720 mV to 860 mV (SHE).

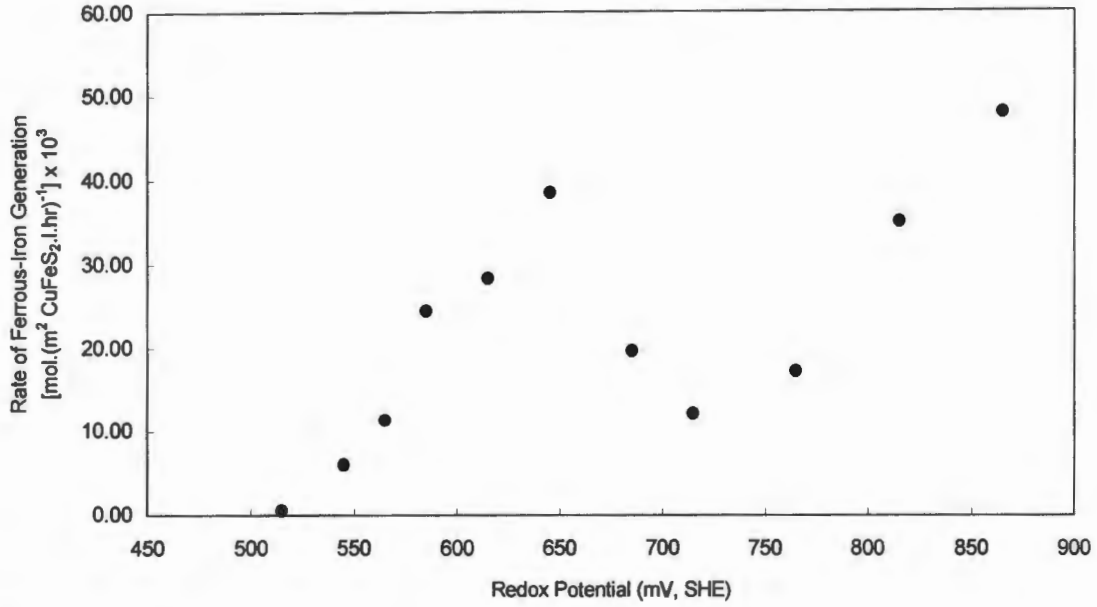

Figure 3.2: Rate of ferrous-iron generation versus redox potential
T = 90°C, 1M H_2SO_4

The temperature at which the rates were determined is much higher than the temperature at which mesophilic and thermophilic bioleaching operations takes place. Kametani and Aoki (1985) reported the amount of permanganate added at various temperatures at 615 mV (SHE), Figure 3.3.

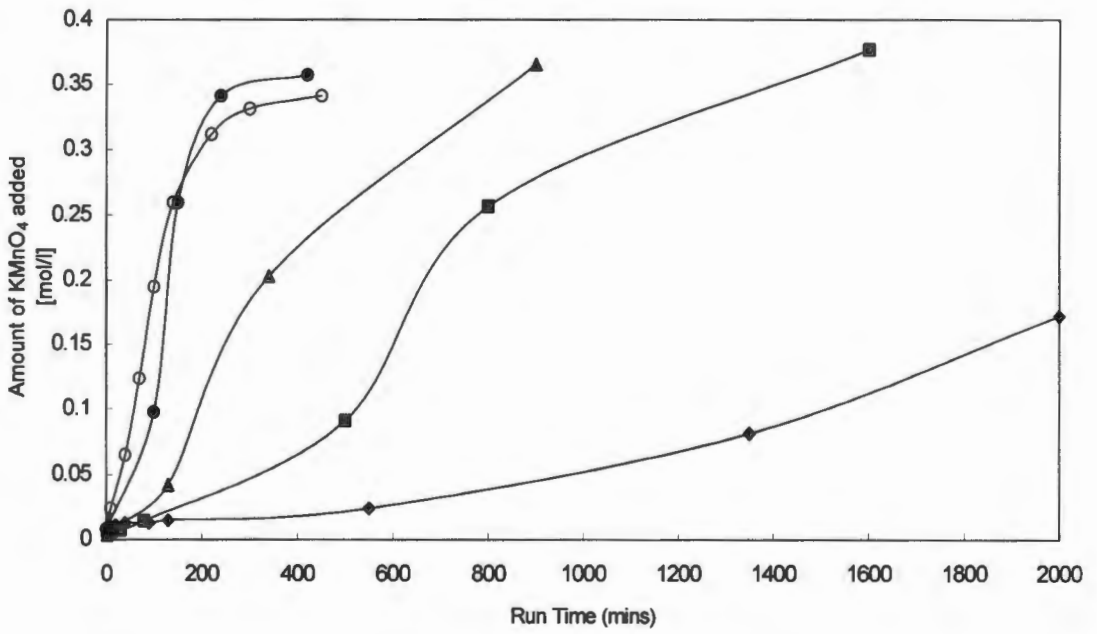

Figure 3.3: Amount of potassium permanganate added for oxidation of chalcopyrite at 615mV(SHE) from 50°C to 90°C.
[♦] 50° C; [■] 60°C ;[▲] 70°C; [●] 80°C ;[O] 90°C

The Arrhenius equation was used to calculate the rates of ferrous-iron generation at the lower temperatures. The activation energy for the reaction control regime was 93kJ/mol. This is higher than the reported activation energy of 47kJ/mol, which included both the reaction and diffusion controlled regime. The rate of ferrous-iron production at the different redox potential at any temperature was calculated using the following scaling factor.

$$r_{Fe^{2+},T_2} = r_{Fe^{2+},T_1} \frac{e^{\frac{Ea}{RT}}}{e^{\frac{Ea}{RT}}} \qquad [3.3]$$

The rates of ferrous-iron generation at 35°C and 70°C are illustrated in Figure 3.4. The rate of ferrous-iron production has been used as a measure of the rate of chalcopyrite dissolution. The high rate of ferrous-iron production observed within the redox potential of 550 to 670 mV (SHE) has been associated with chalcopyrite leaching. The increased ferrous-iron generation between 750 mV and 880 mV (SHE) has been associated with both chalcopyrite and pyrite leaching.

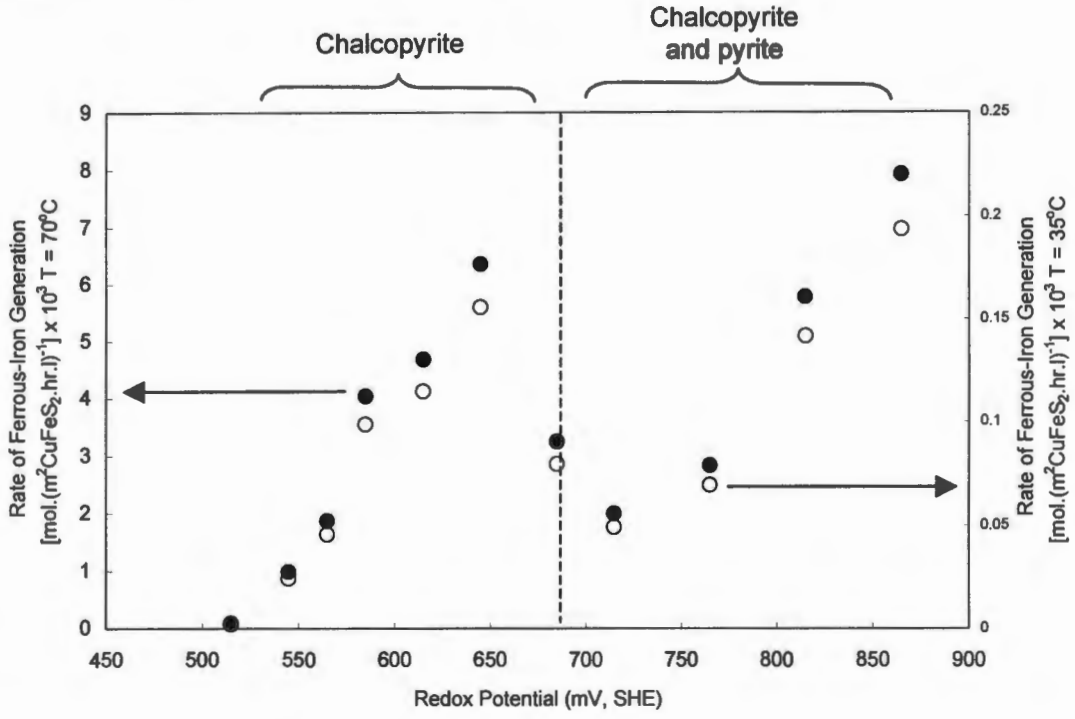

Figure 3.4: Variation in the rate of ferrous formation as a function of redox potential.
[O] 35°C; [●] 70°C

Analysis of leached residue after complete oxidation of the mineral at different redox potential indicated an increased dissolution of iron at higher redox potentials (Figure. 3.5). Ferric leaching of pyrite at higher redox potential accounted for the increase in ferrous-iron generation within this range. Based on the elemental sulfur results at various redox potentials, it was concluded that chalcopyrite in the concentrate was oxidised to form elemental sulfur over the whole redox potential range, while the oxidation of pyrite yielded sulfate ions.

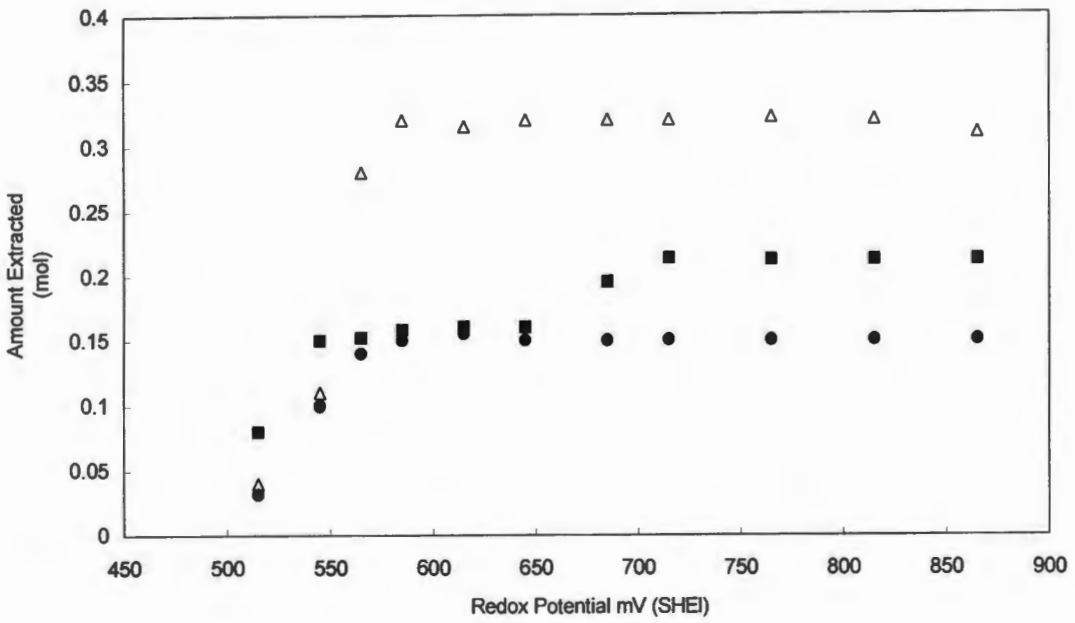

Figure 3.5: Variation in the amount of sulfur, iron and copper formed as a function of redox potential.
[●]Cu; [■] Fe; [Δ] S

Hiroyoshi *et al.* (2000) performed chalcopyrite leach experiments within a lower redox potential range of 520 to 680 mV (SHE), using fine particle size of 6μm. The experiments were conducted in 50mℓ shake flasks at 35°C over a 24 hr leach period. 0.1g of chalcopyrite was leached in 10mℓ of leaching solution. Based on XRD analysis, only chalcopyrite was observed in the concentrate. The redox potential was monitored at the start and end of the experiment and samples were extracted for copper and iron analysis at various stages in the experiment. However, only the concentration of copper extracted at the end of the leach was reported, making it impossible to establish initial copper leach rates. The authors proposed that chalcopyrite leaching occurs in the presence of enhanced copper and ferrous-iron concentrations. Leach experiments were performed with varying initial concentration of copper sulphate from 0.001. to 0.01 M.

The data was re-worked to obtain rates of chalcopyrite leaching. The rates were then normalised to copper extraction per unit surface area. The re-evaluated data is presented in Figure 3.6. These results indicate a much lower and narrower optimal chalcopyrite leach range of 520 to 580 mV (SHE). The experiments were conducted with varying initial copper concentrations, in all the cases the amount of copper extracted was higher at the lower redox potential range. The authors support the theory that chalcopyrite leaching is promoted by ferrous-iron. Therefore, the rate of chalcopyrite leaching decreased at higher redox potentials, because the amount of ferrous-iron present in the solution decreased.

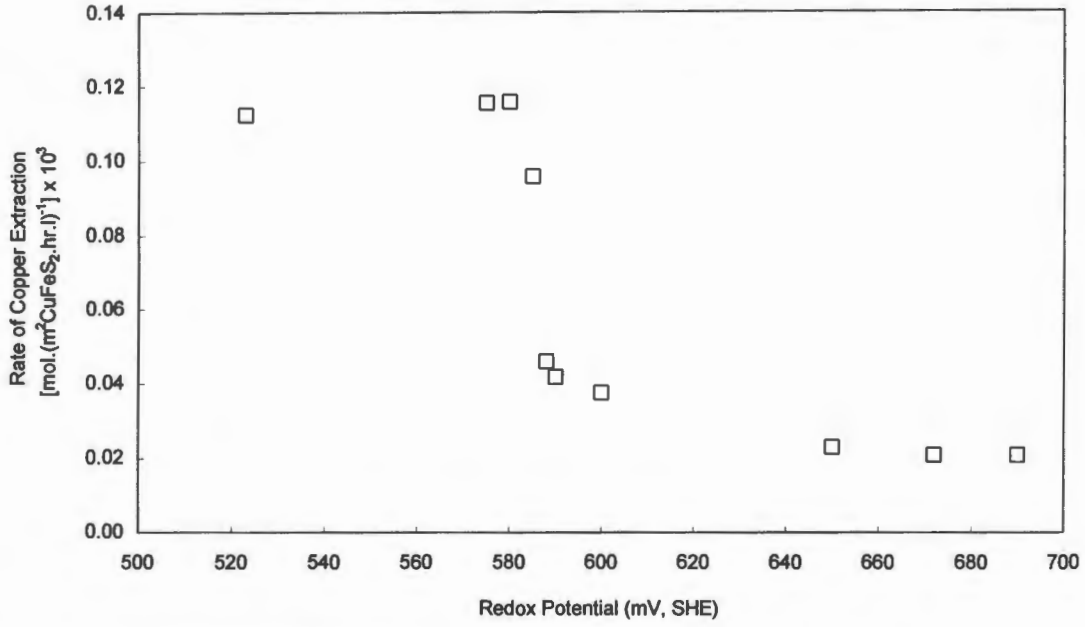

Figure 3.6: The re-evaluated data from Hiroyoshi *et al.*, (2000) indicating the rate of copper extraction at various redox potentials

Literature has presented varying redox potential ranges where chalcopyrite leaching occurs, this prompted the need for further work on the effect of redox potential on chalcopyrite leaching over a wide redox potential range of 550 to 850 mV (SHE). The constant redox potential method established by Kametani and Aoki (1985) was adopted to obtain initial chalcopyrite leach rates under bioleach conditions, which entails operating at temperatures of 35 and 70°C at a pH of 1.5.

Chapter Four

Materials and Methods

The constant redox potential method developed by Kametani and Aoki (1985) was used to establish initial chalcopyrite chemical leach rates under bioleach conditions, which entails operating at temperatures of 35°C and 70°C and pH of 1.5. Controlled addition of potassium permanganate was used to maintain a constant solution redox potential. Concerns about the methodology such as stoichiometry of ferrous-iron oxidation by potassium permanganate and the effect of permanganate on the ore have already been validated by tests presented in Furamera's (2000) thesis.

Preliminary experiments were carried out using pyrite as a base case. This was followed by experiments on chalcopyrite. This chapter presents a concise description of the chemical and physical characteristics of the pyrite and the mixed copper sulphide mineral used, the experimental procedures followed, and the experimental apparatus used.

4.1 MINERAL ANALYSIS

4.1.1 Pyrite Mineral Analysis

The pyrite concentrate used in the preliminary experiments was obtained from Durban Roodepoort Deeps (DRD) gold mine, South Africa. Initially, XRD analysis was used to confirm the presence of pyrite in the concentrate. The total iron and sulfur content of the concentrate was determined by digesting a representative sample of a known mass in hydrofluoric, nitric and perchloric acid. The amount of iron solubilised was determined by Flame Atomic Adsorption Spectroscopy, AAS. The sulfur content was determined by using a Leco SC32 sulfur analyser. The elemental analysis of the concentrate is listed in Table 4.1.

Table 4.1: Elemental analysis of the Durban Roodeport Deep flotation concentrate sample

ELEMENT	CHEMICAL ASSAY (%)
Iron	33.3%
Sulfur	50.5%

The concentrate was wet sieved to obtain the required size fraction. Ore, in the size range of +75 - 106μm was used for the experiments. The Malvern Laser Master Sizer was used to determine the size distribution of the ore sample. The size analysis of the concentrate is listed in Table 4.2.

Table 4.2: Malvern Laser Master Size analysis of the pyrite concentrate

SIZE FRACTION	MASS PERCENT (%)
+106	29.06
-106 +75	45.58
-75+53	10.79
-53+ 38	1.68
- 38	2.79

4.1.2 Chalcopyrite Mineral Analysis

The chalcopyrite concentrate used in all the experiments was obtained from Otjihase mine in Namibia. The chemical composition of the concentrate was determined by QuemSEM and elemental analysis. The elemental analysis of the concentrate is listed in Table 4.3. The composition of the different minerals in the concentrate was determined by the suppliers, using XRD analysis, Table 4.4. The ore was wet sieved and ore in the size range of +53 - 75μm range was used in the experiments. Malvern Laser Master Sizer was used to determine the particle size distribution and the results are presented in Table 4.5.

Table 4.3: QuemSEM analysis of the chalcopyrite concentrate

ELEMENT	QUEMSEM ASSAY (%)	ESTIMATED CHEMICAL ASSAY (%)
Copper	27.99	32.8
Iron	31.55	34.0
Sulphur	35.69	33
Zinc	0.85	

Table 4.4: The mineral composition of the chalcopyrite concentrate (obtained from suppliers)

MINERAL	WEIGHT PERCENT (%)
Chalcopyrite	80.77
Pyrite	13.11
Sphalerite	1.26
Cubanite/Idaite	0.09
Bornite	0.01
Other Sulphides	0.13
Quartz	1.62
Feldspar	0.05
Other Silicates	1.73
Fe-oxides	1.06
Other	0.16

Table 4.5: Malvern Laser Master Size analysis of the chalcopyrite concentrate

SIZE FRACTION	MASS PERCENT (%)
+150	-
+106 – 150	8.35
-106+75	25.48
-75+53	40.71
-53+38	15.92
-38	8.54

4.2 EXPERIMENTAL EQUIPMENT

The experiments were carried out in a 2 litre jacketed, Z61104CT04, Applikon® vessel made of borosilicate glass. The vessel has a working volume of 1 litre. The vessel was covered with a head plate in order to minimise evaporation at high temperatures. The head plate was made up of stainless steel and contained a number of ports for baffles, probes and nitrogen sparging. Baffled reactors were chosen in order to ensure adequate mixing. Three baffles 10 mm wide, 220 mm long and constructed of stainless steel were located at 120 degrees to each other.

The temperature in the reactors was controlled by circulating water from a Grant Y6 constant temperature water bath through the reactor jackets. Agitation and gas

dispersion was achieved by using a 6 bladed, pitched blade impeller driven by a variable speed overhead electric motor set at a rotation speed of 400 rev.min^{-1}.

The solution redox potential was controlled by the addition of potassium permanganate using an automatic titration unit. The Metrohm 718 Stat Titrino, obtained from Swiss Lab, is a remote controlled facility that allows full control of the unit through a desktop computer. The redox potential set point was controlled to within 1 mV of the set point by the optimal adjustment of the control dynamics, maximum and minimum dosing rate.

The leach solution was continuously sparged with nitrogen, via an air sparger located under the impeller. The system was sparged with nitrogen to prevent the possible oxidation of ferrous iron to ferric iron by atmospheric oxidation. This ensures that permanganate was the only oxidant present to oxidise ferrous to ferric-iron.

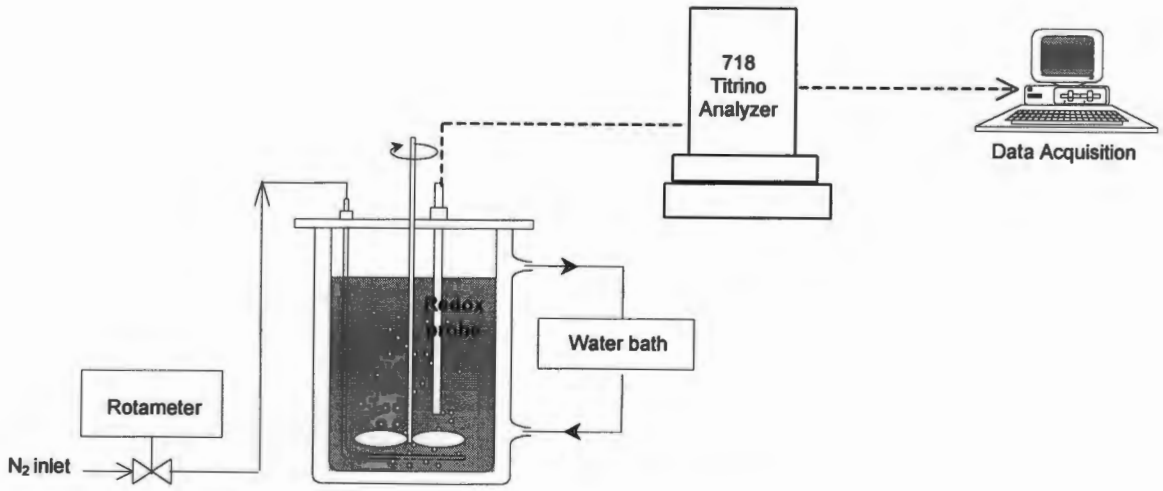

Figure 4.1: Schematic representation of experimental apparatus

4.3 EXPERIMENTAL PROCEDURE

4.3.1 Ore Pre-treatment

The presence of attached mineral fines on ore surfaces leads to a rapid initial copper dissolution. Therefore, the fines were removed from each concentrate sample by an ultrasonic pre-treatment procedure before leaching. The pre-treatment procedure entailed adding 30 mℓ of deionised water to 15g of concentrate in a 500mℓ beaker immersed in an ultrasonic bath. The concentrate was left in the ultrasound bath for a minute, after which the cloudy supernatant was decanted. The procedure was repeated using fresh deionised water.

4.3.2 Probe Calibration

The measured solution redox potential is related to the ratio of the free ferric to free ferrous-iron in the solution via the Nernst equation, Equation 4.1.

$$E = E^{\circ} + \frac{RT}{zF} \ln \frac{[Fe^{3+}]}{[Fe^{2+}]} \qquad [4.1]$$

The literature parameters for E° and RT/zF are ideal values, therefore the probe has to be calibrated for the system in use. The probe calibration was carried out at a constant temperature of 35°C and 70°C. The redox probe was calibrated by making up ferrous and ferric sulfate solutions of similar concentrations. The total iron concentration in solution was determined by both Flame Atomic Adsorption Spectroscopy and titrations with potassium dichromate (Broadhurst, 1993). The ferrous-iron concentration was also determined by titration with cerium (IV) sulfate (Broadhurst, 1993). A detailed description of the titration procedure and the preparation of the reagents are described in Appendix I. A known volume of ferric sulfate was added to a jacked vessel, the redox probe inserted and the solution agitated. The temperature in the reactor was maintained at the required temperature by circulating water from the Grant Y6 constant temperature bath through the reactor jacket. Once thermal equilibrium was reached, an aliquot of ferrous sulfate was added and the redox potential of the solution recorded. The procedure was continued until the solution contained equal volumes of ferric- and ferrous sulfate. Thereafter, the measured redox potential was plotted against $\ln([Fe^{3+}]/[Fe^{2+}])$, and the Nernst parameter, RT/zF (slope) and E° (intercept) was determined.

4.3.3 Measurement of Solution Redox Potential

The redox potential of the solution was measured using a Metrohm platinum wire-Ag/AgCl combination redox probe, filled with liquid 3M KCl electrolyte. The responsiveness of the more robust Mettler Toledo® redox electrodes (Pt-Ag/AgCl) filled with gell-electrolyte was also tested. The liquid probe was more appropriate for initial rate determination than the gell probe, because the free flow of KCl permits quicker redox potential response. At the start of each experiment, the redox probe was calibrated and the accuracy of the redox probe reading was tested against a redox buffer solution. At the end of each run the probe was regenerated by removing the filling solution and soaking the probe in a 10% HCl and acetic acid solution, then rinsing it in distilled water and KCl, before being refilled. Solution redox potential was measured using a platinum-Ag/AgCl combination redox probe, but the potential was reported as values against Standard Hydrogen Electrode (SHE).

4.3.4 Constant Potential Experimental Procedure

At each temperature, a series of runs were performed within the redox potential range of 550 to 850 mV (SHE) at 20 mV intervals. The procedure for each run is described below.

Leach solution with of a desired redox potential was prepared by mixing 10g/ℓ of ferric and ferrous sulfate in a ratio determined by the redox probe calibration. The solution was placed in reactor and allowed to reach the required reaction temperature. The pH of the solution was adjusted and maintained manually to 1.5 by the addition of 98% sulphuric acid and 5M Lithium hydroxide. Lithium hydroxide was used, rather than the more commonly used sodium hydroxide because lithium salts do not form jarosite-type precipitates in ferric sulfate medium (Dutrizac, 1981). The measured potential was set as the set point in the Titrino analyser. At the start of the experiment, 15g of washed concentrate was added to the solution. During the run, the pH of the system was controlled manually rather than by a control system, because there was negligible change in pH during the course of the experiment

As the chalcopyrite oxidises, the amount of ferric-iron decreases and the amount of ferrous-iron increases. As the ratio of the ferric to ferrous-iron in solution decreases, the redox potential drops as predicted by the Nernst Equation. The redox probe measures the solution potential and relays it to the Titrino analyser. The Titrino compares the value of the set point and the measured value and takes corrective measures by adding a controlled amount of potassium permanganate to get the solution potential back to its set point. The potassium permanganate reacts with the ferrous- iron to produce ferric iron according to the following reaction:

$$MnO_4^- + 5Fe^{2+} + 8H^+ \rightarrow Mn^{2+} + 5Fe^{3+} + 4H_20 \qquad [4.2]$$

A diagrammatic representation of the control system is illustrated in Figure 4.2. The amount of potassium permanganate added and the redox potential change during the run was recorded to a file on a personal computer.

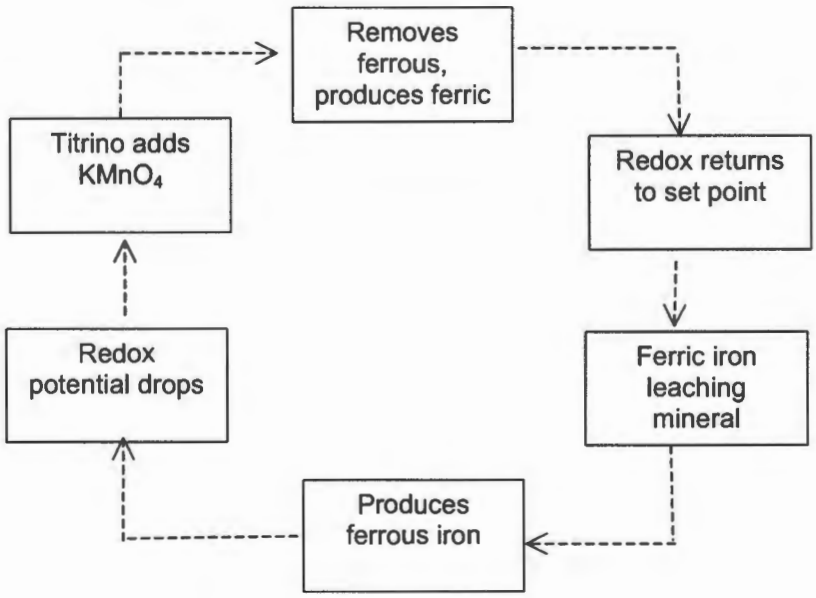

Figure 4.2: Schematic representation of the control system

During the run, samples were extracted at regular intervals to determine the concentration of dissolved copper, zinc and iron using Flame Atomic Adsorption Spectroscopy, AAS. A detailed explanation of the preparation of sample for AAS analysis is given in Appendix I.

Analytical grade chemicals and deionised water were used in the preparation of all the chemicals.

4.4 STOICHIOMETRY OF CHALCOPYRITE LEACHING

Dynamic leach experiments were performed to determine the stoichiometry of chalcopyrite ferric leaching. According to literature, ferric leaching of chalcopyrite proceeds according to either of the following equations:

$$CuFeS_2 + 4Fe^{3+} \rightarrow Cu^{2+} + 5Fe^{2+} + 2S_o \quad [4.3]$$

$$CuFeS_2 + 16Fe^{3+} + 8H_2O \rightarrow Cu^{2+} + 17Fe^{2+} + 2SO_4^{2-} + 16H^+ \quad [4.4]$$

Dynamic leach experiments were performed using both ferric and ferrous sulfate media, at 35°C and 70°C. The system was sparged with nitrogen to avoid the possibility of atmospheric ferrous-iron oxidation to ferric-iron. The ferrous-iron concentration was plotted against the copper concentration, in order to determine the relationship between the ferrous-iron and copper concentration during the experimental run. To establish if the ratio changes with time, the ferrous-iron to copper ratio was determined over a short one hour leach period and over a 20 day leach period.

4.5 RATE DETERMINATION

The rate of pyrite and chalcopyrite ferric leaching can be represented by the rate of ferrous-iron generation within the leach system. A detailed description of the calculations used in determining the rate of ferric leaching is described in the following section.

4.5.1 Rate of Ferrous-Iron Generation

Ferrous-iron generated can be related to the amount of potassium permanganate added to re-oxidise ferrous-iron to ferric-iron, according to Equation 4.2. Furamera (2000) confirmed the spontaneity and the stoichiometry of the reaction under different temperature and pH. The following equation represents the rate of ferrous-iron generation due to ferric leaching of the sulphide minerals:

$$-5r_{KMnO_4} = -r_{Fe^{2+}} \quad [4.5]$$

The rate of ferrous-iron generation over the initial one hour leach period can be calculated based on the performance equation of a constant volume batch reactor.

$$-r_{Fe^{2+}} = \frac{dFe^{2+}}{dt} \qquad [4.6]$$

The volume of potassium permanganate added and volume extracted for analysis during the experimental runs did not exceed 10mℓ. This represented a 1% change in volume, which is considered negligible. Under certain circumstances when the volume changes exceeded this amount the concentration of the analysed copper was corrected accordingly.

4.5.2 Rate of Copper Extracted From Chalcopyrite

The AAS analysis was used to determine the amount of copper which solubilised with time. The rate of copper extracted was determined from the slope of copper extracted versus time plot.

Chapter Five

Results and Discussion

In order to test the applicability and reproducibility of the use of the potassium permanganate method to maintain a constant redox potential, initial leach experiments were performed using pyrite. Pyrite was chosen as a base case because the kinetics of ferric leaching of pyrite has been extensively studied and the leach stoichiometry well established. The results obtained were compared with the dynamic leach experiments performed by May (1997) in order to compare the rate of leaching using these different methods.

Before the start of the experiments the redox probe was calibrated under the condition applied in these experiments. The values of the Nernst parameters E° and RT/zF are reported in the following table:

Table 5.1: The measured Nernst parameters from calibration data

Total Iron Concentration g/ℓ	Temperature	RT/zF	E°	Correlation Coefficient R^2
10g/ℓ	35°C	28.3	475.3	0.997
10g/ℓ	70°C	30.63	483.2	0.997
Standard values	25°C	25.7	573	

5.1 CONSTANT POTENTIAL LEACH EXPERIMENTS USING PYRITE

Constant potential pyrite leach experiments were performed under similar conditions as the dynamic leach tests performed by May (1997). Experiments were performed using the same mineral concentrate, under the same leach conditions such as total iron concentration, pH and temperature. However, the experiments were conducted in a larger 1ℓ baffled reaction vessel as opposed to the 100 mℓ glass reactor system used by May. The system was also sparged with nitrogen to prevent atmospheric ferrous-iron oxidation to ferric-iron.

5.1.1 Reproducibility

To get a measure of the reproducibility of the data, two experimental runs at similar redox potentials were performed under the same conditions. The change in ferrous-

iron generated over time was normalised, and reported as ferrous-iron generation per unit area of chalcopyrite. The results of the ferrous-iron production over time are presented in Figure 5.1. The rates of ferrous-iron generation at 859 mV and 862 mV (SHE) were $7.19*10^{-6}$ and $7.32*10^{-6}$ mol $Fe^{2+}(m^2.FeS_2.\ell.s)^{-1}$ respectively.

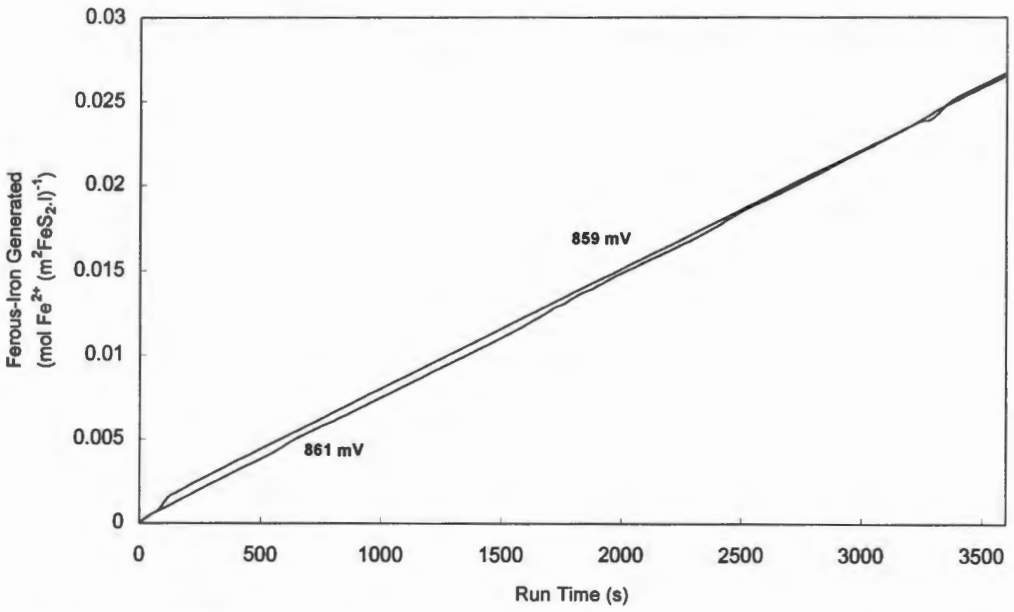

Figure 5.1: Reproducibility of experimental data
T = 35°C, pH = 1.5, Total Iron = 10g/ℓ

These results represent a difference of 2% in the rates obtained, thus demonstrating reproducibility. Rates of ferrous-iron generation were determined at regular 10 mV to 20 mV intervals within the pyrite leaching range of 750 mV to 870 mV (SHE).

5.1.2 Variation of Ferrous-Iron Production With Time At Constant Redox Potential

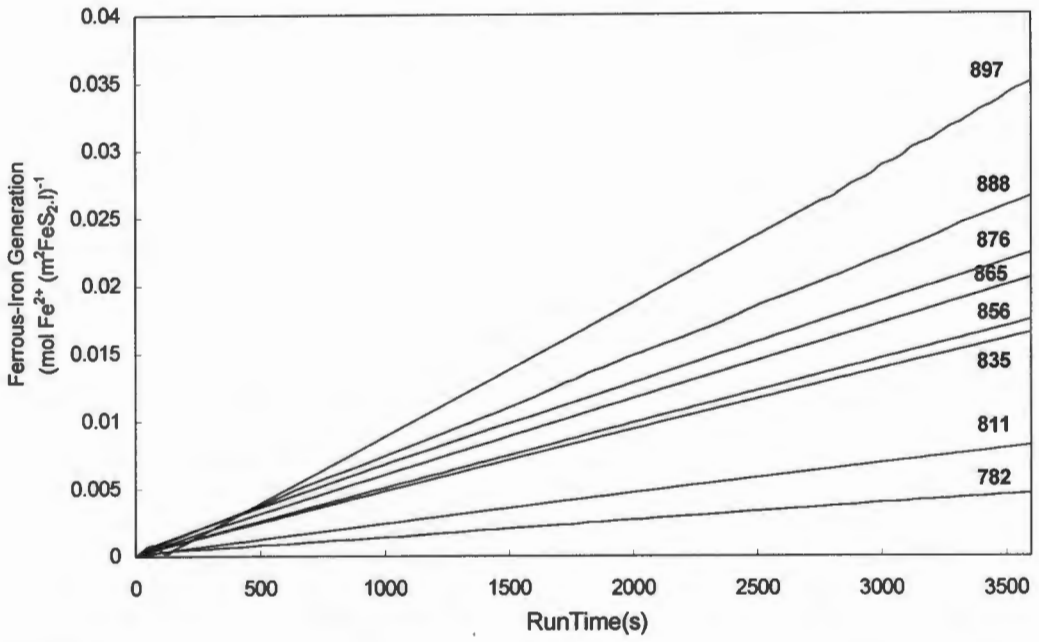

Figure 5.2: Ferrous-iron production at various redox potentials:
T = 35°C, pH = 1.5, Total Iron = 10g/ℓ

The average rate of ferrous-iron generation at each redox potential was determined from the slopes of the ferrous-iron generated plotted against the time curve. The rate of ferrous-iron generation within the redox potential range of 730 to 900 mV (SHE) is illustrated in Figure 5.3.

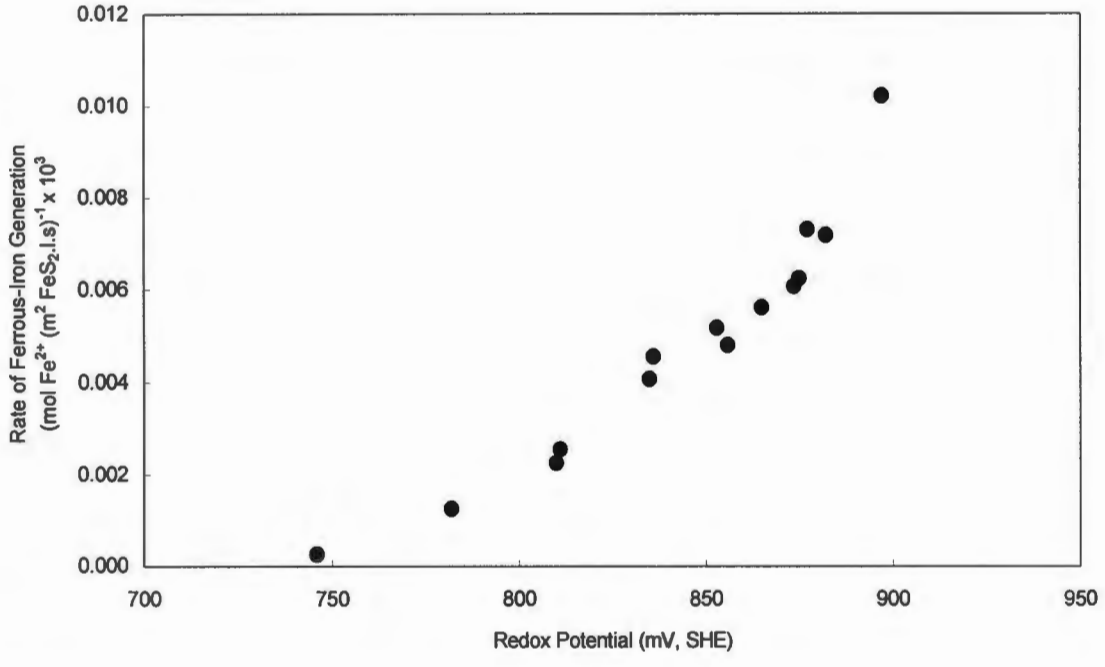

Figure 5.3: Rate of ferrous-iron production at different redox potential
T = 35°C, pH = 1.5, Total Iron = 10g/ℓ

The rate of ferrous-iron production increases exponentially with an increase in redox potential. The same trend was observed by May (1997). These data were then fitted to the Butler-Volmer equation, Equation 5.1, and compared to the rate of leaching obtained by May (1997).

$$r = r_o\left(\exp(\alpha\beta(E-E^\circ) - \exp((1-\alpha)\beta(E-E^\circ)\right) \qquad [5.1]$$

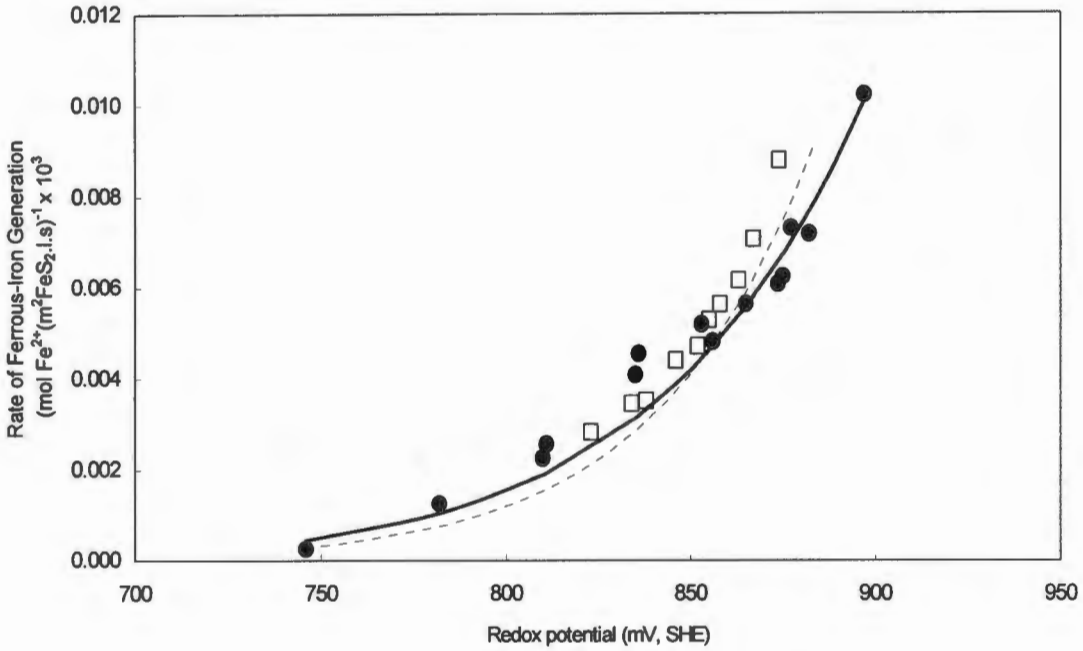

Figure 5.4: Comparison of Butler-Volmer fit to current data and data from May (1997)
[●] Experimental Data; [□] May (1997)
[—] Butler-Volmer fit to current data; [---] Butler-Volmer fit to data from May (1997)

The rate of leaching at higher redox potentials was lower than the rate of leaching predicted by May (1997). In a dynamic leach system, the initial higher rates were attributed to a transient effect, which was probably caused by highly reactive surface sites or a non-faradaic charging effect (May *et al.*, 1997). The author also reported that the larger the difference in redox potential between the mineral and the ferric/ferrous solution, the greater the initial rate (May, 1997).

Comparison of the Butler-Volmer constants from the current study and data from May (1997) are presented below. The values are comparable.

Table 5.2: Table of comparison of Butler-Volmer constants

	Units	May (1997)	Current study
α		0.565	0.53
β	mV^{-1}(SHE)	0.039	0.028
E	mV (SHE)	630	658
r_o	mol. $(m^2FeS_2.s.l)^{-1}$	$8.79*10^{-7}$	$3.02*10^{-8}$

The data was also fitted to the electrochemical model proposed by Nagpal *et al.* (1994). This model assumes a linear dependency of the rate of mineral leaching to the over potential (η). The over potential is the difference between the redox potential and the rest potential.

$$r_{Fe^{2+}} = kA_{FeS}\left(E - E^0\right) \qquad [5.2]$$

The values obtained for the two constants are presented in the following table

Table 5.3: Table of comparison Nagpal *et al.*, (1994) rate constants

	Units	Current Study	Nagpal *et al.* (1994)
E	mV (SHE)	698	748
r_o	Mol. $(m^2FeS_2.s.l.mV)^{-1}$	$3.5*10^{-8}$	$8.0*10^{-5}$

The experimental data was fitted to the electrochemical models by minimising the sum of squares of the error (SSE) between experimental data and the model . The SSE for fit to Butler-Volmer equation was $1.48*10^{-9}$ and $3.39*10^{-5}$ for fit to Nagpal *et al.* (1994) electrochemical model. The experimental results showed a better fit to the Butler-Volmer equation.

Since the rates of pyrite leaching determined using the dynamic and constant potential method are comparable, it can be concluded that the constant potential methodology is reliable and can be used to determine the rate of chalcopyrite leaching.

5.2 STOICHIOMETRY OF CHALCOPYRITE LEACHING

Dynamic leach experiments were carried out to determine the mechanism of chalcopyrite ferric leaching at 70°C and 35°C. Chalcopyrite ferric leaching results in the formation of sulfur or sulfate, according to either of the following reactions (Beckstead *et al.,* 1976; Munoz *et al.,* 1979; Dutrizac and MacDonald, 1974; Dutrizac, 1989 and 1982):

$$CuFeS_2 + 4Fe^{3+} \rightarrow Cu^{2+} + 5Fe^{2+} + 2S_o \qquad [5.3]$$

$$CuFeS_2 + 16Fe^{3+} + 8H_2O \rightarrow Cu^{2+} + 17Fe^{2+} + 2SO_4^{2-} + 16H^+ \qquad [5.4]$$

There is no published data on the stoichiometry during the initial phases of reaction. Furthermore, the initial effect of acid on the leaching of chalcopyrite also has to be taken into consideration

The ferrous-iron to copper ratio was plotted to predict the mechanism of chalcopyrite ferric leaching. If the reaction proceeds to form sulfur then a ferrous-iron to copper ratio of five is expected. If the reaction proceeds to form sulfate then a ratio of 17 is expected. Figure 5.5 shows the ratio of ferrous-iron production to copper extraction during the course of the ferric leach experiment at 70°C and 35°C.

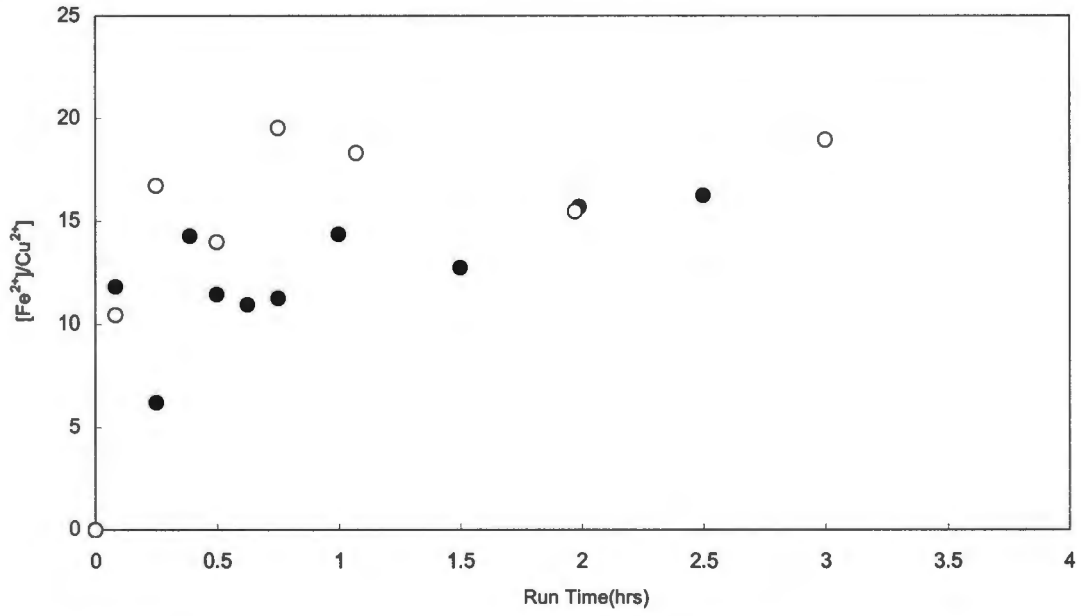

Figure 5.5: Ratio of ferrous-iron to copper production over a short period of time.
[●] 70°C, [O] 35°C, pH = 1.5, Total Iron = 10g/ℓ

It can be seen from the data that the ratio in the early stages of leaching is approximately 15. Ferric leach experiments were also conducted over an extended period of time to determine whether the stoichiometry changed over time. After a prolonged leach period the ratio decreased to five suggesting that the stoichiometry is changing during the course of the reaction, as illustrated in Figure 5.6.

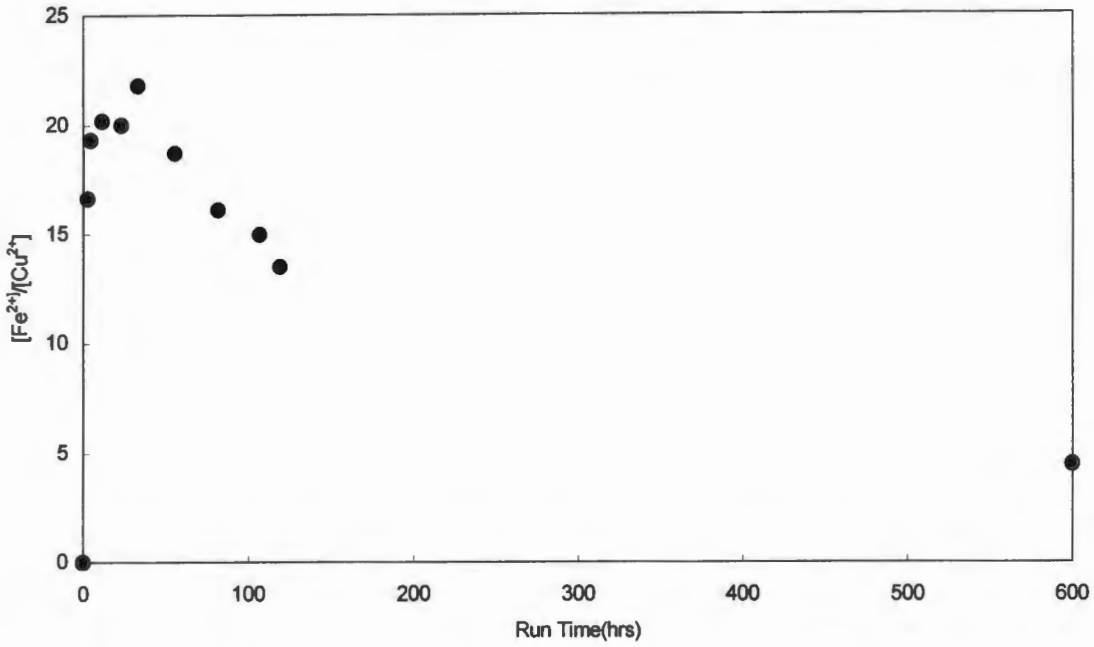

Figure 5.6: Ratio of ferrous-iron to copper over an extended period of time
T = 70°C, pH = 1.5, Total Iron = 10g/ℓ

The ratios of ferrous-iron to copper ratio under the various conditions have been tabulated in Table 5.4.

Table 5.4: Ratio of ferrous-iron to copper concentration at 35°C and 70°C

Leach time	Temperature	Ratio ferrous-iron to copper
3hr run	70°C	16
3hr run	35°C	17

There is evidence of sulfur formation throughout a leach experiment, when a pure chalcopyrite concentrate was used (Dutrizac, 1989). On the otherhand, there is evidence of a varying stoichiometry, when a concentrate of unclear purity was used (Jones and Peters, 1976). The authors reported a decrease in ratio from 12 to 7 only after 12 days of leaching in a ferric sulfate medium. A similar trend was observed in the long run, as shown in Figure 5.6, where the ferrous-iron to copper ratio decreased from 16 to 5 after about 20 days of leaching. However, it is beyond the scope of this investigation to identify reasons for the change in mechanism

The presence of other impurities within the chalcopyrite concentrate such as sphalerite and other sulfides, which are readily oxidised by ferric-iron, causes variation in ferrous-iron to copper ratio. Dutrizac (1982) performed ferric chloride leach experiments on different concentrates and observed that the decrease in chalcopyrite purity caused the molar ratios to become erratic, and thus reflect complex dissolution of pyrite and sphalerite. The more impure concentrate (75 to 80% chalcopyrite) exhibited varied ferrous-iron to copper ratios between 8 to 13,

whereas the more purer chalcopyrite concentrated exhibited ratios close to 5. Subsequently, a very pure chalcopyrite concentrate was used to establish the stoichiometry of ferric sulfate leaching of chalcopyrite, and a ferrous-iron to copper ratio of 5 was obtained (Dutrizac, 1989).

In this study, samples were taken at regular intervals for zinc and iron analysis. Analysis of the zinc, indicated an increase in zinc concentration with time. Based on the zinc analysis, the amount of ferrous-iron generated during ferric leaching of sphalerite was calculated based on Equation [5.5]

$$ZnS + 2Fe^{3+} \rightarrow Zn^{2+} + S^{0} + 2Fe^{2+} \qquad [5.5]$$

Increase in ferrous-iron to copper ratio due to the ferric leaching of sphalerite is not considered significant, and only contributed in part. The amount of copper and zinc extracted during an hour run is illustrated in Figure 5.7.

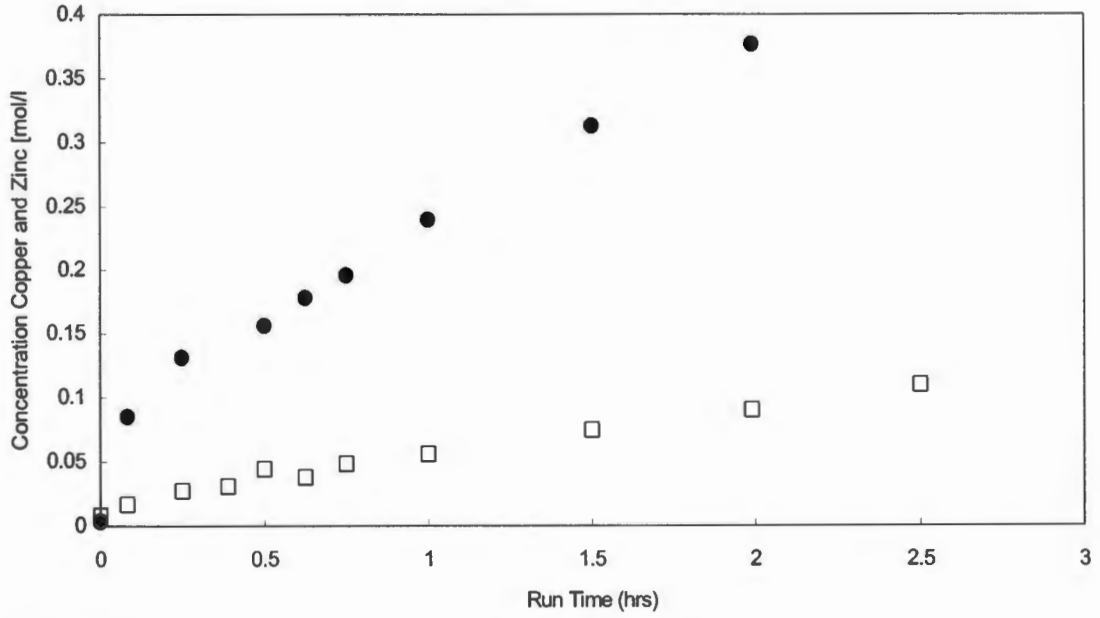

Figure 5.7: Amount of copper and zinc extracted during a ferric leach experiment
[□] Zinc concentration, [●] Copper concentration
T = 70°C, pH = 1.5 Total Iron = 10g/ℓ

During the initial phases of chalcopyrite leaching, the effect of acid on chalcopyrite leaching has to be taken into consideration. Acid leach experiment was conducted to investigate the effect of acid on the leaching of chalcopyrite, the results are illustrated in Figure 5.8

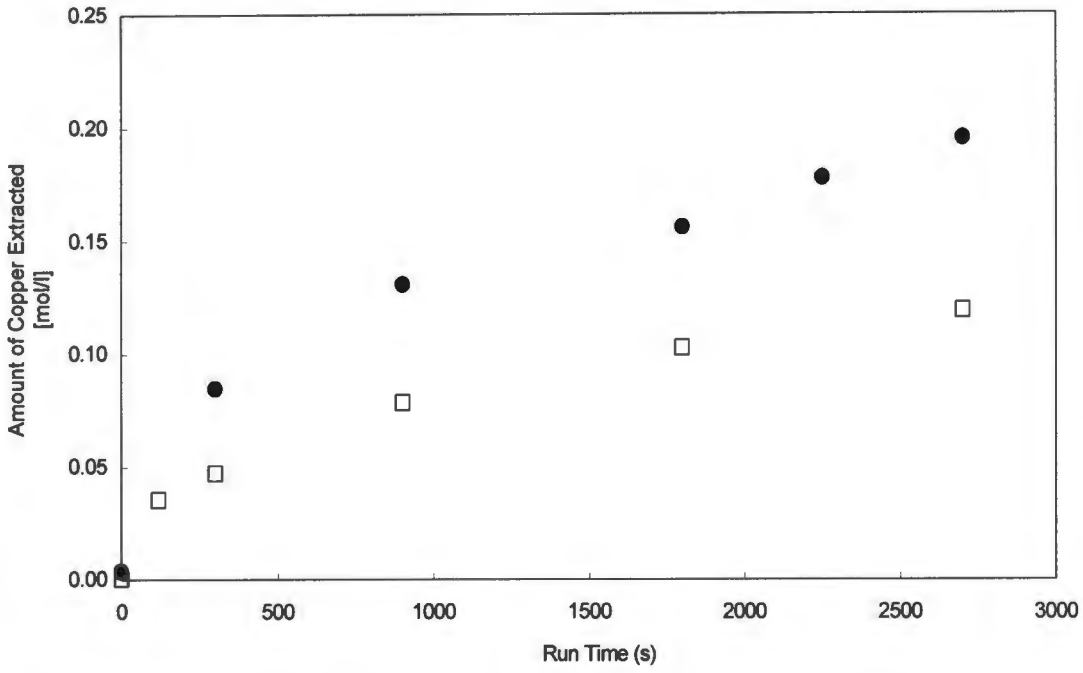

Figure 5.8: Comparison of copper extracted with time during acid leach and ferric leach
[□] Acid leach [●] Ferric leach
T = 70°C, pH = 1.5

The results indicate that acid leaching has a significant effect during the initial phases of the leach experiment. During a one hour run, both acid and ferric leaching are taking place.

5.3 RATE OF CHALCOPYRITE LEACHING

The rate of chalcopyrite leaching can be represented by the rate of ferrous-iron generation and the rate of copper extracted at the various redox potentials. In this section the rate of ferrous-iron generation and rate of copper extraction at 35°C and 70°C is discussed. Following this, an attempt is made at developing a relationship between the rate of ferrous-iron generation and the rate of copper extracted based on the expected ferric leach stoichiometry.

5.3.1 The Rate of Ferrous–Iron Generation

The rate of mineral oxidation is calculated based on the amount of potassium permanganate added during the experimental run, which is then related to the amount of ferrous-iron generated during the ferric leach process. The procedure for determining the rate of ferrous-iron generation has been explained in Section 4.5.1. The rate of ferrous-iron generation at 70°C and 35°C has been illustrated in Figure 5.9 and 5.10, respectively. Similar trends are observed in the rates of ferrous-iron generation at both temperatures. The results show an increase in the ferrous-iron generation between 590 mV and 640 mV (SHE). This is followed by a decrease in

rate of ferrous-iron generation up to 680 mV (SHE). The rate increases again up to approximately 840 mV (SHE).

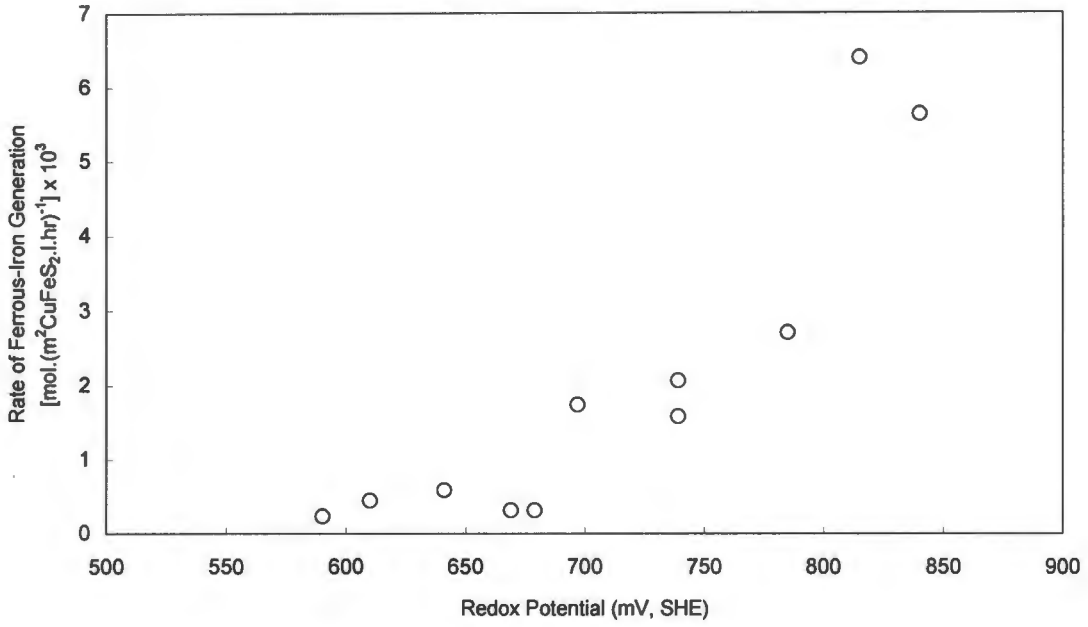

Figure 5.9: Initial rate of ferrous iron generation, calculated using the rate of permanganate addition .
T = 35°C pH = 1.5, Total Iron = 10g/ℓ

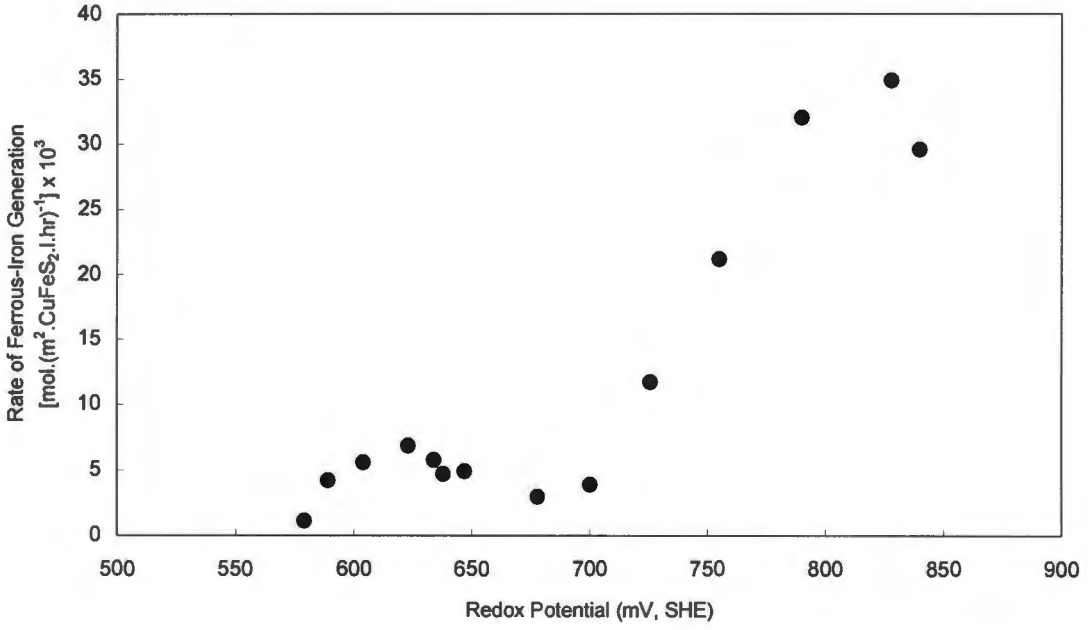

Figure 5.10: Initial rate of ferrous iron generation, calculated using the rate of permanganate addition .
T = 70°C pH = 1.5, Total Iron = 10g/ℓ

5.3.2 Rate of Copper Extraction

The amount of copper extracted from the chalcopyrite concentrate was determined by Atomic Adsorption Spectroscopy. The rate of copper extraction at different redox potentials is illustrated in Figure 5.11.

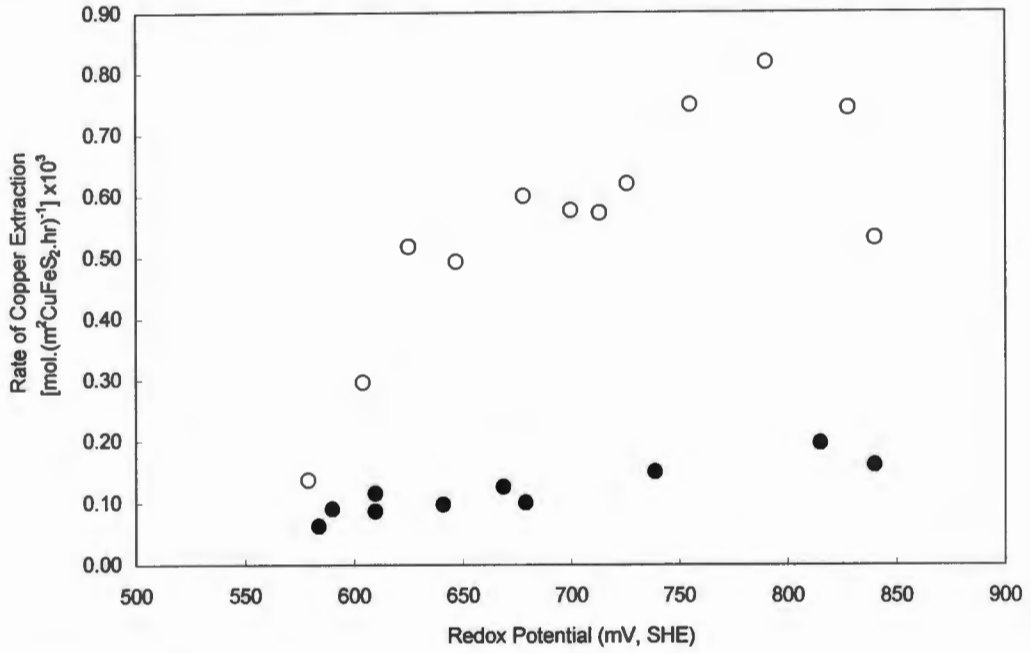

Figure 5.11: Initial rate of copper extraction versus redox potential
[O] 70°C, [●] 35°C pH = 1.5, Total Iron = 10g/ℓ

An increase in temperature gives rise to an increase in the rate of copper extraction. The optimal rate of copper extraction for the 70°C runs is from 600 mV to 800 mV (SHE). There is a slight decrease in the rate of copper extraction at 647 mV (SHE). Similar trends in rate of copper extraction are observed at 35°C. At 35°C, the rates of copper extraction are very low. There is a higher rate of copper extraction within the higher redox potential range of 680 to 840 mV (SHE).

5.3.3 Relating Ferrous Ion Production to Copper Extracted

The expected rate of copper extraction can be calculated from the rate of ferrous-iron production assuming that the reaction proceeds according to Equation 5.3 or 5.4.

The ratio of ferrous-iron production to copper extracted would be either 5 or 17 depending if the reaction proceeds to sulfur or sulfate. Based on the amount of ferrous-iron generated at different redox potentials, the predicted copper extraction was calculated. These results have been compared to the copper analysis obtained from the AAS analysis. Figure 5.12, illustrates some of the predicted copper rates obtained at various redox potentials at 70°C.

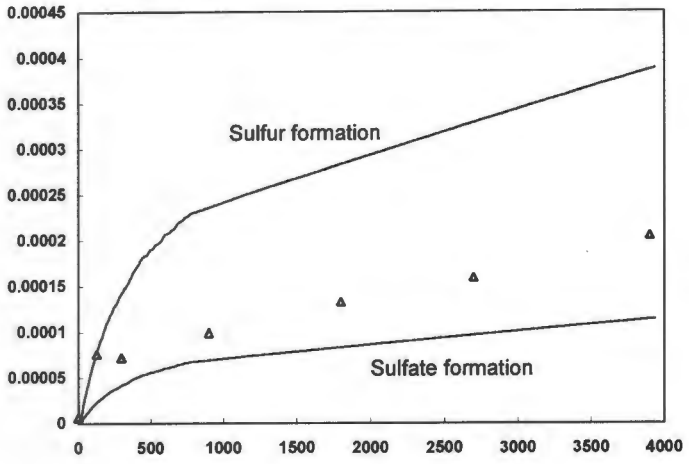

Figure 5.12a: 650 (mV, SHE)

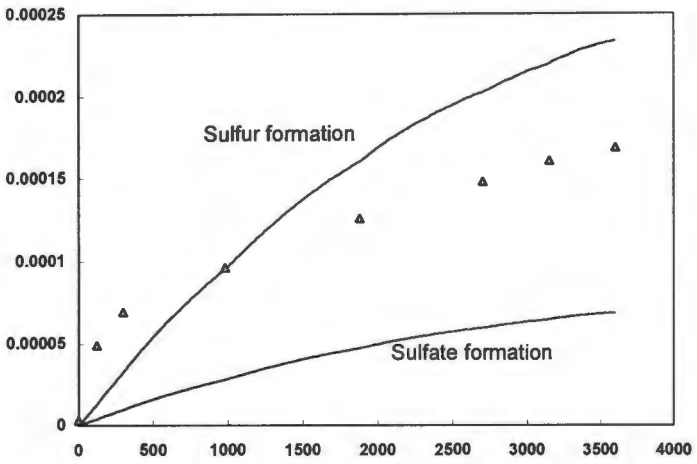

Figure 5.12b: 673 (mV, SHE)

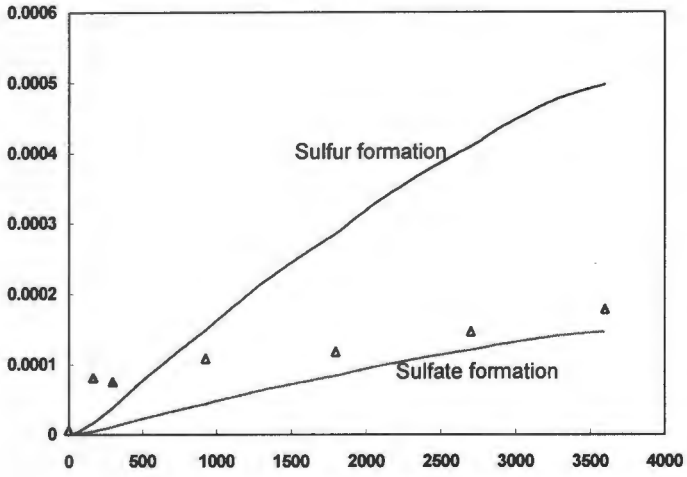

Figure 5.12c: 689 (mV, SHE)

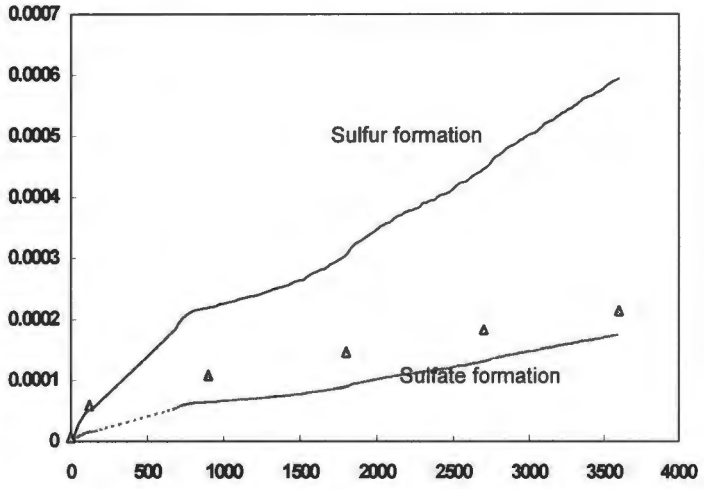

Figure 5.12d: 752 (mV, SHE)

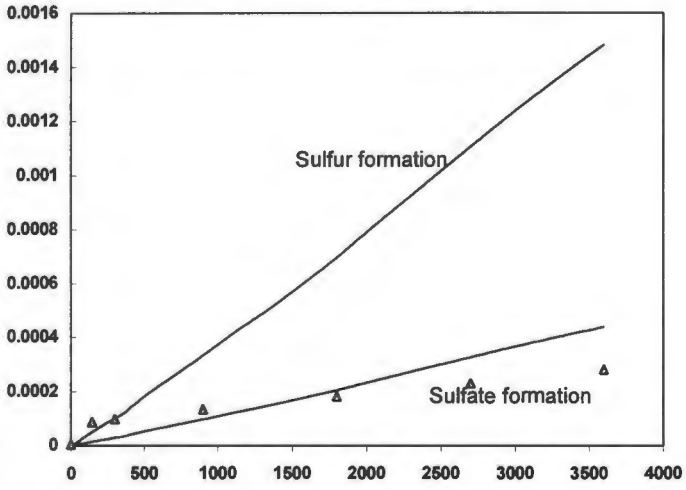

Figure 5.12e: 816 (mV, SHE)

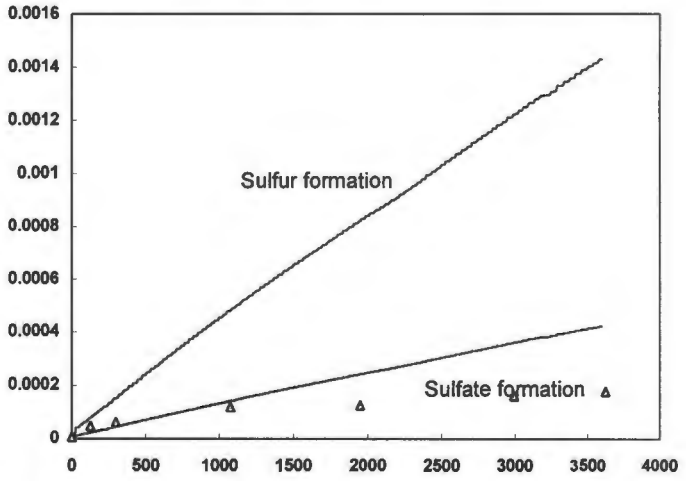

Figure 5.12f: 866 (mV, SHE)

Figure 5.12 Comparison of predicted copper extraction and copper analysis from AA. The predicted copper extraction is based on whether the reaction follows Equation 5.2 or 5.3

A comparison of the predicted copper extraction and the amount of copper extracted determined from AAS analysis, showed that the mechanism of sulfate formation is favoured in most of the redox potentials. There results were expected, because the dynamic ferric leach tests showed a ferrous-iron to copper ratio of 17 within the initial leach period, Section 5.2. The initial rapid dissolution of copper within the first ten minutes could be attributed to acid leaching. The zinc analysis was used to calculate the amount of ferrous-iron generated during the ferric leaching of sphalerite according to Equation 5.5. Sphalerite had negligible effect on the increase in ferrous-iron concentration.

Total iron analysis using titration, indicated a slight increase in the ferrous-iron concentration over time. Therefore, ferric leaching of pyrite also contributed to increase in ferrous-iron generation at higher redox potentials. However, the iron analysis did not show a distinct increase in iron dissolution at redox potential above 700 mV (SHE) as observed by Kametani and Aoki (1985). Iron analysis were also conducted on leached residue, these results were inconclusive, since negligible change in iron concentration were observed over the redox potential range. Analysis of leached residue is not reliable, since the experiments were conducted over a short period of time, within which negligible copper and iron dissolution is expected and the surface does not change significantly.

Chapter Six

Comparison of Results with Literature

The results obtained from this study, on the kinetics of chalcopyrite leaching are compared to the re-evaluated chalcopyrite leach kinetics from Kametani and Aoki (1985) and Hiroyoshi *et al.* (2000). The procedure used to re-evaluate the data was explained in detail in Chapter Three. Preliminary tests were also performed to evaluate whether ferrous–promoted chalcopyrite oxidation by dissolved oxygen is the predominant reaction during chalcopyrite leaching, as proposed by Hiroyoshi *et al.* (1997). These results have been compared to the results obtained by Hiroyoshi *et al.* (1997).

A comparison between to the re-evaluated rate of ferrous-iron generation obtained from Kametani and Aoki (1985), and the rate of ferrous-iron generation at the different redox potential is illustrated in Figure 6.1. The data obtained from Kametani and Aoki (1985) was re-evaluated to obtain rate of ferrous-iron generation at 70°C, using the Arrhenius equation.

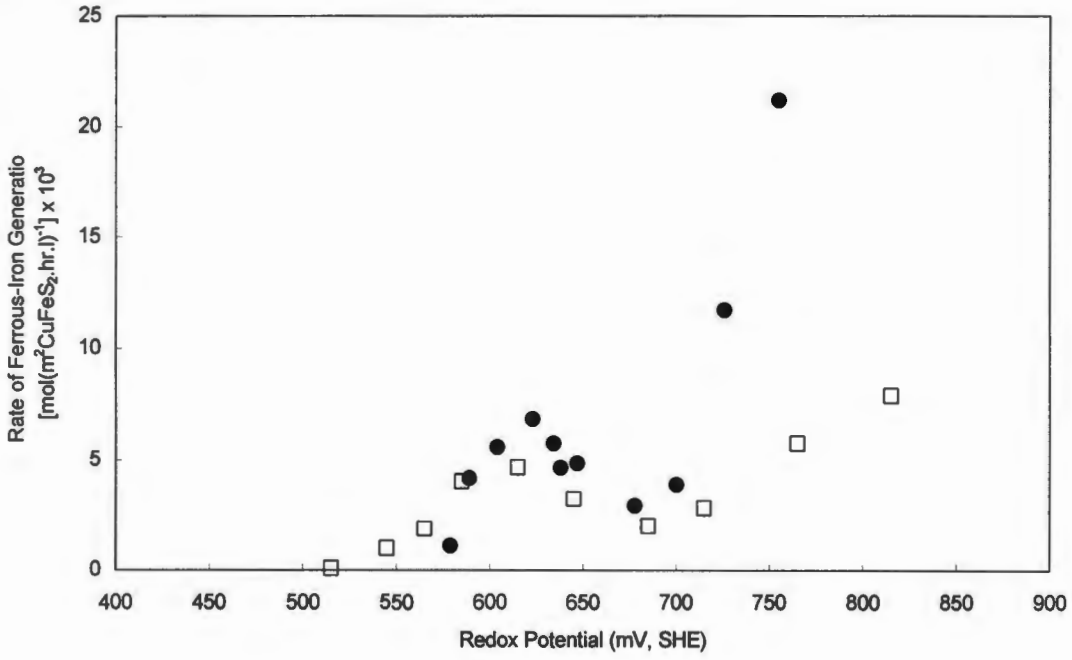

Figure 6.1: Comparison of the rate of ferrous-iron generation from experimental data with rate re-evaluated from Kamatani and Aoki (1985)
[●] Experimental data; [□] Kametani and Aoki (1985)

Similar trends in chalcopyrite leaching were observed both in the experimental data and the reworked data from Aoki and Kametani (1985). The rates from the experimental data were higher than the rates obtained from reworked data above a redox potential range of 700 mV (SHE).

Kametani and Aoki (1985) used elemental analysis of leached residue, Figure 3.5, to show that above the critical redox potential of 685 mV (SHE), the increase in the rate of ferrous-iron was due to the ferric leaching of pyrite and chalcopyrite. Subsequently, the authors performed an independent study on the rate of ferrous-iron generation at various redox potentials using a purer chalcopyrite concentrate. The authors claimed that the same trend in rate of ferrous-iron generation was observed, however, they did not report these results. Based on their findings, Kametani and Aoki (1985) suggested that the change in the rate of ferrous-iron generation above the critical potential was not just due to pyrite oxidation, but could have been caused by a change in the nature of chalcopyrite or chemical reaction. However, they did not show any evidence on how the nature of the chalcopyrite changed, or how the reaction mechanism shifted.

The experimental results from this investigation, on the rate of copper extraction, Figure 5.11, indicate that there is an increase in copper concentration beyond the critical potential. This supports the suggestion by Kametani and Aoki (1985) that there might have been a change in the mechanism or nature of the chalcopyrite concentrate, which leads to an increased chalcopyrite extraction at higher potentials

Hiroyoshi *et al.* (2000) reported that the redox potential range where chalcopyrite leaching occurs was within the potential range of 520 to 700 mV (SHE). The rates of copper extraction were re-evaluated and normalised to the rate of copper extraction per unit area of chalcopyrite. A comparison between the rate of copper extracted at 35°C from the published data and experimental data is shown in Figure 6.2.

The experimental results indicate an increase in the rate of copper extraction from 700 to 800 mV (SHE). Hiroyoshi *et al.* (2000) reported a decrease in rate of copper extraction from 580 to 700 mV (SHE). They did not perform leach experiments above this redox potential range.

The chalcopyrite concentrate used by Kametani and Aoki (1985) and the concentrate used in this study had similar sulfide compositions. The results exhibited similar trends in the redox potential range where chalcopyrite leaching occurs. Hiroyoshi *et al.* (2000) used a purer chalcopyrite concentrate and observed a lower redox potential range within which optimal chalcopyrite leaching occurs. Natarajan (1992) have reported increase in copper extraction from chalcopyrite concentrates containing both chalcopyrite and pyrite due to galvanic interaction. There is a possibility that the galvanic interaction due the presence of other sulfide minerals could have caused enhanced copper extraction at higher redox potentials. This however requires further investigation.

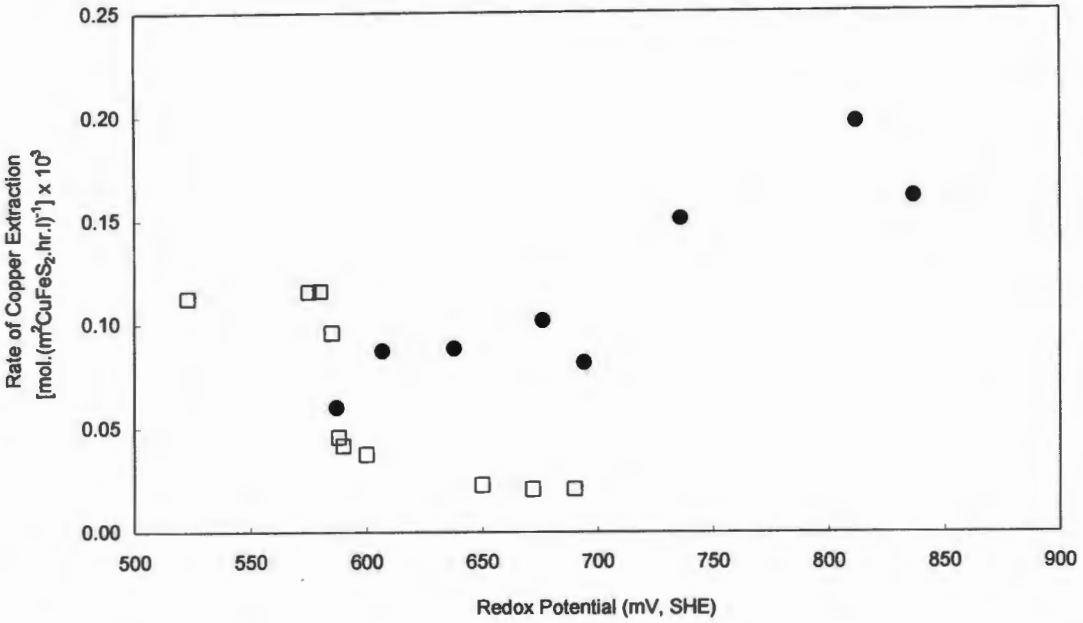

Figure 6.2: Comparison of the rate of copper extracted between experimental data at 35°C and re-evaluated rate at 25°C from Hiroyoshi *et al.*, (2000)
[●] Experimental data [□] Hiroyoshi *et al.* (2000)

6.1 FERROUS-PROMOTED CHALCOPYRITE LEACHING

Hiroyoshi *et al.* (1997) proposed that for a specific concentrate the dominant chalcopyrite leach reaction was:

$$CuFeS_2 + O_2 + 4H^+ \rightarrow Cu^{2+} + Fe^{2+} 2S^\circ + 2H_2O \qquad [5.4]$$

They conducted chalcopyrite leach experiments in shake flasks using both ferric and ferrous sulfate media to determine the extent of chalcopyrite leaching. Three out of four samples showed enhanced chalcopyrite leaching in the ferrous sulfate medium rather than in the ferric sulfate medium. All the samples indicated significant differences on the extent of copper extraction using both the ferric and ferrous sulfate media. The authors suggested that the type of concentrate used affected the type of leaching.

Based on the preliminary results on the extent of copper extraction using the different concentrates in the ferric and ferrous sulfate systems, the authors performed further experiments on the concentrate that exhibited the highest amount of copper extraction in the ferrous sulfate medium. The nitrogen sparged ferrous sulfate showed negligible copper extraction, indicating that ferrous-iron does not leach chalcopyrite. The oxygen sparged ferrous system exhibited the highest copper extraction results. Sparging with oxygen promotes the oxidation of ferrous-iron to ferric-iron. Thus, a similar copper dissolution behaviour should have been observed in ferric and oxygen sparged ferrous sulfate systems. However, on comparison with the ferric sulfate leaching results, the copper extracted in the oxygen sparged ferrous medium was much higher. The authors however, did not monitor the redox potential

change within the system. The results obtained from these experiments are illustrated in Figure 6.3. Based on the oxygen consumption results they showed that chalcopyrite leaching is enhanced in ferrous medium and requires the presence of oxygen to oxidise chalcopyrite, according to Equation 5.4.

Subsequently, preliminary experiments were conducted in this study to establish whether oxidation of chalcopyrite by dissolved oxygen was promoted by the presence of ferrous-irons, as postulated by Hiroyoshi *et al.* (1997). Chalcopyrite leach experiments were conducted using ferric sulfate and oxygen sparged ferrous sulfate media. This was done to establish whether the copper extraction rate in the ferrous sulfate was higher than that in the ferric sulfate system as observed by Hiroyoshi *et al.* (1997). The results contradicted observations from Hiroyoshi *et al.* (1997), because the extent of copper extraction using either a ferric or ferrous system were similar. These results seem to show that ferrous-promoted chalcopyrite oxidation by dissolved oxygen did not improve copper extraction. However, the results in this investigation were preliminary and not conclusive.

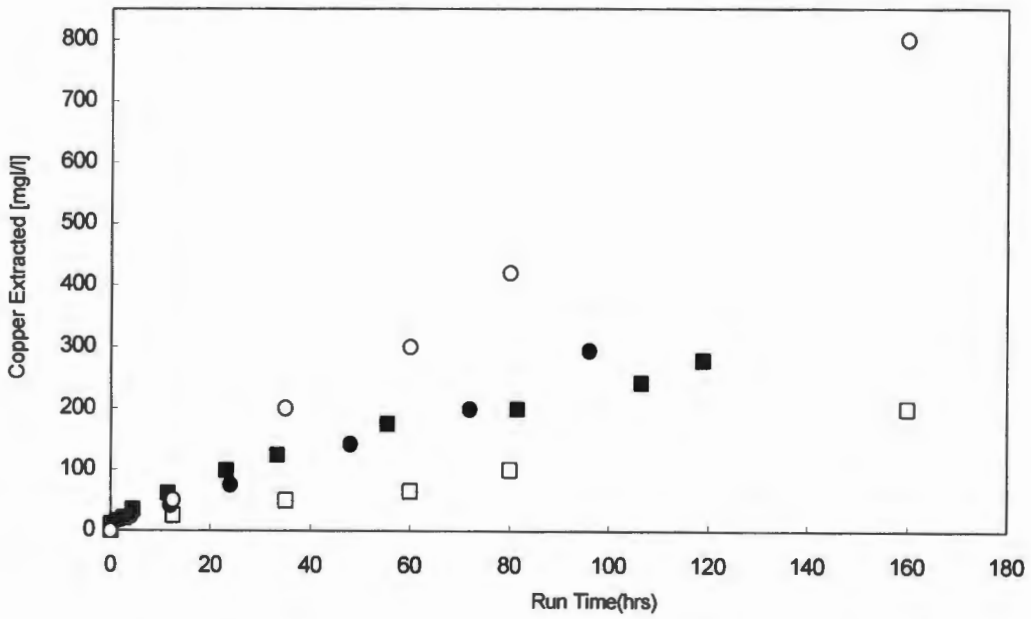

Figure 6.3: Comparison of copper extraction with time in a ferric and ferrous sulfate system with data from Hiroyoshi *et al.*, (1997).
Experimental Results:
[■] 0.2M, Fe^{3+}; [●]: 0.2M Fe^{2+}, sparged in air;
Data from Hiroyoshi *et al.* (1997)
[O] 0.04M, Fe^{2+}, sparged in Air; [□] Hiroyoshi, 0.2M Fe^{3+}, Air

However, the experiments show that different concentrates have different effect on the leaching rates.

Chapter Seven

Conclusions and Recommendations

In this thesis, the ferric leaching of chalcopyrite was investigated as a sub-process in the multi-subprocess mechanism of chalcopyrite bioleaching.

This investigation had two objectives. Firstly, to survey the literature on the nature of the passivating layer formed during the ferric leaching of chalcopyrite. Secondly, to determine the initial rates and the optimal redox potential range at which chalcopyrite ferric leaching occurs. The conclusions drawn from the literature and the experimental results are outlined below.

Various theories on the nature of the passivating layer formed during the ferric leaching of chalcopyrite have been proposed. However, the most recent rigorous work by Klauber *et al.* (2001) and Parker *et al.* (2001) has shown evidence that elemental sulfur is the chief cause of passivation during the initial leach period. Over extended period of time under chemical and bioleaching conditions, ferric-hydroxy sulfate followed by jarosite formation were identified as possible passivating layers

Literature has shown evidence that chalcopyrite leaching undergoes various phases during the leach process. An electrochemical model which predicts chalcopyrite leach kinetics has not yet been developed.

Previous researchers have investigated the kinetics of chalcopyrite leaching under dynamic leach conditions. However, work by Kametani and Aoki (1985), Furamera (2000) and this study has demonstrated that the methodology for determining rate of chalcopyrite leaching using potassium permanganate to maintain constant redox potential is a valid and applicable approach. The applicability of this method was tested on pyrite, a mineral that has been extensively studied and its kinetics well established. The rates were comparable to rates obtained from a previous study using the dynamic leach method.

This investigation has shown that below 580 mV (SHE) the initial rate of chalcopyrite leaching is low. It appears that the leaching of chalcopyrite is favoured from 600 mV to 780 mV (SHE). Higher potentials above 780 mV (SHE) show a decrease in rate of copper production.

The rate of chalcopyrite leaching from this investigation is comparable with rates from Kametani and Aoki (1985).

During the initial phase of chalcopyrite leaching, a variable ferrous-iron to copper ratio was observed. It appears that acid leaching causes a significant amount of copper dissolution, especially during the first ten minutes of the leaching process.

This research is limited and preliminary, the initial rates of chalcopyrite leaching was established using one concentrate. This study has established that the methodology for determining rate of chalcopyrite leaching at constant redox potential is valid. Further work using chalcopyrite concentrates of varying purity is needed to establish whether, the redox potential range where chalcopyrite leaching occurs varies with the type of concentrate used.

REFERENCES

1. Ammou-Chokroum, M., P.K. Sen and F. Fouques (1981), "Electro-oxidation of chalcopyrite in acid chloride medium; kinetics, stoichiometry and reaction mechanism", in: Laskowski, J. (Ed.), Proceedings of the 13th International Minerals Processing Congress, June 4-9, 1979, Warsaw, Poland, Elsevier Scientific Publishers, New York, USA, 759-809.

2. Barrett, J., M.N. Hughes, A. N. Islam and C. Simons (1991), "Nature of stability of precipitated solids form arsenopyrite bio-oxidation effluents", in: Proceedings of Randol Gold Forum, April, 1991, Cairns, Australia, Randol International Ltd., Colarado, USA, 179-183.

3. Barriga Mateos, F., I. Palencia and F. Carranza (1987), "The passivation of chalcopyrite subjected to ferric sulphate leaching and its reactivation with metal sulphides", *Hydrometallurgy*, **19**, 159-167.

4. Beckstead, L.W., B. Munoz and J.L. Sepulveda (1976), " Acid ferric sulfate leaching of attritor-ground chalcopyrite concentrates", in: Yannapolous, J.C and J.C Agarwal (Eds.), "Extractive Metallurgy of copper: Hydrometallurgy and Electrowinning", Proceedings of the International Symposium on Copper Extraction and Refining, February 22-26, 1976, Las Vegas, Nevada, The Metallurgical Society of the AIME©, New York, USA, 611-630.

5. Beckstead, L.W. and J.D. Miller (1976), "Ammonia, oxidation leaching of chalcopyrite - reaction kinetics", *Metall. Trans.*, **8B**, 19-29.

6. Biegler, T. and M.D. Horne (1985), "The electrochemistry of the surface oxidation of chalcopyrite", *J. Electrochem. Soc.*, 1363-1369.

7. Boon, M. (1996), "Theoretical and Experimental Methods in the Modelling of Biooxidation Kinetics of Sulphide Minerals", Ph.D Thesis, Technische Universiteit Delft, The Netherlands.

8. Boon, M., G.S. Hansford and J.J. Heijnen (1995), "The role of bacterial ferrous iron oxidation in the bio-oxidation of pyrite", in: Vargas, T., C.A. Jerez, J.V. Wiertz and H. Toledo (Eds.), Biohydrometallurgical Processing: Proceedings of the International Biohydrometallurgy Symposium IBS-95, November 19-22, 1995, Vina del Mar, Chile, University of Chile, Santiago, Chile, 153-163.

9. Braithwaite, J.W. and M.E. Wadsworth (1976), " Oxidation of chalcopyrite under simulated conditions of deep solution mining", in Yannapolous, J.C and J.C Agarwal (Eds.), "Extractive Metallurgy of Copper: Hydrometallurgy and Electrowinning", Proceedings of the International Symposium on Copper Extraction and Refining, February 22-26, 1976, Las Vegas, Nevada, The Metallurgical Society of the AIME©, New York, USA, 752-770.

10. Broadhurst, J.L. (1993), "Determination of arsenic and iron, and their oxidation states, in BIOX® process liquors", Report No. PR 93/85C of Project No. PR 93/128, GENMIN Process Research, Johanessburg, South Africa, 1-13.

11. Breed, A.W. (2000), " Studies on the Mechanism and Kinetics of Bioleaching with Special Reference to the Bioleaching of Refractory Gold-Bearing Arsenopyrite/Pyrite Concentrates", Ph.D. Thesis, University of Cape Town, South Africa.

12. Brierley, C.L. (1997)," Mining biotechnology research to commercial development and beyond," in: Rawlings, D.E. (Ed.), "Biomining: Theory, Microbes and Industrial Processes", Springer-Verlag and Landes Bioscience, Berlin, Germany, 3-17.

13. Brierley, C.L. and J.A. Brierley (1999), " Copper bioleaching: state of the art", in: Eltringham, G.A, B.A. Hancock, J.E. Dutrizac, S.K. Young, D.B. George and C. Diaz (Eds.), Proceedings of the Copper – Fourth International Conference, Copper; COMBRE 99, October 10-13, 1999, Phoenix, Arizona, USA, TMS.

14. Brierley, J.A. and C.L. Brierley (2001), " Present and future applications of biohydrometallurgy", *Hydrometallurgy*, **59**, 233-239.

15. Burkin, A.R. (1969), "Solid state transformation during leaching", *Min. Sci. Engng.*, 4-4.

16. Colmer, A.R. and M.E. Hinkel (1947), "The role of micro-organisms in acid mine-drainage", *Science*, **106**, 253-256.

17. Crundwell, F.K. and P.I. Harvey (1997), "Growth of *Thiobacillus Ferrooxidans*: A novel experimental design for batch growth and bacterial leaching studies", *Appl. Environ. Microb.*, **63**, 2586-2592.

18. Dew, D.W., E.N. Lawson and J.L. Broadhurst (1997), "The BIOX process for biooxidation of gold-bearing ores or concentrates", in: Rawlings, D.E. (Ed.), "Biomining: Theory, Microbes and Industrial Processes", Springer-Verlag and Landes Bioscience, Berlin, Germany, 45-80.

19. Dew, D.W., R. Muhlbauer and C. Van Buuren (1999), "Bioleaching of copper sulphide with mesophiles and thermophiles", in: Taylor, A. (Ed.), Proceedings of 5th Annual Forum ALTA Copper 1999 Copper Sulphide Symposium, September 6-8, 1999, Gold Coast, Australia, ALTA Metallurgical Services, Melbourne Australia.

20. Dreisinger, D. (2001), "New developments in the hydrometallurgical treatment of copper and copper-precious metal", in: Ibanez, J.P., E. Patino and X. Veloso (Eds.), Proceedings of II Mining Meeting Of South America VII Mining Meeting Of Tarapaca, August 22 –25, 2001, Iquique, Chile, Arturo Prat University, Iquique, Chile, 1-13.

21. Dry, M.J. (1984), "Kinetics of Leaching of a Low Grade Matte in Ferric Sulphate solution, PhD thesis, University of Witswatersrand, South Africa.

22. Dutrizac, J.E. and R.J. MacDonald (1974), "Ferric ion as a leaching medium", *Miner. Sci. Eng.*, **6** (2), 59-99.

23. Dutrizac, J.E. (1978), "The kinetics of dissolution of chalcopyrite in ferric ion media", *Metall. Trans.*, **9B**, 431-439.

24. Dutrizac, J.E. (1981), "The dissolution of chalcopyrite in ferric sulphate", *Metall. Trans.*, **12B**, 371-378.

25. Dutrizac, J. E. (1982), "Ferric ion leaching of chalcopyrite from different localities", *Metall. Trans.*, **13B**, 303-309.

26. Dutrizac, J. E. (1989), "Elemental sulphur formation during the ferric sulphate leaching of chalcopyrite", *Can. Metall. Quart.*, **28**, 337-344.

27. Furamera, A.T. (2000), "A Preliminary Investigation of the Ferric Leaching of a Mixed Sulphide Copper Concentrate at Controlled Redox Potential", M.Sc. (Science). Thesis, University of Cape Town, South Africa.

28. Gomez, C., M. Figueroa, J. Munoz, M.L. Blazquez and A. Blaster (1996), "Electrochemistry of chalcopyrite", *Hydrometallurgy*, **43**, 331-344.

29. Habashi, F. (1978), "Structural and physical properties", in: "Chalcopyrite Its Chemistry and Metallurgy", McGraw-Hill, New York, USA, 15-21.

30. Habashi, F. (2001), "Clean technology in the metallurgical industry", in: Ibanez, J.P., E. Patino and X. Veloso (Eds.), Proceedings of II Mining Meeting Of South America VII Mining Meeting Of Tarapaca, August 22 –25, 2001, Iquique, Chile, Arturo Prat University, Iquique, Chile, 17-28.

31. Habashi, F. and T. Toor (1979), "Aqueous oxidation of chalcopyrite in hydrochloric acid", *Metall. Trans.*, **10B**, 49-56.

32. Habashi, F. (1999), "The future of extractive metallurgy", *CIM Bull.*, **92**, 162-165.

33. Hackl, R. P., D. B. Dreisinger, E. Peters, and J. A. King (1995), "Passivation of chalcopyrite during oxidative leaching in sulphate media", *Hydrometallurgy*, **39**, 25-48.

34. Haines, A.K. and P.C. Van Aswegen (1990), "Process and engineering challenges in the treatment of refractory gold ores", in: "Innovations in Metallurgical Plant, Proc. International Deep Mining Conference", Proceeding of SAIMM Conference, Johannesburg, South Africa, 103-110.

35. Hansford, G.S., T.A. Furamera, M.A. Jaffer, and G.E Searby (1999), "Preliminary results of an investigation on the mechanism of bioleaching of chalcopyrite", in: Taylor, A. (Ed.), Proceedings of 5th Annual Forum ALTA Copper 1999 Copper Sulphide Symposium, September 6-8,1999, Gold Coast, Australia, ALTA Metallurgical Services, Melbourne, Australia.

36. Hansford, G.S. and T. Vargas (2001), "Chemical and electrochemical basis of bioleaching process", *Hydrometallurgy*, **59**, 135-145.

37. Havlik, T. and R. Kammel (1995), " Leaching of chalcopyrite with acidified ferric chloride and carbon tetrachloride addition", *Miner. Eng.*, **8**, 1125-1133.

38. Hearne, T.M., R. Haegele, and R.D. Beck (1998), "Hydrometallurgical recovery of zinc from sulphide ores and concentrates", in: Dutrizac J.E., J.A. Gonzalez, G.L. Bolton and P. Hancock (Eds.), Proceeding of 37th Annual Conference of Metallugist –CIM Zinc and Lead Processing, August 16-19, 1998, Calgary, Canada, Canadian Institute of Mining, Metallurgy and Petroleum, Montreal, Canada, 765-780.

39. Holiday, R.I. and W.R. Richmond (1990), "An electrochemical study of the oxidation of chalcopyrite in acidic solution", *J. Electro. Chem.*, **288**, 83-98.

40. Holmes, P.R. and F.K. Crundwell (2000), "The kinetics of the oxidation of pyrite by ferric ions and dissolved oxygen: An electrochemical study", *Geochimica et Cosmochimica Acta*, **64**(2), 263-274.

41. Homes, P.R. and F.K. Crundwell (1995), "Kinetic aspects of galvanic interactions between minerals during dissolution", *Hydrometallurgy*, **39,** 353-375.

42. Hiroyoshi, N., M. Hajime, T. Hirajima and M. Tsunekawa (2000), " A model for ferrous-promoted chalcopyrite leaching", *Hydrometallurgy*, **57**, 31-38.

43. Hiroyoshi, N., M. Hirato, T. T. Hirajima and M. Tsunekawa (1997), "A case of ferrous-sulphate addition enhancing chalcopyrite leaching", *Hydrometallurgy*, **47**, 37-45.

44. Hiskey, J.B. (1993), "Chalcopyrite Semiconductor Electrochemistry and Dissolution", in: Reddy, R.G., C. A. Landolt and R.N. Weizenbach (Eds.), Proceedings of the Paul E. Queneau International Symposium: Extractive Metallurgy of Copper, Nickel and Cobalt, Denver, Colorado, USA, TMS, Warrendale, Pennsylvania, USA.

45. Hirato, T., M. Kinoshita, Y. Awakura and M. Majima (1986), "The leaching of chalcopyrite with ferric chloride", *Metall. Trans.*, **17B**, 19-28.

46. Hirato, T., Y. Awakura and M. Majima (1987), "The leaching of chalcopyrite with ferric sulphate", *Metall. Trans.*, **18B**, 489-495.

47. Jones, D.L. and E. Peters (1976), "The leaching of chalcopyrite with ferric sulphate and ferric chloride", in: Yannapolous J.C and J.C Agarwal (Eds.), "Extractive Metallurgy of copper: Hydrometallurgy and Electrowinning", Proceedings of the International Symposium on Copper Extraction and Refining, February 22-26, 1976, Las Vegas, Nevada, The Metallurgical Society of the AIME, New York, USA, 633-653.

48. Kametani, H. and A. Aoki (1985), "Effect of suspension potential on the oxidation rate of copper concentrate in a sulphuric acid solution", *Metall. Trans.*, **16B**, 695-705.

49. Kelly, D.P. and A.P. Wood (2000), "Reclassification of some species of *Thiobacillus* to the new genera *Acidithiobacillus* gen. nov., *Halothiobacillus* gen. nov. and *Thermithibacillus* gen. nov.", *Int. J. Syst. Evol. Micr.*, **50**, 511-516.

50. Klauber, W., A. Parker, C. van Bronswijk and H. Watling (2001), " Sulphur speciation of leached chalcopyrite surfaces determined by X-ray photoelectron spectroscopy", *Int. J. Miner. Process,* **62**, 65-94.

51. Lawson, E.N., C.N. Nicholas and H. Pellat (1995), "The toxic effects of chloride ions on *Thiobacillus ferrooxidans"*, in: Vargas, T., C.A. Jerez, J.V. Wiertz and H.

Toledo (Eds.), Biohydrometallurgical Processing: Proceedings of the International Biohydrometallurgy Symposium IBS-95, November 19-22, 1995, Vina del Mar, Chile, University of Chile, Santiago, Chile, 201-208.

52. Linge, H. G. (1976), "A study of chalcopyrite dissolution in acidic ferric nitrate by potentiometric Titration", *Hydrometallurgy*, **2**, 51-64.

53. Lu, Z.Y., M.I. Jeffrey and F. Lawson (2000), " The effect of chloride ions on the dissolution of chalcopyrite in acidic solutions", *Hydrometallurgy*, **56**, 189-202.

54. May, N. (1997), " The Ferric Leaching of Pyrite", M.Sc. (Applied Science) Thesis, University of Cape Town, South Africa.

55. May, N., D. E Ralph and G.S. Hansford (1997), "Dynamic redox potential measurement for determining the ferric leach kinetics of pyrite", *Miner. Eng.*, **10**, 1279-1290.

56. Miller, P.C., M.K. Rhodes, R. Winby, A. Pinches and P.J. van Staden (1999), "Commercialization of bioleaching for base-metal extraction", *Miner. Metall. Proc.*, **16**(4), 42-50.

57. Miller, J.D. and H.Q. Portillo (1981), "Silver catalysis in ferric sulfate leaching of chalcopyrite", in: Laskowski, J. (Ed.), Proceedings of the 13th International Minerals Processing Congress, June 4-9, 1979, Warsaw, Poland, Elsevier Scientific Publishers, New York, USA, 851-901.

58. Munoz, P. B., J. D. Miller and M. E. Wadsworth (1979), "Reaction mechanism for the acid ferric sulphate leaching of chalcopyrite", *Metall. Trans.*, **10B**, 149-158.

59. Murr, E., A.E. Torma and J.A. Brierley (1978), "Metallurgical applications of bacterial leaching and related microbiological phenomena", Academic Press, New York, USA, XVIII, 53.

60. Nagpal, S., D. Dahlstrom and T. Dolman (1994), "A mathematical model for bacterial oxidation of sulphide ore concentrate", *Biotech. Bioeng.*, **43**(5), 357-364.

61. Natarajan, K.A. (1990), " Electrochemical aspects of bioleaching of base metal sulphides", in Ehrlich H.L. and C.L. Brierley (Eds.), "Microbial Mineral Recovery", McGraw-Hill, USA, 79-106.

62. Natarajan, K.A. (1992), "Electroleaching of base metal sulphides", *Metall. Trans.*, **23B**, 5-11.

63. Natarajan, K.A., and I. Iwasaki (1974), "Eh measurements in hydrometallurgical systems", *Miner. Sci. Eng.*, **6**, 35-44.

64. Parker, A. J., R. L. Paul and G. P. Power (1981), "Electrochemical aspects of leaching copper from chalcopyrite in ferric and cupric salt solutions", *Aust. J. Chem.*, **34**,11-34.

65. Parker, A. J., C. Klauber, H.R. Watling and W. van Bronswijk (2001), "An X-Ray photoelectron spectroscopy study of the mechanism of chalcopyrite leaching", in: Ciminelli, V.S.T. and O. Garcia (Eds.), Biohydrometallurgy: Fundamentals, Technology and Sustainable Development: Proceedings of the International Biohydrometallurgy Symposium IBS-'01, September 16-19, 2001, Minas Gerais, Brazil, Elsevier Scientific Publishers, Amsterdam, Netherlands, 547-555.

66. Peters, E. and F.M. Doyle (1989), "Leaching and decomposition of sulphide minerals", in: Sastry, K.V.S. and M.C. Fuerstenau (Eds.), Proceedings of symposium: Challenges in Mineral Processing, December 7-9, 1988, Berkley, California, USA, Society of Mining Engineering Inc, Littleton, Colorado, USA, 509-526.

67. Peterson, J., D.G. Dixon, M. Timmins and R. Ruitenburg (2001), "Batch reactor studies of the leaching of a pyrite/chalcopyrite concentrate using thermophilic bacteria," in: Ciminelli, V.S.T. and O. Garcia (Eds.), Biohydrometallurgy: Fundamentals, Technology and Sustainable Development: Proceedings of the International Biohydrometallurgy Symposium IBS-'01, September 16-19, 2001, Minas Gerais, Brazil, Elsevier Scientific Publishers, Amsterdam, Netherlands, 525-533.

68. Record, G.H. (1965), 'The use of Redox Potential in Chemical Process Control' – Description and Measurement", *Instrument Engineer*, 69-75.

69. Riekkola-Vanhanen, M. and S. Heimala (1993), "Electrochemical control in the biological leaching of sulfidic ores", in: Torma, A.E., J.E. Wey and V.L. Lakshmanan (Eds.), Biohydrometallurgical Technologies: Bioleaching processes: Proceedings of the International Biohydrometallurgy Symposium IBS-93, August 22-25, 1993, Jackson Hole, Wyoming, USA, TMS, Warrendale, Pennsylvania, USA, 561-570.

70. Rossi, G. (1990), "Kinetic Models" in: "Biohydrometallurgy", McGraw-Hill, Hamburg, Germany, 293-309.

71. Schippers, A., and W. Sand (1999), "Bacterial leaching of metal sulphides proceeds by two indirect mechanisms via thiosulphate or via polysulphides and sulphur." *Appl. Environ. Microb.*, **65**, 319-321.

72. Schnell, H.A. (1997), "Bioleaching of Copper", in Rawlings, D.E. (Ed.), "Biomining: Theory, Microbes and Industrial Processes", Springer-Verlag and Landes Bioscience, Berlin, Germany, 21-43.

73. Taylor, A. and M.L. Jansen (1999), "Hydrometallurgical treatment of copper sulphides – are we on the brink?", in: Taylor, A. (Ed.), Proceedings of 5th Annual Forum ALTA Copper 1999 Copper Sulphide Symposium, September 6-8,1999, Gold Coast, Australia, ALTA Metallurgical Services, Melbourne, Australia.

74. Tiwari, B.L., J. Kolbe and H.W. Hayden (1980), "Leaching of high solids, attritor ground chalcopyrite concentrate by *in-situ* generated ferric sulphate solution", *Metall. Trans.*, **11B**, 89-93

75. Van Aswegen, P.C. (1993), "Bio-oxidation of refractory fold ores, the GENMIN experience", in: Proceedings Biomine '93, March 22-23, 1993, Adelaide, Australia, Australian Mineral Foundation, Glenside SA, 15.1-15.14.

76. Wan, R. Y., J.D.Miller, J. Foley and S. Pons (1984[a]) "Electrochemical features of the ferric sulphate leaching of $CuFeS_2$/C aggregates", in: Richardson, P.E. S. Srinivasan and R. Woods (Eds.), Proceedings International Symposium on

Electrochemistry in Mineral and Metal Processing, Cincinnati, USA, Pennington, New Jersey: Industrial Electrolytic Division, Energy Technology Group, 391-416.

77. Wan, R. Y., J. D. Miller, and G. Simkovich (1984[b]), "Enhanced Ferric Sulphate Leaching of Copper from $CuFeS_2$ and C Particulate Aggregates", in: Haughton, L. F. (Ed.), Mintek 50 – Proceedings of International Conference on Mineral Science and Technology, Randburg, South Africa, Council of Mineral Technology, Randburg, South Africa, 575-588.

78. Warren, G.W., M.E. Wadsworth and S.M. El-Raghy (1982), "Passive and transpassive anodic behaviour of chalcopyrite in acidic solutions", *Metall. Trans.*, **13B**, 571-579.

79. Wadsworth, M.E. (1987), "Leaching – metal applications," in: Rousseau, R.W (Ed.), "Handbook of Separation Process Technology", John Wiley & Sons, New York, 529-531.

APPENDIX I

ANALYTICAL METHODS

STANDARDISATION OF A SOLUTION OF POTASSIUM PERMANGANATE

The procedure used to calculate the concentration of the potassium permanganate used in the experimental determinations is described in this section.

Method

The burette was filled with the potassium permanganate solution. The pipette was washed with water and rinsed with small amounts of the oxalic acid solution. Exactly 20 ml of oxalic acid solution (0.05 M) was pipetted into a clean flask. Approximately 20 ml of 3M sulphuric acid was added and the solution was heated to about 60 °C. The hot solution was titrated with the potassium permanganate until the first permanent pink tinge. This procedure was repeated with further aliquotes of oxalic acid solution until three titres which agreed within 0.1ml of each other was obtained. If a brown suspension or precipitate had occurred, then insufficient sulphuric acid would have been added or the titration could have been carried out too quickly.

The equation for the reactions which occurred is:

$$2KMnO_4 + 3H_2SO_4 + 5(COOH)_2 \rightarrow 2MnSO_4 + K_2SO_4 + 10CO_2 + 8H_2O$$

Calculations

The permanganate ion (MnO_4^-) was converted to the manganese (II) ion (Mn^{2+}) while carbon dioxide was liberated. The reaction involved the hydrogen ion (H^+), thus the addition of sulphuric acid to the oxalic acid solution before titration.

Using the equation above, the following relationship was used to calculate the concentration of the potassium permanagante.

$$\frac{C_{oxalic\ acid} \times V_{oxalic\ acid}}{5} = \frac{C_{KMnO_4} \times V_{KMnO_4}}{2}$$

TITRATIONS METHODOLOGIES USED FOR DETERMINATING FERROUS-IRON AND TOTAL ION CONCENTRATIONS

Determination of Ferrous Ion Concentration

The required aliquot (5 ml) was pipetted into a conical flask. 10 ml of spekker was added, followed by 3 – 4 drops of barium diphenyl sulfonate indicator. The sample was titrated with potassium dichromate until the first permanent colour change from orange to purple.

$$Fe(II)\ (mol.l^{-1}) = \frac{[K_2Cr_2O_7] \times V_{titre} \times 55.85 \times 6}{V_{titre}}$$

Determination of Total Iron Concentration

The required aliquot (5 ml) of sample was pipetted into a conical flask. 30 ml ferric acid was added and the solution was heated to boiling point. Stannous chloride was added drop-wise until the yellow colour of the solution disappeared. One extra drop was added and the total amount of stannous chloride added was recorded. The solution was cooled to room temperature and 10 ml mercuric chloride solution was added forming a silky white precipitate. If no precipitate formed, too little stannous chloride would have been added, and if the precipitate was heavy and grey, too much stannous chloride would have been added. In either case the experiment had to be aborted. 4-8 drops of barium sulfonate indicator were added and the sample titrated with potassium dichromate until the first permanent colour change from yellow/green to purple.

$$Fe(II)\ (mol.l^{-1}) = \frac{[K_2Cr_2O_7] \times V_{titre} \times 55.85 \times 6}{V_{titre}}$$

Preparation of Reagents

The chemical reagents used in the procedures mentioned above were prepared as described below.

Potassium Dichromate Solution

About 10 g of potassium dichromate was dried in an oven at about 105 °C for 1-2 hours. About 8.8 g of the dried potassium dichromate was dissolved in 2 litres of distilled water, to form a standard solution of concentration about 0.015 M.

Spekker Acid

450 ml concentrated (98 %) sulphuric acid and 450 ml concentrated (32 %) hydrochloric acid were slowly added to 1200 ml distilled water with stirring. The solution was allowed to cool before transferring to a storage bottle.

Ferric acid solution

300 ml of spekker acid solution and 600 ml concentrated (32 %) hydrochloric acid were slowly added to 1200 ml distilled water with stirring. The solution was allowed to cool before being transferred to a storage bottle.

Stannous chloride solution

50 g stannous chloride ($SnCl_2$) was weighed out into a 100 ml beaker. 50 ml of concentrated (32 %) hydrochloric acid was added and the solution was heated to about 50 °C and agitated until all the salt had dissolved. After cooling, the solution was diluted to 1 litre with distilled water and stored in a glass container with a few granules of tin metal.

Mercuric chloride solution (saturated)

One litre of distilled water was added to 50 g mercuric chloride ($HgCl_2$) and agitated for 2 hours. If all the mercuric chloride had dissolved, a further amount was added and the solution agitated for a further 2 hours.

Barium Diphenylamine Sulfonate Indicator

1 g barium diphenyl sulfonate ($C_{24}H_{20}BaN_2O_6S_2$) was weighed out in a 250 ml beaker. 100 ml of concentrated (98 %) sulphuric acid was added and the solution was agitated until the salt had completely dissolved.

SAMPLE PREPARATION FOR AAS ANALYSIS

Samples were extracted at regular intervals and analysed for copper, zinc and total iron. The samples were diluted 1 part sample in 10 parts acidified de-ionised water for copper and zinc analysis. The samples were not diluted further for copper and zinc analysis, since the concentrations of these elements were very low, and further dilution could result in measuring a lower copper concentration. The optimal dilution strength was determined by preparing standards of 1mg/ℓ, 5mg/ℓ and 10mg/ℓ of copper sulfate in 10g/ℓ and 5g/ℓ of ferric and ferrous sulfate media. These samples were then diluted at various ratios in acidified de-ionised water and analysed using AAS, to determine the optimal dilution factor which gave the most accurate readings.

The samples were diluted 1 part sample to 100 parts acidified de-ionised water for total iron analysis.

APPENDIX II

CALCULATION OF RATE PER UNIT AREA OF CHALCOPYRITE

$$(m^2 CuFeS_2)mol^{-1} = [(m^2 CuFeS_2).kg^{-1}][(0.183kgCuFeS_2)mol^{-1}]$$

$$= \frac{\pi d^2}{\rho\pi\frac{d^3}{6}}.\left[(0.183kgCuFeS_2)mol^{-1}\right]$$

$$= \frac{6}{\rho d}.\left[(0.183kgCuFeS_2)mol^{-1}\right]$$

$$= \frac{6}{4087d}.\left[(0.183kgCuFeS_2)mol^{-1}\right]$$

Assumptions: Molar mass of chalcopyrite = 183 g. mol $^{-1}$

Density of Chalcopyrite = 4087 kg.m^{-3}